Abstract

Conventional methods for soil compaction mapping, such as penetrometers, although accurate, work as stop-and-go providing point measurements. This process is both time consuming and labour intensive. On-the-go electrical Conductivity (EC) measurements such as electromagnetic induction (e.g. *EM38*) are affected by key soil properties including texture, moisture content and compaction, so offer a possible rapid alternative for compaction detection. Therefore, the aim of this work is the detection of the within-field variability of soil compaction using soil electrical conductivity for improved soil management.

A methodology for identification of within-field variability and for comparison of the data collected by contact and contact-less EC sensors, soil compaction sensor (which contains of eight instrumented wedge faces attached to the leading edge of a tine) and cone penetrometer was developed and a randomised block design experiment was performed. The data was evaluated statistically, the maps of spatial variability were created and the areas for targeted soil loosening were determined.

A key finding was the development of application maps for targeted soil loosening, based on soil electrical conductivity measurements. The practical utilisation of this method assumes the presence of two maps that would be compared. The initial map has to be created for the soil in desirable loosened conditions and will be used as a standard for further comparisons. Further map will characterize the conditions of the compacted soil. It is recommended that both maps would be obtained in similar conditions to minimize the effect of soil moisture. The application map can be then created either manually using visual comparison of both initial (loosened soil condition) and further map (compacted areas), or using an appropriate geostatistical tool, in this case a ratio of the two maps.

It was found out that the EC readings collected by the Conductometer at depth range of 0-0.3 m are able to distinguish the soil areas with no compaction above 0.3 m and the soil compacted within whole profile. The EC readings obtained at depth range of 0-0.9 m can distinguish the soil zones with no compaction above 0.6 m from the rest

of the field. Using the EC data obtained at both depth ranges it is possible to determine three different environments within the field: one with no compaction above 0.3 m, one with no compaction above 0.6 m and one containing the soil compacted within whole profile.

The best results for determining the areas with different depths of soil compaction were obtained by soil compaction sensor and cone penetrometer. However the absolute values of soil compaction sensor were affected by small changes in soil texture. The slow data collection speed of point penetration resistance measurement technique practically limits the spatial resolution of final data set. The soil compaction sensor has to be attached on the frame of the subsoiler and although it provides precise readings, it has high energy requirement. The high labour and time requirements are the main disadvantages of penetration resistance measurements. Second most precise determination of the areas with different soil compaction presence was provided by the EC data collected by the Conductometer which is able to collect data on-the-go with much lower power requirements. *EM38* operated in horizontal mode distinguished the areas with no compaction above 0.3 m and areas with soil compacted at whole profile with less precision. The same instrument operated in vertical mode was not sensitive enough to measure any differences in soil bulk density.

Table of Contents

Abstract i

Table of Contents iii

Table of Figures viii

List of Tables xviii

Acknowledgements xxii

List of Abbreviations xxiii

1 Introduction 1

1.1 Background 1

1.2 Aim 2

1.3 Objectives 2

1.4 Outline methodology 2

2 Literature review 3

2.1 Soil and soil degradation 3

2.1.1 Effects of soil compaction on plants and soils 3

2.1.2 Principles of soil compaction formation 4

2.2 Methods of detection of soil compaction within-field variability 6

2.2.1 Vertical measurement systems 7

2.2.2 Horizontal measurement systems 8

2.2.3 Non-contact sensors 10

2.3 Measuring of soil electrical conductivity 12
2.3.1 Definition 12
2.3.2 Theory of conducting electrical current in the soil 12
2.3.3 Factors that affect soil EC 13
2.3.4 Devices and methods for soil EC measurements 14
2.3.5 Depth of sensing 16
2.3.6 Relations between EC and other soil properties 19
2.3.7 Using EC measurements in different industries 21
2.4 Chapter summary 22
3 System operation parameters 24
3.1 Cone penetrometer 24
3.2 Soil compaction sensor 25
3.3 EM38 26
3.4 Conductometer 27
3.5 Operating characteristics 30
3.5.1 Introduction 30
3.5.2 Objectives 30
3.5.3 Time stability of EC readings 30
3.5.4 Relationship between the depth of the discs and the EC readings 35
4 Initial field experiments 38
4.1 Introduction 38

4.2 Objectives 38

4.3 Site characteristics 38

4.4 Comparing the readings obtained from trafficked and non-trafficked areas 40

4.4.1 Methodology 40

4.4.2 Results and discussion of results 41

4.5 Measurement performed in the same line at both directions 45

4.5.1 Methodology 45

4.5.2 Results and discussion of results 46

4.6 Localization of the trafficked areas using the perpendicular EC survey 49

4.6.1 Methodology 49

4.6.2 Results and discussion of results 51

4.7 Soil sampling 59

4.7.1 Methodology 59

4.7.2 Results and discussion of results 60

4.8 Conclusions of initial field experiments 62

5 Randomized block design (RBD) experiment 64

5.1 Introduction 64

5.2 Site characteristics 64

5.3 Methodology 65

5.4 Results and discussion of results 67

5.4.1 Conductometer compaction measurements - stationary and dynamic 67

5.4.2 Compaction treatment maps using Conductometer EC data 72

5.4.3 *EM38* compaction measurements 76

5.4.4 Penetrometer compaction measurements 78

5.4.5 Soil compaction sensor 82

5.4.6 Summary of ANOVA for RBD experiment 84

5.4.7 Regression analysis 85

5.5 Soil sampling 86

5.5.1 Methodology 86

5.5.2 Results and discussion of results 86

5.6 Conclusions of randomized block design experiment 88

6 Conclusions 90

7 Recommendations 93

8 References 94

Appendix I. *EM38* operating instructions i

Calibration procedure i

Appendix II. Time stability of EC readings iii

Appendix III. Weather data vi

Appendix IV. Relationship between the depth of the discs and the EC readings vii

Appendix V. Statistical analyse of the EC readings obtained from the trafficked and non-trafficked areas viii

The Conductometer viii

The *EM38* operated in vertical mode.....x

Appendix VI. Statistical analyse of the EC readings obtained in the same line in both directions xi

The Conductometer.....xi

The *EM38* operated in vertical mode.....xi

Appendix VII. Statistical analyse of the EC readings obtained within and between tramlines xii

The Conductometer.....xii

The *EM38* operated in vertical mode.....xiv

Appendix VIII. Methodology of soil laboratory analyses.....xvi

Particle size distribution.....xvi

Electrical conductivity by saturated paste.....xx

Loss on ignition.....xxi

Determination of soil pH xxii

Appendix IX. Bar charts – graphical interpretation of ANOVA results.....xxiv

Appendix X. Graphs of regression analyses.....xxxi

Appendix XI. Maps of EC readings obtained by the Conductometer at speed of 0.05 $m.s^{-1}$ xl

Appendix XII. Coordinates of EC measurements obtained by the Conductometer in different modes xlii

Table of Figures

Figure 2.1 Effect of soil compaction on soil pores' orientation and spacing. 4

Figure 2.2 Map of inherent susceptibility of European soils to compaction. 5

Figure 2.3 Soil cone penetrometer. 7

Figure 2.4 The geometry of the cone of *Veris® Profiler 3000*. 8

Figure 2.5 Schematic of a soil mechanical resistance measurement device. 9

Figure 2.6 Acoustic plow pan detection sensor. 10

Figure 2.7 Schematic of a subsurface soil reflectance optical sensor. 11

Figure 2.8 Ground penetrating radar. 11

Figure 2.9 Three different pathways of electrical conductance in soil. 12

Figure 2.10 Contours of electromagnetic array created by EMI. 15

Figure 2.11 A – Contours of an electric array created by *Veris® 3100*; and B – Wiring scheme of Soil Doctor® equipment. 16

Figure 2.12 A – *Veris® 3100*; and B – Soil Doctor®. 16

Figure 2.13 Soil electrical resistance equipment developed by Rhoades. 16

Figure 2.14 Spacing of sensing electrodes for a Wenner array. 17

Figure 2.15 Wenner's diagram showing four electrodes in the soil during soil EC measurement. 18

Figure 2.16 Relative response of both *EM38* and *Veris® 3100* (Shallow and Deep) sensors in dependence on soil depth. 19

Figure 2.17 Metal detector. 21

Figure 3.1 Soil cone penetrometer (Penetrologger from Eijkelkamp).....24

Figure 3.2 Flap of the instrumented tine and the horizontal forces acting on it. 25

Figure 3.3 Soil compaction sensor. A – callibration procedure, B – mounting on the frame of the subsoiler.....26

Figure 3.4 *EM38* attached to a non-metallic cart and plugged to a PDA. 27

Figure 3.5 Conductometer during field survey (A) and the sketch of sensed soil profiles (B). 28

Figure 3.6 Flow chart of the Conductometer. 29

Figure 3.7 EC measurement performed within the Sports ground. 31

Figure 3.8 Soil EC readings collected in measuring point no. 1 within the depth range of 0-0.3 m. 32

Figure 3.9 Soil EC readings collected in measuring point no. 1 within the depth range of 0-0.9 m. 33

Figure 3.10 Soil EC readings collected within the depth range of 0-0.3 m before and after rainfalls. 34

Figure 3.11 Soil EC readings collected within the depth range of 0-0.9 m before and after rainfalls. 34

Figure 3.12 The dependency between the soil EC within the soil profile 0-0.3 m and the depth of discs. 36

Figure 3.13 The dependency between the soil EC within the soil profile 0-0.9 m and the depth of discs. 37

Figure 4.1 Aerial photograph of the experimental sites used in this work. 39

Figure 4.2 Soil series present within Downings field. 40

Figure 4.3 Layout of the experiment aimed at the investigation of the differences between the EC readings obtained from trafficked and non-trafficked areas.....41

Figure 4.4 Positions of the coulter disc electrodes while running within the tramline. 41

Figure 4.5 Coulter disc electrodes within wheel mark (A) and in non-trafficked soil (B). 42

Figure 4.6 Soil EC readings collected at depth range of 0-0.3 m within and between the tramlines. 43

Figure 4.7 Soil EC readings collected at depth range of 0-0.9 m within and between the tramlines. 43

Figure 4.8 Difference of soil EC readings collected at depth range of 0-0.3 m and 0-0.9 m (EC30-EC90) within and between the tramlines. 44

Figure 4.9 Soil EC readings collected at depth range of 0-1.5 m within and between the tramlines. 45

Figure 4.10 Layout of the experiment aimed at the investigation of the repeatability of the EC measurements. 46

Figure 4.11 Soil EC readings collected in the same line in both directions (1st run and 2nd run) in depth range of 0-0.3 m.....47

Figure 4.12 Soil EC readings collected in the same line in both directions (1st run and 2nd run) in depth range of 0-0.9 m.....47

Figure 4.13 Detail view of the disc running in the groove created during the 1st run. 48

Figure 4.14 Soil EC readings collected in the same line in both directions (1st run and 2nd run) in depth range of 0-1.5 m.....49

Figure 4.15 Layout of the experiment aimed at the localization of the tramlines using the EC readings. 50

Figure 4.16 Soil EC readings collected within the Downings field perpendicularly across the tramlines. Detail shows the various widths along the tramlines dimensioned in meters that were used for data processing as it is described further. 50

Figure 4.17 Soil EC readings collected perpendicularly across the tramlines 51

Figure 4.18 Soil EC readings collected perpendicularly across the tramlines (1st run within "Strip 3"). 52

Figure 4.19 Sketch of Downings field cross-section along "Strip 3" showing different soil layering. 53

Figure 4.20 Natural break intervals of residuals of the soil EC readings measured by the Conductometer within the depth range 0-0.3 m. 56

Figure 4.21 Natural break intervals of residuals of the soil EC readings measured by the Conductometer within the depth range 0-0.9 m. 56

Figure 4.22 Natural break intervals of residuals of the soil EC readings measured by the *EM38* within the depth range 0-1.5 m. 57

Figure 4.23 Soil electrical conductivity measured by the Conductometer within the depth range 0-0.3 m used to delineate soil texture boundaries. 58

Figure 4.24 Soil electrical conductivity measured by the Conductometer within the depth range 0-0.9 m used to delineate soil texture boundaries. 58

Figure 4.25 Soil electrical conductivity measured by the *EM38* within the depth range 0-1.5 m used to delineate soil texture boundaries. 59

Figure 5.1 Soil series present within Avenue field. 65

Figure 5.2 Layout of randomised block experiment performed within trial plot within Avenue field. 65

Figure 5.3 EC readings obtained by the Conductometer operated in stationary mode from the trial plot at both depth ranges 0-0.3 m and 0-0.9 m before treatment applying.....69

Figure 5.4 EC readings obtained by the Conductometer operated in stationary mode from the trial plot at both depth ranges 0-0.3 m and 0-0.9 m after treatment applying. 69

Figure 5.5 EC readings obtained by the Conductometer operated in dynamic mode (at speed of 0.05 $m.s^{-1}$) from the trial plot at both depth ranges 0-0.3 m and 0-0.9 m before treatment applying. 70

Figure 5.6 EC readings obtained by the Conductometer operated in dynamic mode (at speed of 0.05 $m.s^{-1}$) from the trial plot at both depth ranges 0-0.3 m and 0-0.9 m after treatment applying. 70

Figure 5.7 Scatter plot of EC readings collected by the Conductometer at depth of 0-0.3 m in stationary and dynamic mode (at speed of 0.05 $m.s^{-1}$). 71

Figure 5.8 Scatter plot of EC readings collected by the Conductometer at depth of 0-0.9 m in stationary and dynamic mode (at speed of 0.05 $m.s^{-1}$). 71

Figure 5.9 Map of EC readings obtained by the Conductometer operated in stationary mode from the trial plot at depth range of 0-0.3 m before (left) and after (right) treatment applying. 74

Figure 5.10 Application map created by “EC30 before treatment application / EC30 after treatment application” (simple ratio). 74

Figure 5.11 Map of EC readings obtained by the Conductometer operated in stationary mode from the trial plot at depth range of 0-0.9 m before (left) and after (right) treatment applying. 75

Figure 5.12 Application map created as “EC90 before treatment application / EC90 after treatment application” (simple ratio). 75

Figure 5.13 EC readings obtained by *EM38* operated in vertical mode from the trial plot at depth range 0-1.5 m before treatment applying. 76

Figure 5.14 EC readings obtained by *EM38* operated in vertical mode from the trial plot at depth range 0-1.5 m after treatment applying. 77

Figure 5.15 EC readings obtained by *EM38* operated in horizontal mode from the trial plot at depth range 0-0.75 m after treatment applying. 77

Figure 5.16 Map of EC readings obtained by the EM operated in horizontal mode from the trial plot at depth range of 0-0.75 m after treatment applying. 78

Figure 5.17 Diagram of soil penetration resistance measured within different treatments. 79

Figure 5.18 Soil penetration readings obtained from the trial plot after treatment applying and averaged at depth range 0.1-0.3 m. 79

Figure 5.19 Soil penetration readings obtained from the trial plot after treatment applying and averaged at depth range 0.1-0.5 m. 80

Figure 5.20 Map of soil penetration resistance readings obtained from the trial plot and averaged at depth range of 0-0.3 m before (left) and after (right) treatment applying..... 80

Figure 5.21 Application map created by “PR30 before treatment application / PR30 after treatment application” (simple ratio). 81

Figure 5.22 Map of soil penetration resistance readings obtained from the trial plot and averaged at depth range of 0-0.5 m before (left) and after (right) treatment applying..... 81

Figure 5.23 Application map created by “PR50 before treatment application / PR50 after treatment application” (simple ratio). 82

Figure 5.24 Bending moment measured by soil compaction sensor within the trial plot at multiple depth ranges. 83

Figure 5.25 Map created on the base of the bending moment readings sensed by the soil compaction sensor obtained from the trial plot after treatment applying. 83

Figure VIII.1 Samples placed onto hotplate. xvi

Figure VIII.2 Measuring cylinders placed into a water bath. xviii

Figure VIII.3 Triangle for soil particle size distribution determination. xix

Figure VIII.4 Procedure for preparation of saturated extract and own measurement.xxi

Figure VIII.5 Silica dishes placed in a desiccator.....xxii

Figure VIII.6 Procedure for preparation of the suspension. xxiii

Figure VIII.7 Procedure for own measurement. xxiii

Figure IX.1 Stationary data obtained after treatment.....xxiv

Figure IX.2 Ratio of the stationary data (before/after treatment). xxv

Figure IX.3 Dynamic (0.05 $m.s^{-1}$) EC data obtained after treatment.....xxvi

Figure IX.4 Ratio of the dynamic (0.05 $m.s^{-1}$) data (before/after treatment).....xxvi

Figure IX.5 Dynamic (1 $m.s^{-1}$) EC data obtained after treatment.....xxvi

Figure IX.6 Ratio of the dynamic (1 $m.s^{-1}$) data (before/after treatment).....xxvii

Figure IX.7 Stationary data obtained after treatment..... xxviii

Figure IX.8 Ratio of the stationary data (before/after treatment). xxix

Figure IX.9 Dynamic (0.05 $m.s^{-1}$) EC data obtained after treatment.....xxix

Figure IX.10 Ratio of the dynamic (0.05 $m.s^{-1}$) data (before/after treatment).....xxix

Figure IX.11 Dynamic (1 $m.s^{-1}$) EC data obtained after treatment.....xxx

Figure IX.12 Ratio of the dynamic (1 $m.s^{-1}$) data (before/after treatment).....xxx

Figure X.1 Scatter plot of the soil electrical conductivity measured at stationary mode at depth range of 0-0.3 m and the penetration resistance averaged within the depth range of 0.1-0.3 m. xxxi

Figure X.2 Scatter plot of the soil electrical conductivity measured at stationary mode at depth range of 0-0.75 m and the penetration resistance averaged within the depth range of 0.1-0.3 m. xxxi

Figure X.3 Scatter plot of the soil electrical conductivity measured at stationary mode at depth range of 0-1.5 m and the penetration resistance averaged within the depth range of 0.1-0.3 m. xxxii

Figure X.4 Scatter plot of the bending moment measured by the soil strength sensor and averaged at depth range of 0.2-0.4 m and the penetration resistance averaged within the depth range of 0.1-0.3 m. xxxii

Figure X.5 Scatter plot of the soil electrical conductivity measured at stationary mode at depth range of 0-0.3 m and the penetration resistance averaged within the depth range of 0.1-0.5 m. xxxiii

Figure X.6 Scatter plot of the soil electrical conductivity measured at stationary mode at depth range of 0-0.75 m and the penetration resistance averaged within the depth range of 0.1-0.5 m. xxxiii

Figure X.7 Scatter plot of the soil electrical conductivity measured at stationary mode at depth range of 0-0.9 m and the penetration resistance averaged within the depth range of 0.1-0.5 m. xxxiv

Figure X.8 Scatter plot of the soil electrical conductivity measured at stationary mode at depth range of 0-1.5 m and the penetration resistance averaged within the depth range of 0.1-0.5 m. xxxiv

Figure X.9 Scatter plot of the bending moment measured by the soil strength sensor and averaged at depth range of 0.2-0.4 m and the penetration resistance averaged within the depth range of 0.1-0.5 m. xxxv

Figure X.10 Scatter plot of the bending moment measured by the soil strength sensor and averaged at depth range of 0.2-0.4 m and the soil EC readings measured within the depth range of 0-0.3 m. xxxv

Figure X.11 Scatter plot of the bending moment measured by the soil strength sensor and averaged at depth range of 0.2-0.4 m and the soil EC readings measured within the depth range of 0-0.75 m. xxxvi

Figure X.12 Scatter plot of the bending moment measured by the soil strength sensor and averaged at depth range of 0.2-0.4 m and the soil EC readings measured within the depth range of 0-0.9 m. xxxvi

Figure X.13 Scatter plot of the bending moment measured by the soil strength sensor and averaged at depth range of 0.2-0.4 m and the soil EC readings measured within the depth range of 0-1.5 m. xxxvii

Figure X.14 Scatter plot of the bending moment measured at the depth range of 0.35-0.4 and the soil penetration resistance averaged within the same depth range. xxxvii

Figure X.15 Scatter plot of the bending moment measured at the depth range of 0.30-0.35 and the soil penetration resistance averaged within the same depth range.. xxxviii

Figure X.16 Scatter plot of the bending moment measured at the depth range of 0.25-0.30 and the soil penetration resistance averaged within the same depth range.. xxxviii

Figure X.17 Scatter plot of the bending moment measured at the depth range of 0.20-0.25 and the soil penetration resistance averaged within the same depth range. xxxix

Figure XI.1 Map of EC readings obtained by the Conductometer operated in dynamic mode (speed 0.05 $m.s^{-1}$) from the trial plot at depth range of 0-0.3 m before (left) and after (right) treatment applying. xl

Figure XI.2 Application map created as “EC30 before treatment application / EC30 after treatment application” (simple ratio). xl

Figure XI.3 Map of EC readings obtained by the Conductometer operated in dynamic mode (speed 0.05 $m.s^{-1}$) from the trial plot at depth range of 0-0.9 m before (left) and after (right) treatment applying. xli

Figure XI.4 Application map created as "EC90 before treatment application / EC90 after treatment application" (simple ratio). xli

Figure XII.1 Positions of the individual measurements obtained by the Conductometer operated in stationary mode: left – original coordinates, right – adjusted coordinates. xlii

Figure XII.2 Positions of the individual measurements obtained by the Conductometer operated in dynamic mode (speed 0.05 $m.s^{-1}$): left – original coordinates, right – adjusted coordinates. xlii

Figure XII.3 Positions of the individual measurements obtained by the Conductometer operated in dynamic mode (speed 1 $m.s^{-1}$): left – original coordinates, right – adjusted coordinates. xliii

List of Tables

Table 4.1 Summary table of the t-tests showing the signification of differences of individual measurements performed within and between tramlines.....45

Table 4.2 Summary table of the t-tests showing the signification of differences of individual measurements performed within the same line in both directions. 48

Table 4.3 Summary table of the t-tests showing the signification of differences of individual measurements performed within trafficked and non-trafficked areas and evaluated within different widths along the tramline axes. 55

Table 4.4Soil moisture by weight. 60

Table 4.5 Soil organic matter content (Loss on ignition). 60

Table 4.6 Electrical conductivity by saturated paste. 61

Table 4.7 Soil pH. 61

Table 4.8 Soil texture. 61

Table 5.1 Summary table of the ANOVA showing the signification of differences of individual measurements performed within different treatments. 84

Table 5.2 Soil moisture by weight. 86

Table 5.3 Soil organic matter content (Loss on ignition). 86

Table 5.4 Electrical conductivity by saturated paste. 87

Table 5.5 Soil pH. 87

Table 5.6 Soil particle size distribution. 87

Table II.1 Descriptive statistics of the EC readings collected at depth range of 0-0.3 m in time of 10 minutes. iii

Table II.2 Descriptive statistics of the EC readings collected at depth range of 0-0.9 m in time of 10 minutes. iii

Table II.3 Descriptive statistics of the EC readings collected at depth range of 0-0.3 m in time of 1 minute. iv

Table II.4 Descriptive statistics of the EC readings collected at depth range of 0-0.9 m in time of 1 minute. iv

Table II.5 Descriptive statistics of the EC readings collected in dynamic mode at depth range of 0-0.3 m characterizing one of the measuring points within randomised design experiment. v

Table II.6 Descriptive statistics of the EC readings collected in dynamic mode at depth range of 0-0.9 m characterizing one of the measuring points within randomised design experiment. v

Table III.1 Weather data for Silsoe area collected by the Met station. vi

Table IV.1 Regression analysis for the EC readings obtained within soil depth range of 0-0.3 m in various depths of discs. vii

Table IV.2 Regression analysis for the EC readings obtained within soil depth range of 0-0.9 m in various depths of discs. vii

Table V.1 t-Test of the EC readings collected at depth range of 0-0.3 m at1st pair of runs. viii

Table V.2 t-Test of the EC readings collected at depth range of 0-0.3 m at 2nd pair of runs. viii

Table V.3 t-Test of the EC readings collected at depth range of 0-0.9 m at 1st pair of runs. viii

Table V.4 t-Test of the EC readings collected at depth range of 0-0.9 m at 2nd pair of runs. ix

Table V.5 t-Test of the differences between shallow and deep EC (EC30-EC90) readings collected at 1st pair of runs. ix

Table V.6 t-Test of the differences between shallow and deep EC (EC30-EC90) readings collected at 2nd pair of runs.....ix

Table V.7 t-Test of the EC readings collected at depth range of 0-1.5 m at 1st pair of runs.....x

Table V.8 t-Test of the EC readings collected at depth range of 0-1.5 m at 2nd pair of runs.....x

Table VI.1 t-Test of the EC readings collected at depth range of 0-0.3 m. xi

Table VI.2 t-Test of the EC readings collected at depth range of 0-0.9 m. xi

Table VI.3 t-Test of the EC readings collected at depth range of 0-1.5 m. xi

Table VII.1 t-Test of the EC readings collected at depth range of 0-0.3 m within the 6 m wide strip along the tramline axes. xii

Table VII.2 t-Test of the EC readings collected at depth range of 0-0.3 m within the 4 m wide strip along the tramline axes. xii

Table VII.3 t-Test of the EC readings collected at depth range of 0-0.3 m within the 3 m wide strip along the tramline axes. xii

Table VII.4 t-Test of the EC readings collected at depth range of 0-0.3 m within the 2.2 m wide tramlines..... xiii

Table VII.5 t-Test of the EC readings collected at depth range of 0-0.9 m within the 6 m wide strip along the tramline axes. xiii

Table VII.6 t-Test of the EC readings collected at depth range of 0-0.9 m within the 4 m wide strip along the tramline axes. xiii

Table VII.7 t-Test of the EC readings collected at depth range of 0-0.9 m within the 3 m wide strip along the tramline axes. xiv

Table VII.8 t-Test of the EC readings collected at depth range of 0-0.9 m within the 2.2 m wide tramlines. xiv

Table VII.9 t-Test of the EC readings collected at depth range of 0-1.5 m within the 6 m wide strip along the tramline axes. xiv

Table VII.10 t-Test of the EC readings collected at depth range of 0-1.5 m within the 4 m wide strip along the tramline axes. xv

Table VII.11 t-Test of the EC readings collected at depth range of 0-1.5 m within the 3 m wide strip along the tramline axes. xv

Table VII.12 t-Test of the EC readings collected at depth range of 0-1.5 m within the 2.2 m wide tramlines. xv

Acknowledgements

My first and foremost thanks go to God who has granted me the opportunity to spend a year of my study here in Cranfield University and especially on Silsoe Campus.

I would like to express my deeply gratefulness to my Cranfield supervisor Dr. Toby W Waine and co-supervisor Prof. Richard J Godwin for their valuable advice, suggestions, encouragements and patience towards me. I also thank Dr. Thomas Mayer, the subject adviser in my thesis committee. Thanks to my Slovak supervisor Doc. Ing. Jan Piszczalka, PhD. for his support during realisation of this project.

My thanks goes also to my colleague and friend Ing. Jana Havránková, PhD. who opened the gate of the cooperation between Slovak University of Agriculture (SUA) in Nitra, Slovakia and Cranfield University. I would like to express my gratitude to Prof. Ing. Ladislav Nozdrovický, PhD., the head of Department of Machines and Production Systems at SUA in Nitra, for lending of the Conductometer which was used in this study. I thank to Mr Václav Prošek and Ing. Miroslav Mimra, Ph.D. from Czech University of Life Sciences at Prague, Czech Republic for their valuable advices and support with adjusting of the Conductometer. My great thanks go to Mr Robert J Walker and Mr Peter Grundon for their help with all technical equipment and the realization of my field experiments. I thank to Mrs Maria Biskupska and Mr Richard Andrews for their advices and help with my laboratory analyses. My great thanks go to Ms Liz Farmer, Mrs Pat Bellamy and Mr Charles Marshall for their help with evaluation of my data. Thanks to my friends Petr Vozka for his help with my soil samples and Cephas Kwaku Bosrotsi for his language corrections.. I would like to express many thanks to Dr Kim Blackburn, Mrs Sandra Richardson and all my colleagues and friends from both National Soil Resources Institute at Silsoe and also Department of Machines and Production Systems at SUA in Nitra for their help and support. I thank the Slovak Academic Information Agency (SAIA) for their financial support.

My special and heartfelt thanks go to my family and friends from home for keeping in touch, their help, encouragement and support.

List of Abbreviations

a	Spacing of Disc Electrodes	m
b	Depth of electrode insertion	m
BM	Bending Moment	N.m
C	Mass of pipetted fraction <0.002 mm (clay)	g
D	Dispersant Factor	
d	Oven-dry mass of sodium hexametaphosphate dispersing solution	g
EC	Electrical Conductivity	$S.m^{-1}$
EC150	Electrical Conductivity Measured at depth range of 0-1.5m	$S.m^{-1}$
EC30	Electrical Conductivity Measured at depth range of 0-0.3m	$S.m^{-1}$
EC75	Electrical Conductivity Measured at depth range of 0-0.75m	$S.m^{-1}$
EC90	Electrical Conductivity Measured at depth range of 0-0.9m	$S.m^{-1}$
EC_a	Apparent Soil Electrical Conductivity	$S.m^{-1}$
EM38	Contact-less instrument aimed at soil EC measurement	
EMI	Electromagnetic Induction	
F	Factor	
HR	EC reading obtained by *EM38* operated in horizontal mode	$S.m^{-1}$
I	Electrical Current	A
LOI	Loss on ignition	
LSD	Least Significant Difference	

m_0	Mass of the empty silica dish	g
m_1	Mass of the silica dish and dehydrated soil	g
m_2	Mass of the silica dish and soil after ignition	g
PR	Penetration Resistance	MPa
PR30	Penetration Resistance Averaged at depth range of 0-0.3m	MPa
PR50	Penetration Resistance Averaged at depth range of 0-0.5m	MPa
R	Resistance	Ω
RBD	Randomized block design	
S	Total mass of sand	g
SCS	Soil Compaction Sensor	
V	Electrical Potential	V
VR	EC reading obtained by *EM38* operated in vertical mode	$S.m^{-1}$
Z	Mass of pipetted fraction 0.002 mm – 0.063 mm (silt and clay)	g
γ	Electrical Conductivity	$S.m^{-1}$
π	Pi (~3.14)	
ρ	Electrical Resistivity	Ω.m

1 Introduction

1.1 Background

Soil as a crucial resource for life on our planet is endangered by various degradation processes. One of these processes is the soil compaction that occurs within the topsoil or subsoil layers. Compaction restricts and interferes root growth, reduces the amount and size of soil pores, decreases soil infiltration, causes water-logging and lead to run-off (Brady and Weil, 1999). The seriousness of the problems caused by the soil compaction is highlighted by the directive issued by the Commission of the European Communities (2006).

Conventional methods for soil compaction mapping use devices that sense the soil either vertically or horizontally. The vertical sensors (e.g. penetrometer) work as stop-and-go and provide point measurements. Although they provide accurate characteristics of soil strength acting against plant roots growth in measured profile, the process is often slow and time consuming. The methods utilising the horizontal sensing reflect the soil strength, often in different soil depths, and acting against the implement used for soil reclamation. These sensors work as on-the-go and provide continuous readings. Their disadvantages are the higher energetic requirements and the risk of excessive wearing of sensing tine and all working parts which is caused by the friction between the soil particles and the tool. Many researchers (Jabro et al, 2005; Smith, 2001; Rhoades et al.; 1999; McNeill, 1980) observed dependency between soil bulk density and soil electrical conductivity. Measuring of the soil electrical conductivity is a very practical, simply, cheap and energy efficient tool for within-field variability mapping. The patterns of soil electrical conductivity maps frequently achieve a high degree of correlation with such important parameters as the yield of grain, the soil texture, the soil compaction, or the moisture content.

Previous work conducted by myself at the Slovak University of Agriculture in Nitra, Slovakia used the direct contact method of soil electrical conductivity surveying for within-field variability mapping. This compared the obtained patterns with soil texture, moisture, soil penetration resistance readings, and with a yield. This identified

the need for further investigation and to focus on soil property variability. Using both direct contact and contact-less soil electrical conductivity sensing methods in conjunction with the cone penetrometer and horizontal soil compaction sensor could be used to verify the abilities of mentioned sensors to determine and localise the areas with different soil bulk density.

1.2 Aim

Detection of the within-field variability of soil compaction using soil electrical conductivity (and other soil properties) for improved soil management.

1.3 Objectives

1. To develop a methodology to identify within-field variability of soil compaction using two different electrical conductivity sensors compared with a soil compaction sensor.

2. To create maps of the within-field variability of soil compaction.

3. To suggest improved soil management strategies that could result.

1.4 Outline methodology

It was intended to find out if the soil electrical conductivity (EC) is a suitable tool for identifying the areas with different levels of soil bulk density. The chosen experimental field was surveyed by both contact (Conductometer) and contact-less (*EM38*) method of measuring of soil EC. The obtained EC readings were displayed in GIS software and the obtained patterns were compared with the tramline locations. Subsequently the randomized block design experiment with different depths of soil compaction layer presence was conducted. Such a trial plot was surveyed with both mentioned EC instruments and the readings obtained were compared with the readings collected by the cone penetrometer and soil compaction sensor. The data was evaluated by statistical methods, displayed as spatial variability maps and some soil management strategies were suggested.

2 Literature review

2.1 Soil and soil degradation

Soil as one of most crucial factors for life on Earth as described by the work of Brady and Weil (1999) by the major functions that it fills:

1. Soil is a medium for plant roots and by its properties it often determines the type of the present vegetation.
2. Soil properties determine the soil water quality and water losses, utilization, contamination, and purification.
3. Soil as a recycling system is an environment for decomposition of waste and dead bodies of plants, animals and people as well.
4. Soil is the environment for organism living.
5. Soil also presents the important building material and the foundation for various structures in civil engineering.

For the farmers, the soil is considered the medium and environment for plant roots. Soil is an environment consisting of soil particles and pores filled by water and air. The soil nutrients, water and air have to be in suitable form and amount as well as all other properties (soil temperature, soil mechanical properties) (Allmaras et al, 1973).

2.1.1 Effects of soil compaction on plants and soils

As one of the most serious soil degradation processes identified by Brady and Weil (1999) is soil compaction. Duiker (2004) elaborated a study about effects of soil compaction. He shows that soil compaction due to field traffic can cause yield losses from 1 to 37 percent. The most direct consequence of soil compaction is increased soil bulk density. For each soil type there is a specific range of optimal bulk densities, exceeding these can restrict the root growth. It is important to emphasize that the soil bulk density in no-till soils could reach the higher values than in cultivated soils. Even though, the soil structure can be more favourable due to higher organic matter content and higher soil biological activities within the subsurface layer.

Soil structure is mostly degraded as a result of soil compaction. Soil compaction causes the reduction of gaseous exchange and reduction of water and nutrients (e.g. nitrogen, phosphorus and potassium) that plants are able to uptake. Soil macropores are crushed, micropores are created, and as soil particles are closer together, the soil strength increases. Finally if the soil penetration resistance is higher than 2 MPa (Taylor, Roberson and Parker, 1966), this may lead to restriction of roots penetration and growth. The smaller portion of soil macropores causes the decreasing of soil aeration when the soil is near the field capacity. Increasing proportion of soil micropores decreases the available soil water content for plants. The soil infiltration and percolation are slower which results in the soil being water-logged after substantial rainfalls and finally into soil erosion (Brady and Weil, 1999; Duiker, 2004).

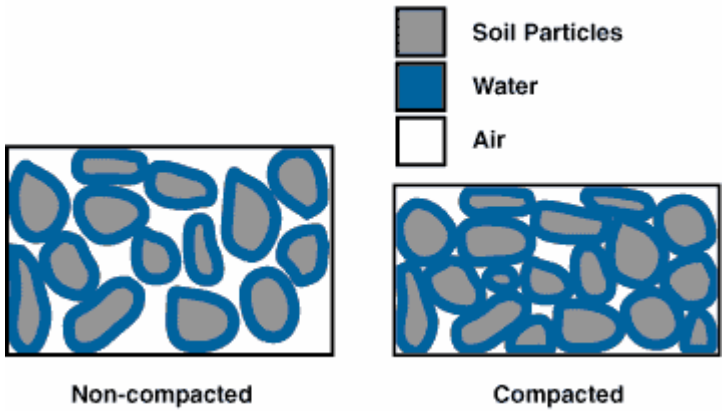

Figure 2.1 Effect of soil compaction on soil pores' orientation and spacing (University of Minnesota, 2001).

2.1.2 Principles of soil compaction formation

Various activities in human society are the major causes of soil compaction. This are either caused deliberately or as a by-product (Coder, 2000). For every soil type there is certain soil moisture content whereat the soil can be compacted by minimal effort. According to the author the soil compaction could occur as an effect of following:

- static or dynamic impacts of humans, animals or traffic,
- soil handling,

- vibrations and explosions, as an intentional and systematic soil compaction under buildings and infrastructure,
- water drops that induce soil crusting and surface compaction.

The loss of an organic matter which serves as food for soil fauna that naturally aerates the soil, leads to soil compaction as well.

Methods for alleviation of soil compaction

The natural conditions as soil texture, the size, shape and properties (e.g. porosity) of soil particles have the most distinguished effect on soil compaction. Jones et al. (2003) created the map of an inherent susceptibility of the European soils to be compacted (Figure 2.2).

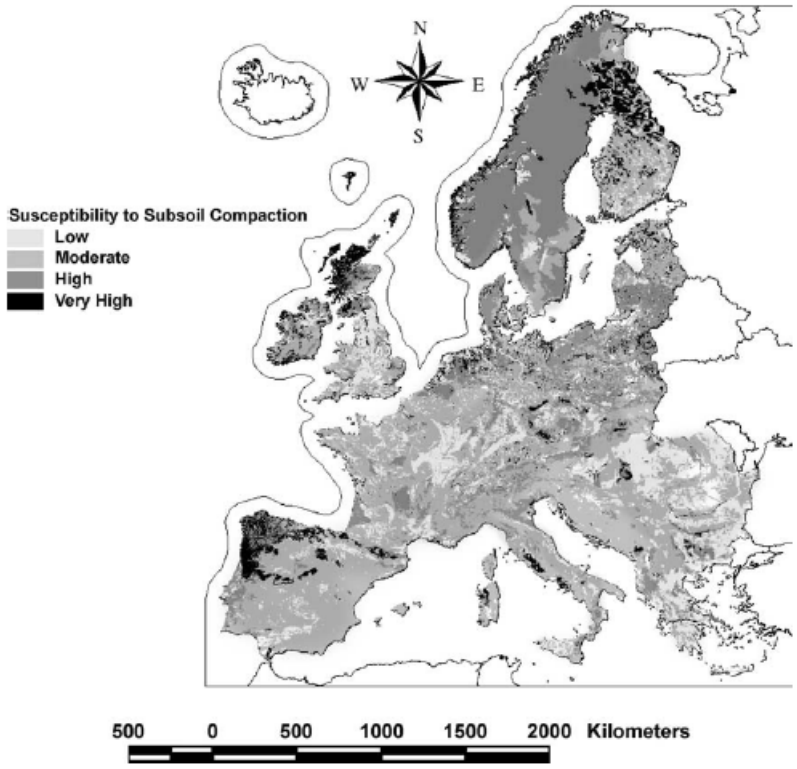

Figure 2.2 Map of inherent susceptibility of European soils to compaction (Jones, et al, 2003).

The controlling of soil compaction is most often possible only using appropriate technology, machines, loads, tyres, and tyre inflation pressures (Sharifi et al., 2007). Duiker (2004) specifies the arrangements to avoid soil compaction as follows:

a) Avoiding trafficking when the soil is plastic and in excessive soil moisture content.
b) Author recommends keeping axle loads below 10 tons or even below 6 tons because it is the axle load that causes the most hazardous subsoil compaction.
c) Decreasing the contact pressure between soil and tyre which is possible to reach by using low inflation pressures, flotation tyres, doubles or using track machinery. Compaction of topsoil is influenced just by contact pressure and the author suggests keeping high inflation pressure tyres (e.g. truck tyres at 700 kPa), out of the field.
d) Minimization of trafficked area by enlarging both the working width and the tread width or decreasing the number of passes. The method of using permanent traffic lanes seems to be a perspective one. Its biggest disadvantage is a need to adjust the track of all vehicles to the same width.
e) Increasing of the soil organic matter content and the number of soil animals. This is possible to achieve by returning the crop residuals such as straw back to the soil, growing cover crops, and by applying compost and manure. To avoid unfavourable losses of organic matter is possible to apply soil protection from erosion and no-till management.
f) Restriction of tillage. The author recommends tillage only in inevitable cases. It is to be recommended to till the soil without inversion while the depth of tillage should be 2 – 5 cm deeper than the depth of hard pan. If hard pan is not present, deep tillage is not necessary.

2.2 Methods of detection of soil compaction within-field variability

The soil compaction or soil strength can be measured by various soil sensors that can be basically classified into one of three groups as:

- those that penetrate the soil in a vertical direction,
- sensors penetrating the soil in horizontal direction,
- and non-contact sensors that use the indirect methods of sensing.

2.2.1 Vertical measurement systems

Cone penetrometer

Cone penetrometer is a simple tool aimed at measuring the soil penetration resistance. Soil moisture content, soil bulk density, soil porosity, and soil firmness are the main soil factors affecting the value of the soil penetration resistance. The diameter of the base, top angle, and the surface coarseness of the cone as the parameters of the penetrometer, affects the value of the soil penetration resistance as well (Bajla, 1998). Over the years various penetrometers were developed. For the ability of comparison the obtained readings the dimensions of cone penetrometer were united and defined by ASAE Standard 313.3 (ASABE, 2004) (Figure 2.3).

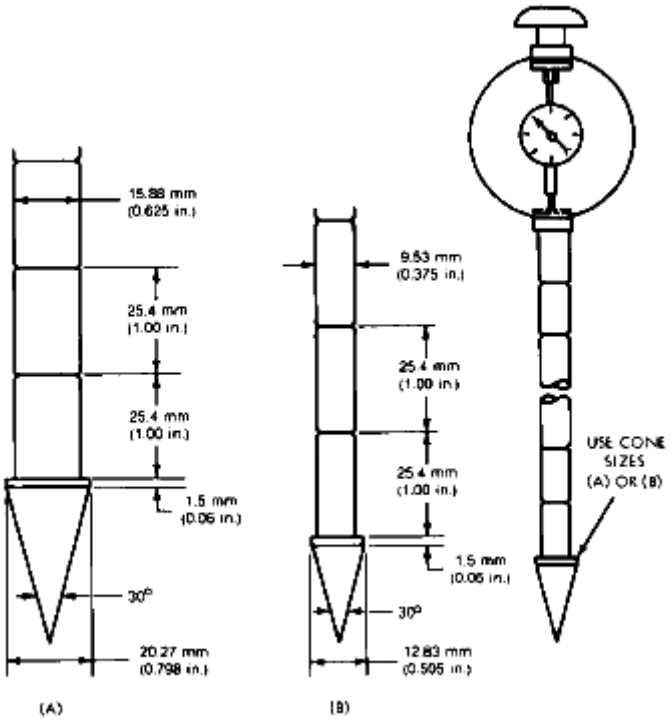

Figure 2.3 Soil cone penetrometer (after ASABE, 2004).

However the different constructions of the penetrometers exist as well. For example, *Veris*® developed an automated *Profiler 3000* which uses a different geometry of a cone, operates in a higher insertion speed. It measures the soil resistance and soil electrical conductivity as well (Sudduth et al., 2004) (Figure 2.4).

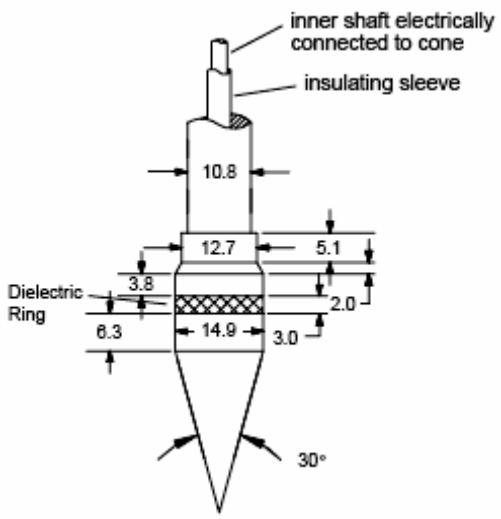

Figure 2.4 The geometry of the cone of *Veris® Profiler 3000* (after Sudduth et al., 2004).

The measurement of soil resistance using the cone penetrometer provides a curve of the soil resistance in whole sensed profile. Even though, the accuracy of this tool is high in a vertical direction, it demands many discrete locations within the field to obtain a sufficient spatial resolution. As a result of above, its usage for a field survey is very time consuming and laborious.

2.2.2 Horizontal measurement systems

Mechanical sensors

An on-the-go soil strength measurement system was developed by Hall and Rapper (2005). The shank of the sensor was equipped by a sensing tip and a force transducer. The researchers tested several different tips. They found out that the readings obtained by this sensor are less influenced by soil moisture than the readings obtained by a cone penetrometer. Therefore there was stronger correlation found with soil bulk density than with soil penetration resistance.

Chung et al. (2006) developed a soil strength profile sensor. This sensor works like a horizontal penetrometer which is able to sense the soil strength in several depths. The body of the profile sensor is created by the metal plate. The soil strength is transmitted by the prismatic tips and it's sensed by load cells.

Similar construction of soil sensor was used by Chukwu and Bowers, Jr. (2005). They tested their sensor equipped by three sensing tips and load cells under soil bin conditions. It allowed sensing soil strength in three different depths of 178, 279, and 381 mm.

Very simple instrument was presented at the work of Adamchuk and Jasa (2002). The working part of the sensor was created by the cutting blade which was basically a beam stressed by the soil strength. The bending moment introduced by the soil strength was sensed by the strain gauges attached on the leg of the sensor (Figure 2.5).

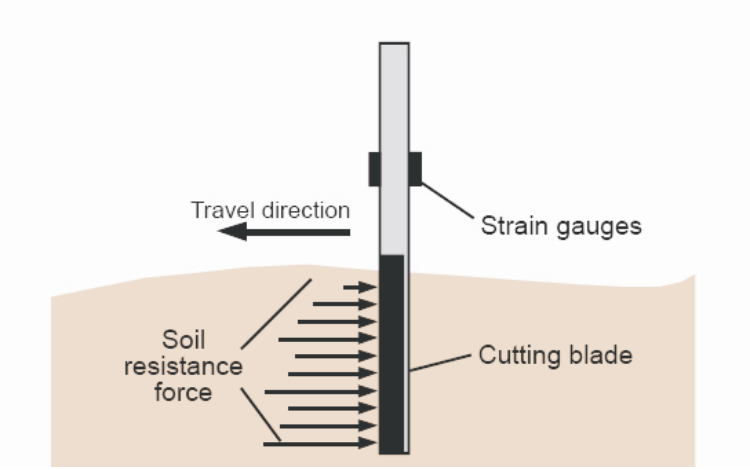

Figure 2.5 Schematic of a soil mechanical resistance measurement device (Adamchuk and Jasa, 2002).

Soil compaction profile sensor of different construction was developed by Sharifi (Sharifi, 2004; Sharifi et al., 2007). The sensor consists of a leg and several instrumented flaps attached with the strain gauges. The soil strength acting on the flaps evokes the bending moment which is sensed by strain gauges and logged by a laptop.

The mechanical on-the-go sensors remove the disadvantage of the cone penetrometers and offer higher spatial resolution. On the other hand they have lower vertical resolution and the friction between the tool and the soil particles causes the wearing of the sensor.

Acoustic sensors

These sensors use to sense the soil texture, basically on the change of the acoustic signal due to soil particles and/or soil compaction. Tekeste et al. (2002) constructed an on-the-go soil sensor aimed at detection of plough pan. The sensing tip of the sensor was equipped with a microphone which sensed the sound caused by drawing the tool through the soil environment. However this method is unable to sense the multiple depth and it is unserviceable because of a low signal-to-noise ratio.

Figure 2.6 Acoustic plow pan detection sensor (Tekeste et al, 2002).

2.2.3 Non-contact sensors

Optical sensors

This type of sensors usually utilizes near-infrared, mid-infrared or polarized light spectrum. They work on the similar principles as a remote sensing (most often realised on the satellite or aeroplane platform) (Adamchuk and Jasa, 2002).

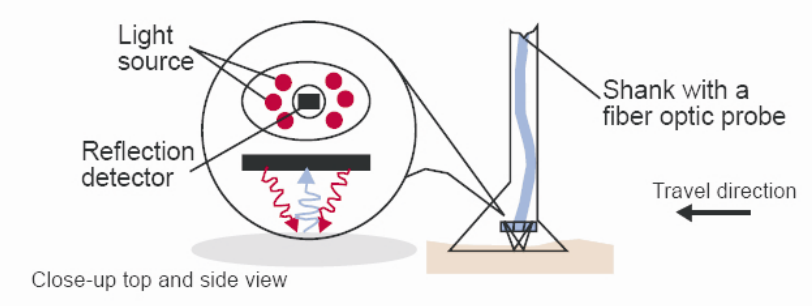

Figure 2.7 Schematic of a subsurface soil reflectance optical sensor (after Adamchuk and Jasa, 2002).

Ground penetrating radar

Instead of optical sensors some researchers use the ground-penetrating radar (Figure 2.8). It transmits the ultra high frequency radio waves (microwave electromagnetic energy) into soil and measures the wave reflections (GeoModel, 2007). Any changes in these reflections can mean the change of soil density or the presence of hardpan.

Figure 2.8 Ground penetrating radar (after GeoModel, 2007).

Soil electrical conductivity sensors

The patterns of soil electrical conductivity often show the within-field variability of soil properties. Many researchers (Jabro et al, 2005; Smith, 2001; Rhoades et al.; 1999; McNeill, 1980) observed similarities between soil bulk density (or soil compaction) and soil electrical conductivity. Because of the many advantages of this method, it is discussed in more details in following chapters.

2.3 Measuring of soil electrical conductivity

2.3.1 Definition

The ability of a material to conduct electrical current is referred to as electrical conductivity. (It is reciprocal of electrical resistivity, sometimes called specific electrical resistance). The basic unit of electrical conductivity is siemens per meter (Oxford reference, 1992).

2.3.2 Theory of conducting electrical current in the soil

There are three different environments presented in soil matter – solid soil particles and soil pores that can be filled both by liquid of soil water often with dissolved salts and also by air (Corwin and Lesch, 2005a; McNeill, 1980). Each of these mediums has different electrical conductivity. Soil particles have very low value of electrical conductivity which can be increased by higher clay content. The higher content of soil pores that can be filled by soil water also increase the electrical conductivity, especially in saturated conditions and when the water contains dissolved salts. Because the air is an extremely good insulator, there are only three possible pathways for electrical current to flow: via (1) solid-liquid (soil particles and pores fill with soil water), via (2) liquid (soil water), and (3) straight through soil particles (Figure 2.9).

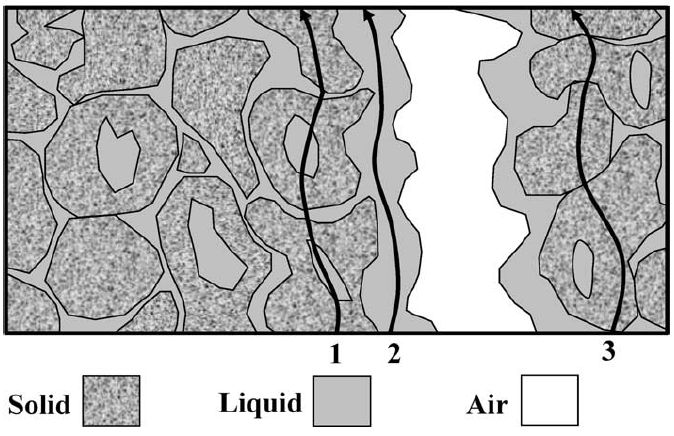

Figure 2.9 Three different pathways of electrical conductance in soil (Corwin and Lesch, 2005a).

2.3.3 Factors that affect soil EC

McNeill (1980) specifies factors that affect soil EC reading as follow:

Soil pore connection – Soils with high ratio of soil pores filled by water better conduct the electrical current. Clayey soils contain huge amount of small pores that increase their electrical conductivity in comparison with sand soils that usually acquire smaller values of electrical conductivity. Despite of mentioned above the soil compaction causes the increasing of soil conductivity values.

Soil moisture – Soil water content positively affected the values of soil electrical conductivity, because it presents the base for electrolyte which creates by dissolving soil salts.

Content of salts – Higher concentration of soil salts increases the consistency of electrolyte in soil matter. Although the salt content has a slight affect on the electrical conductance, there can be specific zones within the field that are significantly affected by soil salts (Hindický, 2007).

Cation exchange capacity – The presence of positive charged ions (Ca, Mg, K, Na, NH4 or H) in water solution presented in soil matter also causes the increasing of electrical conductivity. Principle is similar to soil salts above.

Sensing depth – The strength of sensor signal (for both direct contact and EMI method) becomes weak with higher depth. This means that upper soil layers can be mapped more precisely than deeper soil layers.

Temperature – Decreasing soil temperature causes very slightly decrease of soil EC values. The significant change happens when the soil temperature decrease under the zero point. Then the water in soil pores freezes, soil pores become more insulated each from other and soil EC values decrease significantly. Temperature of the air can markedly affect soil EC readings as well. Waine (1999) developed an equation for normalization EC values collected by EMI.

Veris Technologies (2003) claim that the value and spatial variability of electrical conductivity within specific field is affected mostly by one or two major factors that can be different from field to field. This implies then the interpretation of soil electrical conductivity readings is highly local specific.

In most of fields the soil EC values are mostly affected by clay content. Sudduth et al (2001) say that soil electrical conductivity maps primarily affected by soil texture are not change over time. However the soil EC maps affected by soil salts primarily display significant differences within the year because they reflect the mobility of some salts in the soil matter. Using some agricultural practices the fields with texture base EC may rarely change onto fields with salt base EC.

2.3.4 Devices and methods for soil EC measurements

Basically three different types of soil electrical conductivity sensing exist – electromagnetic induction (EMI), methods utilising the direct contact with the soil, and the time domain reflectometry (TDR). Mostly two of them (EMI and the method of direct contact) are used for surveying of within field variability. Although the TDR allows measuring both soil electrical conductivity and soil moisture in real time, this method is not suitable for field survey because it is not sufficiently simple, accurate, robust and fast (Rhoades et al, 1999).

Adamchuk and Jasa (2002) write that using electromagnetic sensors the soil matter becomes a part of electrical circuit and local change of soil properties immediately affects the readings recorded by data logger (Srinivasan, 2006). They name following three sensors:

- *Veris® 3100* (Veris Technologies, Salina, Kansas) which allows to measure electrical conductivity. The Conductometer used in this study is based on the *Veris® 3100* sensor and uses equivalent electrode spacing.
- *EM38* (Geonics Limited, Mississauga, Ontario, Canada) which measures the transient electromagnetic response.

- *Soil Doctor® System* (Crop Technology, Inc., Bandera, Texas) which uses the electrical response directly for optimisation of application rates.

The EMI (e.g. *EM38*) works on the principle of introducing electrical energy into the soil matter using the current source which is created by transmission coil. This source moves over soil surface and it must not be in physical contact with the soil. The current source transmits the electromagnetic array, it penetrates the soil and the response (the strength of reflected signal) is measured by sensor, which is created by receiver coil (Figure 2.10).

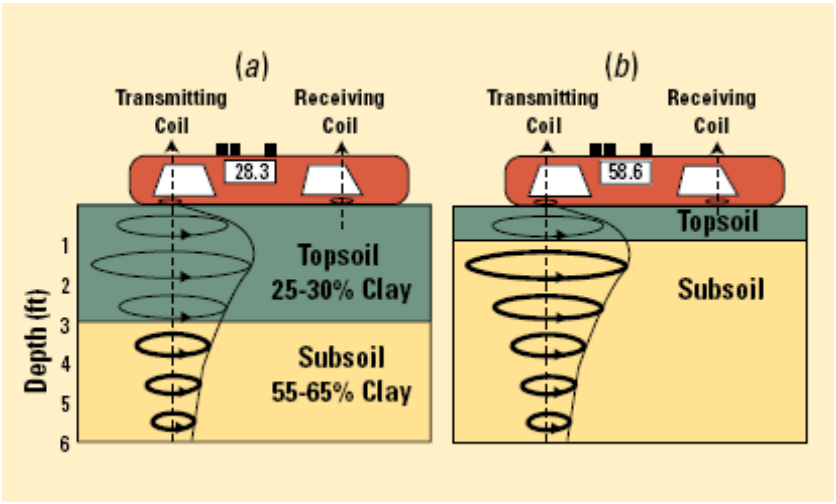

Figure 2.10 Contours of electromagnetic array created by EMI (Davis et al, 1997).

The direct contact method (also known as the electrical resistance method) is based on creating of an electrical circuit which introduces the electrical current into the soil through two single disc electrodes (Figure 2.11). Drop of potential, which is caused by a soil electrical resistance, is sensed by the other pair or by other two pairs (*Veris® 3100*) of disc electrodes. The disc electrodes penetrate the soil only within few centimeters (see Figure 2.12) (Veris Technologies, 2003). Tine electrodes were used by Rhoades (1992, 1993) on the prototype machine (Figure 2.13). Later the disc electrodes start to be mounted for commercial equipment by *Veris®* and *Soil Doctor®*. The difference between these two systems is in different wiring (Figure 2.11).

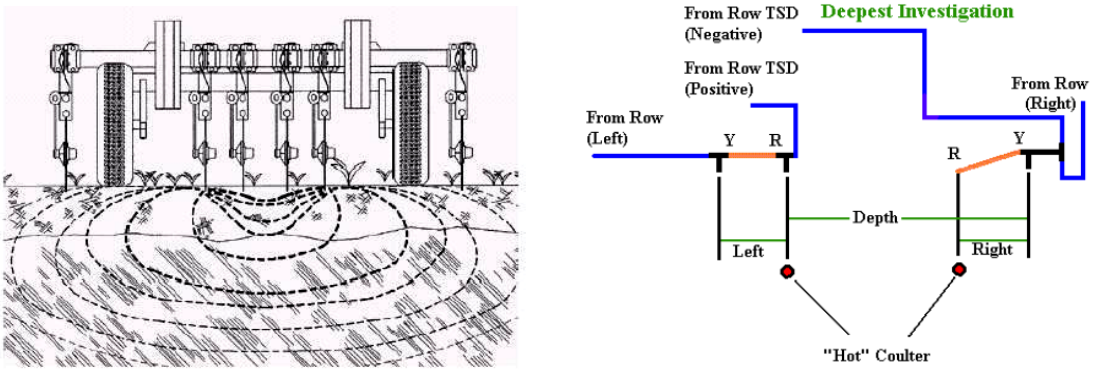

A **B**

Figure 2.11 A – Contours of an electric array created by *Veris® 3100* (Veris Technologies, 2003); and B – Wiring scheme of Soil Doctor® equipment (Crop Technology).

A **B**

Figure 2.12 A – *Veris® 3100* (Veris Technologies, 2003); and B – Soil Doctor® (Crop Technology).

Figure 2.13 Soil electrical resistance equipment developed by Rhoades (1992, 1993).

2.3.5 Depth of sensing

Electrical conductivity is measured in two depth intervals using the direct contact – shallow electrical conductivity 0 – 0.3 m and deep electrical conductivity 0 – 0.9 m.

The range of depth intervals depends on the spacing of individual disc electrodes on the frame of the sensor (Veris Technologies, 2003). Milsom (2003) describes several possible arrangements of electrodes on the frame. *Veris® 3100* uses so called Wenner array for which the spacing between electrodes is identical (see Figure 2.14 and Equation 1).

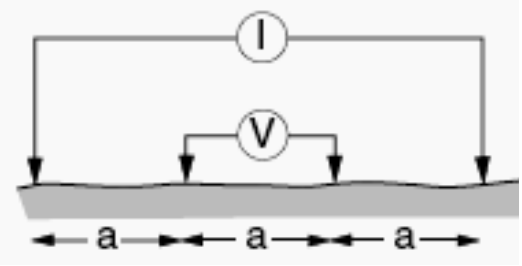

Figure 2.14 Spacing of sensing electrodes for a Wenner array (after Milsom, 2003).

$$\gamma = \frac{1}{\rho} = \frac{I}{2\pi a V}$$ **Equation 1**

where: γ – electrical conductivity ($S.m^{-1}$),

ρ – electrical resistivity (Ω.m),

π – Pi (~3.14),

a – spacing of disc electrodes (m),

V – electrical potential (V).

The depth of sensing is equal to a half of the spacing between outer electrodes for a device uses four electrodes. As the *Veris® 3100* uses six electrodes, it works like two independent sensors where the one of them senses the soil depth of upper 0.3 m and the second one of 0.9 m. Wenner (1916) found out that the depth of electrode insertion into the soil affects the EC readings and he developed the equation (Equation 2) to define this relationship for a Wenner array:

$$EC_a = \frac{\left(1 + \frac{2}{\sqrt{1+4\left(\frac{b}{a}\right)^2}} - \frac{1}{\sqrt{1+\left(\frac{b}{a}\right)^2}} \right)}{4\pi a R}$$

Equation 2

where: EC_a - Apparent Soil Electrical Conductivity ($S.m^{-1}$),

a - spacing of disc electrodes (m),

b – depth of electrode insertion (m),

π – Pi (~3.14),

R – resistance (Ω).

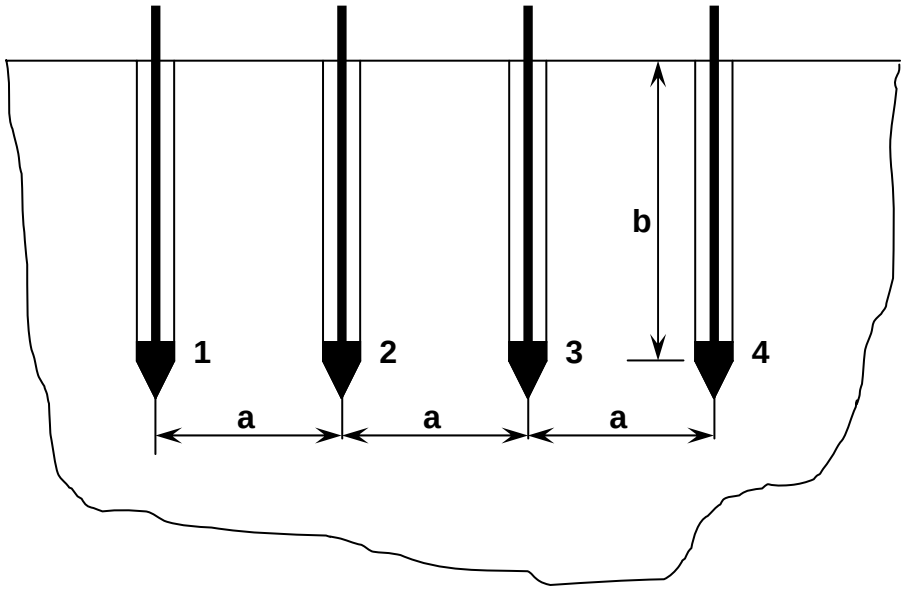

Figure 2.15 Wenner's diagram showing four electrodes in the soil during soil EC measurement (after Wenner, 1916).

Depth of the soil sensing using EMI depends on setting of the measuring mode (vertical or horizontal), the height of the sensor over soil surface and on the spacing of transmitter and receiver coil (Johnson et al, 2003). Most of non-contact sensors of soil electrical conductivity sense the top soil layer at thickness of 1 or 1.5 m. In the case of geological research the depth of measurement can be several tens of meters.

Sudduth et al (1998) and Doolittle et al (2002) say that there are very similar results and comparable gross spatial patterns obtained by both sensors – *EM38* and *Veris® 3100*. Although they found out a significant correlation between all measured data sets, there were significantly important lower mean values found for *Veris® 3100* Shallow in comparison with *Veris® 3100* Deep and *EM38*. The graph of relative responses of both *EM38* and *Veris® 3100* sensors is shown on Figure 2.16.

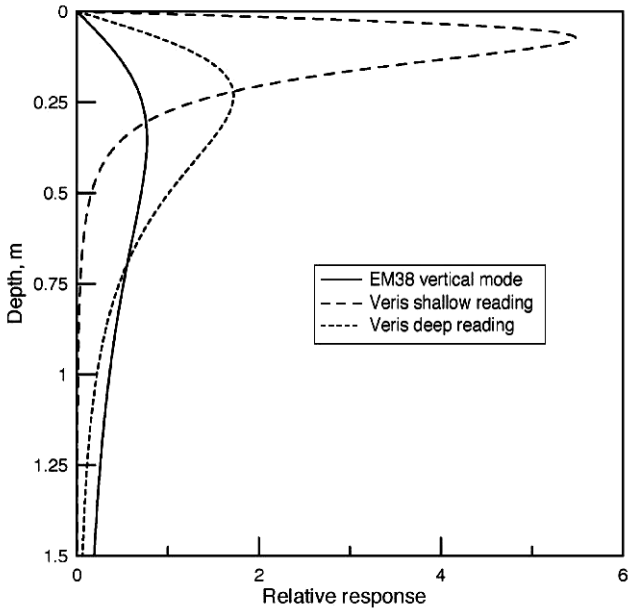

Figure 2.16 Relative response of both *EM38* and *Veris® 3100* (Shallow and Deep) sensors in dependence on soil depth (Sudduth et al., 2005).

2.3.6 Relations between EC and other soil properties

McNeill (1992) and Rhoades et al (1999) specified that apparent soil electrical conductivity (EC_a) sensed by soil sensors can provide useful information about important soil physical and chemical properties. They named soil water content, clay content, clay mineralogy, soil salinity, soil pore size and distribution, and cation exchange capacity (CEC). These are the main factors that affect soil apparent electrical conductivity. Depending on location and specific properties of particular fields the soil EC_a values can be most affected by salt content in saline soils (Williams and Baker, 1982) or by soil texture, water content, and CEC in non-saline soils (Rhoades et al, 1976).

Considering electrical conductivity (EC), Rhoades et al. (1999) say that beside salinity also soil bulk density, density of soil particles, clay content and distribution of soil pores are said to be among the most important properties affecting the soil electrical conductivity readings. They found out some periodicity in higher EC readings collected across the furrows. They reported that this can be caused by a higher compaction in the furrows that were trafficked by the tractor wheels. A similar phenomenon was observed by Corwin and Lesch (2005b). On the contrary Rhoades et al. (1999) found out lower EC values for chisel tilled soils. That can be caused both by creating of trenches (approximately 25 mm wide) and their filling by dry soil particles. Smith (2001) successfully used EMI for mapping of soil compaction caused by field traffic. Clark et al. (2000) in their study compared the hard pan depth sensed by a penetrometer with soil electrical conductivity readings. These authors identify the high spatial variability of soil compaction (e.g. trafficked tramlines) which necessitate the high density of a measurement and collected data. An opportunity of using soil electrical conductivity for soil compaction sensing is described also at work of Samouëlian et al. (2003) who used it for detecting of soil cracking under laboratory conditions.

The *EM38* soil electrical conductivity sensor was successfully used by Waine (1999), Pires (2004), James et al. (2000) and Wolharn (2001) who examined the affect of air temperature, soil salinity, moisture and texture on soil electrical conductivity readings. Obtained electrical conductivity maps are used for redefining soil type boundaries, available water content assessment and yield prediction (Waine, 1999). Wolharn (2001) dealt with factors that affect EMI readings, he compared the EMI maps with the maps of yields and finally he used the soil electrical conductivity maps for targeted soil surveying and pits' locations.

Malo et al (2001a, 2001b) found significantly important positively correlation between soil electrical conductivity sensors (*Veris*® and *EM38*) values and soil moisture (weight and volume). They found correlation between soil electrical conductivity readings collected by *Veris*® *3100* Deep and *EM38* and the average soil bulk density in up 0.3 m. These researchers tried to draw up several models and develop several equations to predict some of soil properties. They found that on the

base of soil EC data they are able to predict soil moisture within 3 % and 4 % for moisture by weight and volume respectively. If they included other soil parameters into the model the soil moisture prediction improved into 2 % for both by weight and volume.

Corwin and Lesch (2005a) provide overall list of researches dealing with soil electrical conductivity used for mapping, modelling or just comparing with other soil properties.

2.3.7 Using EC measurements in different industries

The company OKM Ortungstechnik GmbH. produces several sensors working on the principle of electrical conductivity (EMI). These sensors are used in engineering geology and archeological investigation for exploration of groundwater sources, caverns, voids, caves, fractured zones, and for finding various metallic objects (OKM Ortungstechnik GmbH.).

The same principle of work is used in army metal detectors for searching of weapons and ammunition (Global Security).

Figure 2.17 Metal detector (GeoModel, 2007).

Ground penetrating radars (GPR) that provide the graphic image of the subsurface also work on the principle of EMI (Davis and Annan, 1989). GPR generates electromagnetic signals and detects the electromagnetic field interactions with the surrounding materials.

Sensors working on the principle of measuring of electrical conductivity are also used for measuring of various materials' moisture (Thomson and Ross, 1996) and water quality (Flores and Navar, 2002).

Electrical conductivity is also utilized in medicine. The electrical current injects the human body and the voltage is measured via attached electrodes (direct contact) or contactless measurements on the base of electromagnetic induction are used (Gencer and Tek, 1999). Such functions of a human body as a respiration rate, blood pressure, heart rate or skin conductance are controlled unwillingly and depend on an actual stress. So they are used as a base factors monitored by a polygraph or a lie detector (Committee to Review the Scientific Evidence on the Polygraph, Division of Behavioral and Social Sciences and Education, National Research Council, 2002).

2.4 Chapter summary

Agricultural soils are often endangered by degradation processes. Many of them are caused by soil compaction which restricts, interferes and even impede root growth and development. It also decreases the amount of soil pores and reduces the soil infiltration which may cause a water-logging.

The soil texture containing the fine soil particles and higher portion of the soil micropores is assumed to be compacted more easily. Thus the clayey soils can be compacted more easily than sandy soils. On the other hand while the clayey soils have a natural ability to partially alleviate the soil compaction, the sandy soils do not (Mašek, 2005). The techniques for compaction controlling include the using of appropriate technology, machines, lower load on the axles, wider tyres and lower inflation pressures (Sharifi et al., 2007).

There are two basic methods for direct soil compaction mapping. One of them is measuring of soil penetration resistance using soil penetrometers that penetrate the soil vertically. These allow following the progress of soil vertical strength. Their disadvantages are the necessity of numerous point measurements and high time and labour costs. Other types of sensors sense the horizontal soil strength. Such devices allow soil strength sensing continuously, often in several depths but the shank and

sensing units of the sensor are often exposed to excessive wearing caused by the friction between the soil particles and a tool.

Alternatively, there are also non-direct methods of sensing within-field variability. The soil electrical conductivity (both by direct contact e.g. disc coulter electrical conductivity sensor; and by electromagnetic induction e.g. *EM38*) belongs among such methods. The values of soil electrical conductivity are affected by several factors such as soil pore connection, soil moisture, content of salts, cation exchange capacity, sensing depth, and temperature. The greatest influence is the soil texture, soil moisture, salinity and even compaction (Rhoades et al., 1999). Some authors (Rhoades et al., 1999; Corwin and Lesch, 2005b; Smith, 2001; Jabro et al, 2005; Clark et al. 2000) observed some similarities between soil electrical conductivity patterns and soil compaction sensors readings. Soil electrical conductivity measurement is referred to as a practical and simple practice for within-field variability surveying and EC readings often relate to other soil or yield data.

Previous work conducted by myself at the Slovak University of Agriculture in Nitra, Slovakia used the direct contact method for soil electrical conductivity surveying. This compared the obtained patterns with other soil properties (soil texture, moisture, soil penetrometrical resistance data), and with a yield. This identified the need for further investigation and to focus on the relationship between the soil compaction and the soil EC and compare the outputs from the different sensors. It is intended to examine the suitability of the soil electrical conductivity measuring for determining the compacted areas within the field.

3 System operation parameters

3.1 Cone penetrometer

For performing the soil penetration resistance measurement the Penetrologger set from Eijkelkamp was used (Figure 3.1). It consists of the penetrometer water-resistant casing (1), impact absorber (2), probing rod (3), sensing cone (4), electrically insulated grips (5), communication port (6), GPS antenna (7), LCD screen (8), control panel (9), and bubble-level (10) (Eijkelkamp, 2007).

This penetrometer is able to collect the measurements up to the depth of 0.8 m with 10 mm depth resolution. During the penetration the soil the depth is sensed by the internal ultrasonic sensor using the depth reference plate. Maximal penetration force is 1,000 N and the force resolution is 1 N. All the logged data is saved in the internal memory of the penetrologger. The communication between the instrument and the computer is provided through the cable plugged to the communication port of the device and the computer.

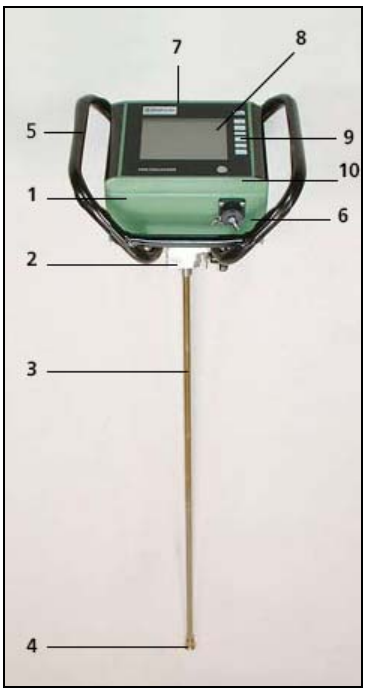

Figure 3.1 Soil cone penetrometer (Penetrologger from Eijkelkamp) (after Eijkelkamp, 2007).

3.2 Soil compaction sensor

Soil compacted sensor developed by Sharifi et al. (2007) is a tine instrumented with the flaps sensitive on the load. One edge of each of eight flaps is attached to the tine. The flaps are 50 mm wide. This design increases the vertical resolution in comparison with previous constructions. The flap is defined as a half-wedge shape sensing element, which is equipped by the strain gauges attached on its rear side. Each flap is equipped with a pair of strain gauges wired into half-active Wheatston bridge. This electronic circuit senses the bending moment caused by the resultant horizontal strength acting on the flap as moving through the soil matter.

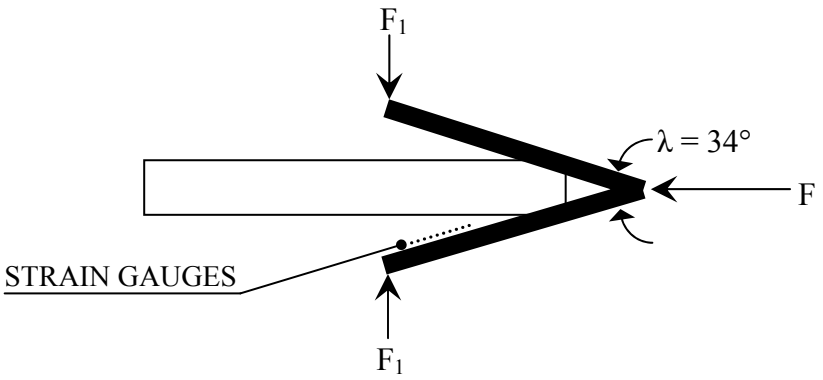

Figure 3.2 Flap of the instrumented tine and the horizontal forces acting on it (after Sharifi et al., 2007).

Strain gauges sensing the bending moment were calibrated by applying a static force on each flap (Figure 3.2 and Figure 3.3). The static force (F_1) was in fact a gravitational force caused by the weights hung on the flap using a special tool. In this case the force acted perpendicularly to the cross section of the body of tine and simulated a force which causes the bending moment during the measurement within the soil matter. The electric signal in millivolts from the strain gauges was immediately processed using the Fyled logger; the bending moment in Newton meters was calculated and logged by a laptop computer with running DaisyLab software. All the calibration curves were linear lines with coefficient of determination (R^2) of 0.99.

A B

Figure 3.3 Soil compaction sensor. A – callibration procedure, B – mounting on the frame of the subsoiler.

3.3 EM38

EM38 (Figure 3.4) is a commercially available soil contact-less sensor working on the principle of electromagnetic induction. The electromagnetic field is induced by electrical current flow through the transmitting coil. The electromagnetic field penetrating the soil to a given depth is reflected and intercepted by receiving coil of the instrument. The soil electrical conductivity is determined by the strength of received signal. This signal is processed and soil electrical conductivity readings are calculated by *Farm Works Software*® run in hand operated PDA used for data logging. The depth of soil penetration depends on the inter-coil spacing, the height of the instrument above the ground and chosen operating mode (horizontal or vertical) (Johnson et al, 2003). The calibration of the instrument should be done at least 3-4 times a day. If the soil resistivity is too high then the calibration is necessary to be repeated more often. It is recommended to follow the calibration procedure attached in appendices (Geonics limited, 2001).

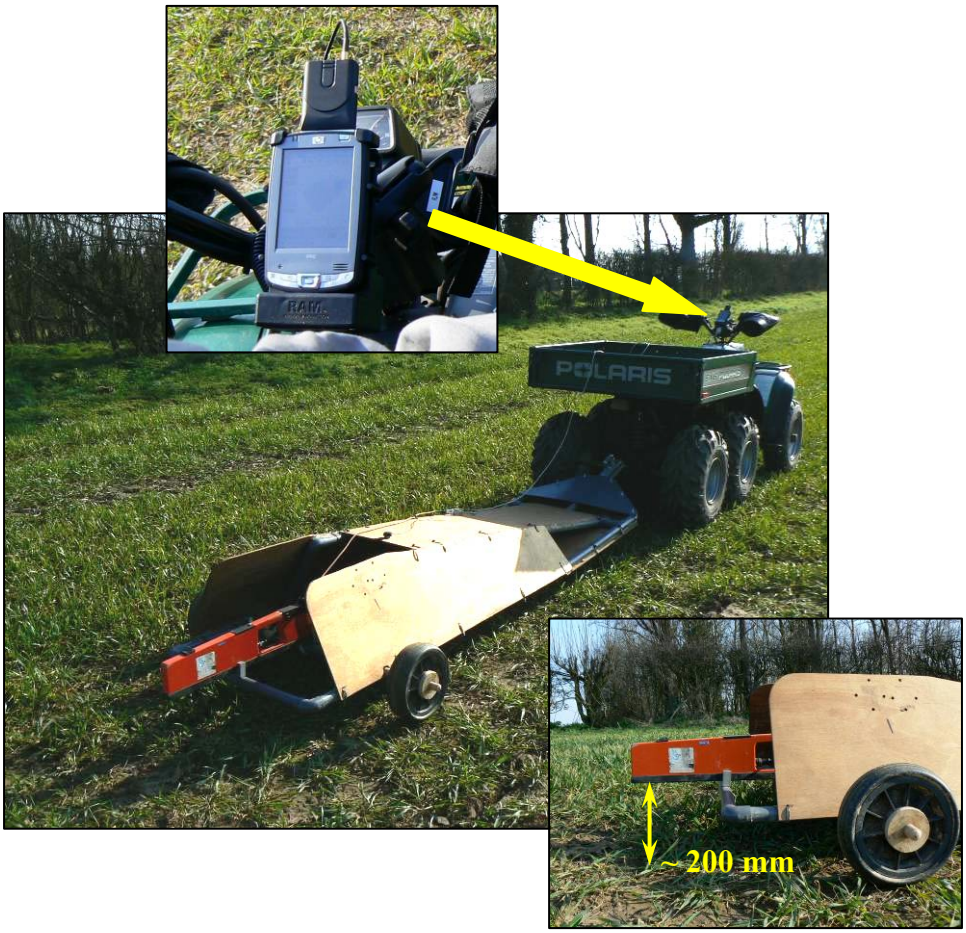

Figure 3.4 *EM38* attached to a non-metallic cart and plugged to a PDA.

3.4 Conductometer

The Conductometer (Figure 3.5) is a coulter disc contact sensor aimed at soil electrical conductivity surveying by direct contact with the soil. It was developed by Czech University of Life Sciences Prague (Czech Republic) and designed in cooperation with Slovak University of Agriculture in Nitra (Slovak Republic). The coulter electrodes penetrate the soil only in a few centimetres. Spacing of them is based on a reference given for Wenner array (Milsom, 2003) for two sensed depth ranges 0-0.3 m and 0-0.9 m. Spacing of sensing (voltage) coulter discs electrodes is equal to 0.2 m for shallow soil profile and 1.8 m for deep soil profile. Identical soil profiles are sensed by commercially available equipment *Veris® Model 3100*. The electronics of the Conductometer allows continual measurement of EC in both soil profiles. The readings of AC voltage measured by outer and inner electrodes, time and

co-located GPS coordinates are logged by laptop at an interval set by an internal processor of 5 seconds (0.2 Hz) or 1.2 seconds (0.833 Hz). The EC readings for both soil depth profiles are subsequently calculated using Equation 1. Electronic circuits and wiring (see Figure 3.6) provide that the EC readings are proportional to the soil properties on the distance moved during the measuring interval (Šařec et al., 2005). The instrument does not need any calibration but as it was necessary to test its behaviour in specific conditions, the experiments detailed in Chapter 3.5 below were conducted.

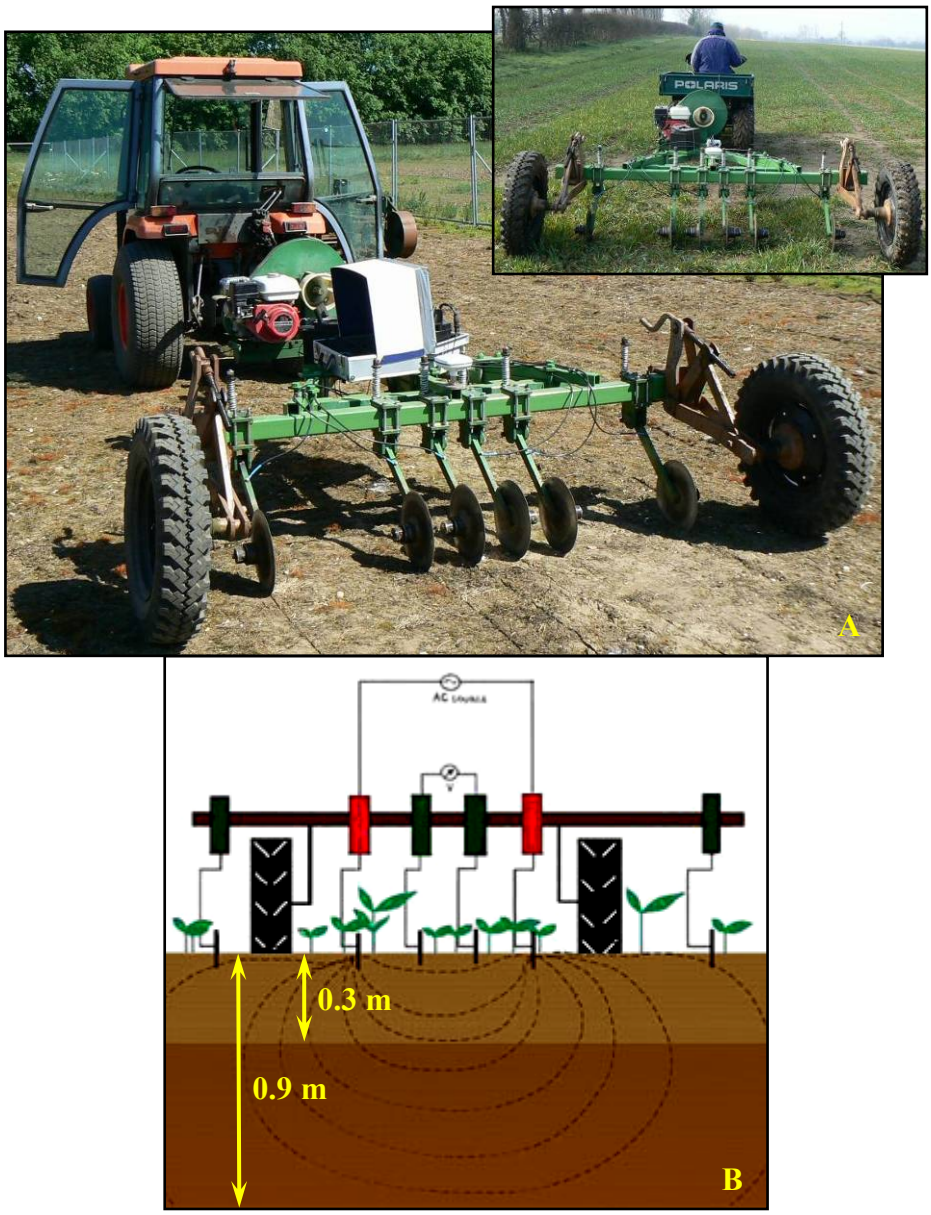

Figure 3.5 Conductometer during field survey (A) and the sketch of sensed soil profiles (B).

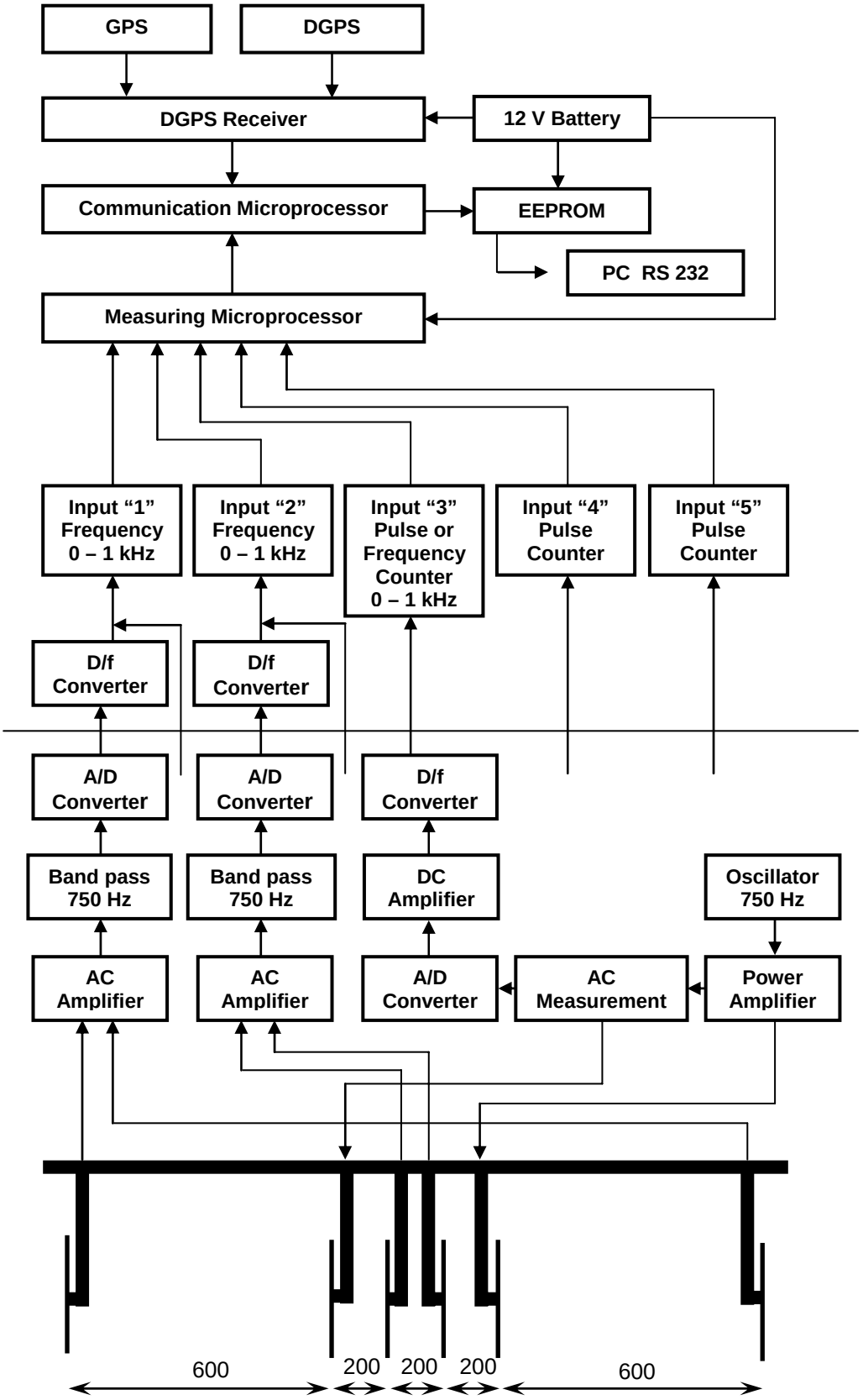

Figure 3.6 Flow chart of the Conductometer (after Šařec et al., 2005).

3.5 Operating characteristics

3.5.1 Introduction

The initial sampling frequency of the Conductometer was only 0.2 Hz. At normal operating speeds about 3 $m.s^{-1}$ it matches with mutual distance of successive readings about 15 m. Such a sampling frequency is sufficient for soil texture mapping but not for identification of compacted areas within the field. Therefore it was necessary either to collect the data in stationary mode or increase the sampling frequency of the Conductometer. For that reason a new processor with a highest possible sampling frequency of 0.833 Hz was ordered from the Czech University of Life Sciences Prague (Czech Republic) and the working speed was reduced for the randomised block design experiment. As some of the data was collected also stationary, yet it was necessary to inspect the time stability of the readings collected in stationary mode.

The coulter disc electrodes of the instrument are pushed into the soil by coil springs. The penetration depth of discs varied due to the different soil densities that were investigated. In order to distinguish if the EC readings are affected by soil bulk density or by depth of discs it was needed to investigate the influence of the depth of discs on the EC reading.

3.5.2 Objectives

1. To investigate the time stability of the electrical conductivity readings obtained by the Conductometer operated in stationary mode.

2. To investigate the effect of the depth of coulter disc electrodes on the EC readings collected by the Conductometer.

3.5.3 Time stability of EC readings

Site characteristics

The experiment aimed at investigation of time stability of collected EC readings was performed on University Sports ground in Silsoe, Bedfordshire in the South-East

England. The Sports ground is situated in the South-East corner of the campus (see Figure 4.1 in Chapter 4.3) on heavy clayey soils and its surface is grown by grass.

Setting up the experiment

The EC readings were collected on 4th May 2007 using the Conductometer working with sampling frequency of 0.2 Hz and operated in the stationary mode. The instrument was stopped in four different measuring points marked with a white paint within the Sports ground (see Figure 3.7). The data collected in each point at time of ten minutes was evaluated by descriptive statistics and the stability of the readings taken in particular points was reviewed. The experiment was replicated after 6 days on 10th May 2007 after substantial rainfalls (38.4 mm) and the effect of the water content was observed.

Figure 3.7 EC measurement performed within the Sports ground.

Results and discussion of results

The EC data collected by the Conductometer within both soil depth profiles (0-0.3 m and 0-0.9 m) is characterized by a high stability (Figure 3.8 and Figure 3.9). As it can be seen the EC readings slightly decrease on the beginning of the measurement and then are stable. This decrease can be caused by the reduction of adhesion between the soil and disc electrode. The descriptive statistics for both datasets was calculated. It

was found out that the coefficient of variation was less than 0.015 for the readings collected in time of 10 minutes (see Table II.1 and Table II.2 in Appendix II) and it did not exceed a value of 0.020 for the data collected within 1 minute (Table II.3 and Table II.4 in Appendix II). For comparison the EC data obtained in dynamic mode and characterizing one of the measuring points within randomised block design experiment (Chapter 5) achieved the variation coefficient of 0.063 and 0.025 for depth ranges of 0-0.3 m and 0-0.9 m respectively (see Table II.5 and Table II.6 in Appendix II). Following these findings the data obtained at a given time within individual points was assumed to be constant. Thus it could be averaged and used for a further processing.

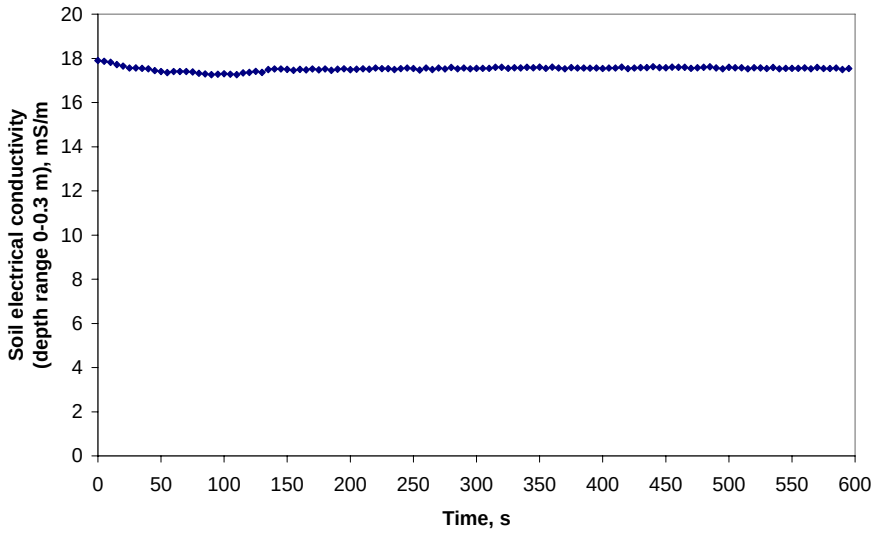

Figure 3.8 Soil EC readings collected in measuring point no. 1 within the depth range of 0-0.3 m.

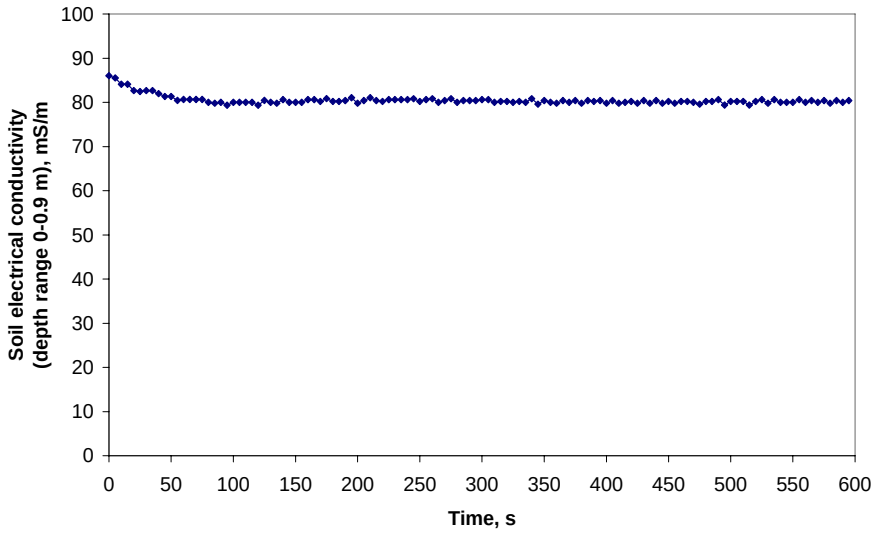

Figure 3.9 Soil EC readings collected in measuring point no. 1 within the depth range of 0-0.9 m.

It was observed that the means of EC readings collected before (4th May 2007) and after rainfalls (10th May 2007) at particular points within the Sports ground were evidently different (see Figure 3.10 and Figure 3.11). Whilst the readings obtained within the shallow soil layer increased, the data within the deeper soil layer decreased. Between both the earlier and the later EC measurement only two differences that could cause above difference were observed. One of them was the higher water content in the top soil layer and the second one was the higher penetration depth of the coulter disc electrodes.

During mentioned time period there was 38.4 mm of rainfall (see Table III.1 in Appendix III). So it was assumed that the raising of the EC values in the upper soil layer was caused by increasing the soil water content in the topsoil. Similarly it was assumed that the decline in the EC readings collected within the deeper soil profile could be possibly caused by the lower water content which could by drawn off by the grass roots.

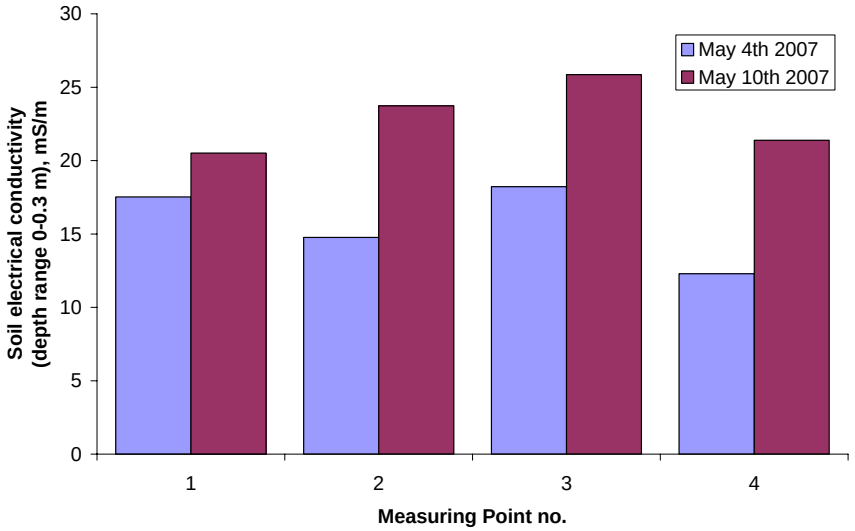

Figure 3.10 Soil EC readings collected within the depth range of 0-0.3 m before and after rainfalls.

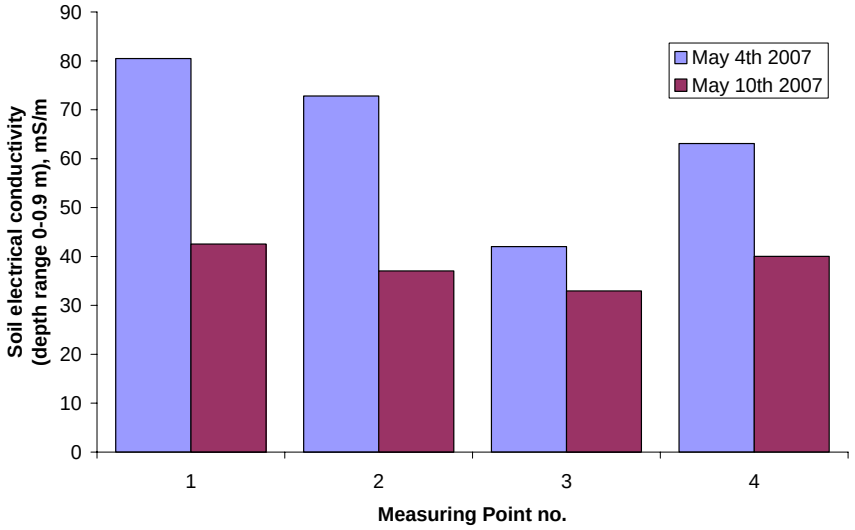

Figure 3.11 Soil EC readings collected within the depth range of 0-0.9 m before and after rainfalls.

The other difference observed between both the earlier and later measurement was a different depth of coulter disc electrodes. Because of the higher water content in the top soil layer during the second measurement the soil softened and the discs pushed by the coil springs penetrated it deeper. This phenomenon affected the surface of the contact area between the soil and the discs. The different contact area surface affected

the conductivity readings but it had not the major contribution on the observed change. The explanation for this statement is that the change in the contact area surface affects the readings collected within the shallow and the deeper layer in the same way - either both of them decrease or increase. This will be confirmed by the following experiment.

3.5.4 Relationship between the depth of the discs and the EC readings

Site characteristics

The effect of the depth of coulter disc electrodes on the EC readings was investigated within Avenue field. This field is situated in the North part of Silsoe College Farm (see Figure 4.1 in Chapter 4.3). The soils are loamy textured with flat surface and without any cover crop.

Setting up the experiment

It was necessary to perform another experiment and examine the influence of the discs penetration depth or rather the contact area surface on the EC readings while the other properties remain unchanged. Such an experiment was performed on 7th June 2007 within the Avenue field. The topsoil layer of the field was loose and the discs were pushed into the soil at several given depths with four replications. It was requested to provide for sufficient electrical contact between the soil and discs in all investigated depths. This was carefully set for each of performed measurements. The only variable was the contact area surface between the soil matter and the discs.

Results and discussion of results

Dependency between the soil EC (for both shallow and deep soil depth range) and the penetration depth of discs was evaluated using the regression analysis which is listed in Table IV.1 and Table IV.2 in Appendix IV. As the "Significance F" value is smaller than 0.05 there is a significant regression and a straight line can be fitted to the data. As the value under "P-value" for both depth ranges is less than 0.05 than the slope of the fitted line is significantly different to zero. In other words the EC readings

increase when the depth of the discs or contact area surface increase. This finding is in contrast with Wenner's formula (see Equation 2 in Chapter 2.3.5) according which the EC should decrease with increased depth of electrodes. This phenomenon is probably caused by the different shape of the electrodes used by Wenner. His sketch shows the tipped electrodes (Figure 2.15). It means that by pushing the electrodes deeper to the soil Wenner really changed only the depth of sensing. However the Conductometer uses the flat disc electrodes. By pushing such electrodes deeper to the soil also the contact area increases. Therefore the relationship given by Wenner is not valid for the coulter electrodes. For this type of electrodes it would be desirable to define the relationship between EC readings and contact area surface rather than depth of insertion of electrodes.

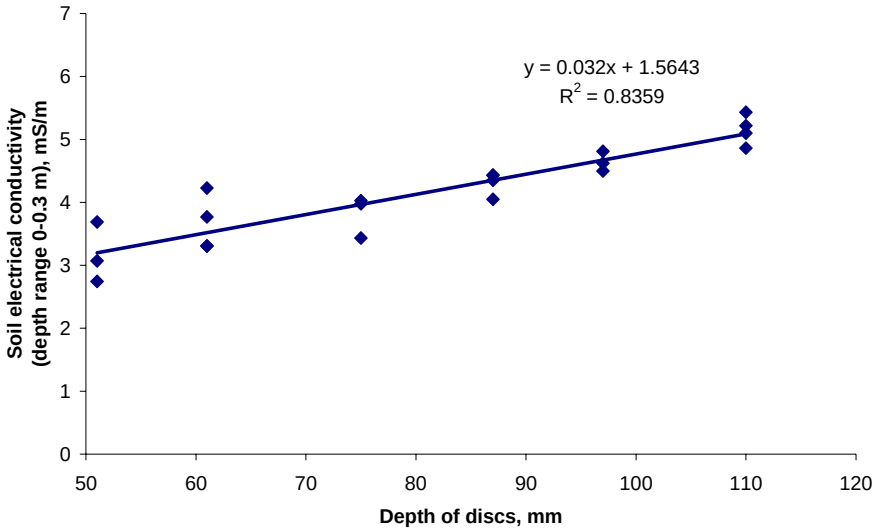

Figure 3.12 The dependency between the soil EC within the soil profile 0-0.3 m and the depth of discs.

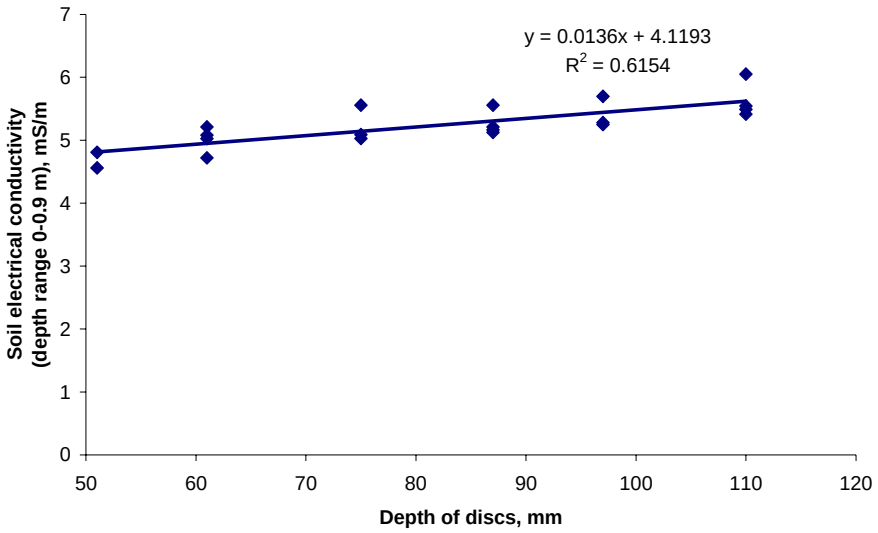

Figure 3.13 The dependency between the soil EC within the soil profile 0-0.9 m and the depth of discs.

4 Initial field experiments

4.1 Introduction

The data collected in this experiment was obtained using both devices – the Conductometer and the *EM38* operated in vertical mode. In order to meet the specified objectives of this experiment the survey has been divided into several steps, when the sensors were pulled through the field in different locations, directions, and operating speeds. The experiments were performed in early spring on 26th March 2007.

4.2 Objectives

1. To investigate differences between conductivity readings obtained from trafficked and non-trafficked areas.

2. To investigate the repeatability of the measurement performed in the same line while the sensor is pulled from side to side.

3. To investigate and identify the areas with a higher soil bulk density within the field, using the soil electrical conductivity measurements. Use both the direct contact (Conductometer) and contact-less (*EM38* operated in vertical mode) sensors. As the compacted zones, thus the areas with a higher soil bulk density, the tramline locations are assumed.

4. To collect the soil samples to characterize the field environment and assess the soil moisture content, soil salinity (electrical conductivity by saturated extract), soil pH and soil organic matter content (loss on ignition method).

4.3 Site characteristics

The experiment was conducted in Silsoe, Bedfordshire in the South-East England. Downings field was chosen as an experimental plot. It is situated in the North-West corner of Silsoe College Farm (see Figure 4.1). The relatively small area of the field which allows early performance of field experiments; the high spatial variability of

soil conditions which could be detected by soil sensors; and the wide information background created by previously conducted researches (Pires, 2004, Wolharn, 2001) were the main criterions for choosing the particular field.

The area of the field is about 5.5 ha. Five different soil series and a soil types range from a sandy loam to clay are present within the field (Figure 4.2) (Pires, 2004). In the time of performing the experiments, the soil samples were collected from the sampling points shown in Figure 4.2. The overall characteristic of the investigated soil properties is described in Chapter 4.7.2. Plot is sloped in East–West direction and the maximum difference in elevation is about 9 meters. The field was cropped by winter wheat. The tramlines are spaced about 20 m apart.

Figure 4.1 Aerial photograph of the experimental sites used in this work (Infoterra Ltd and Bluesky©, 2007).

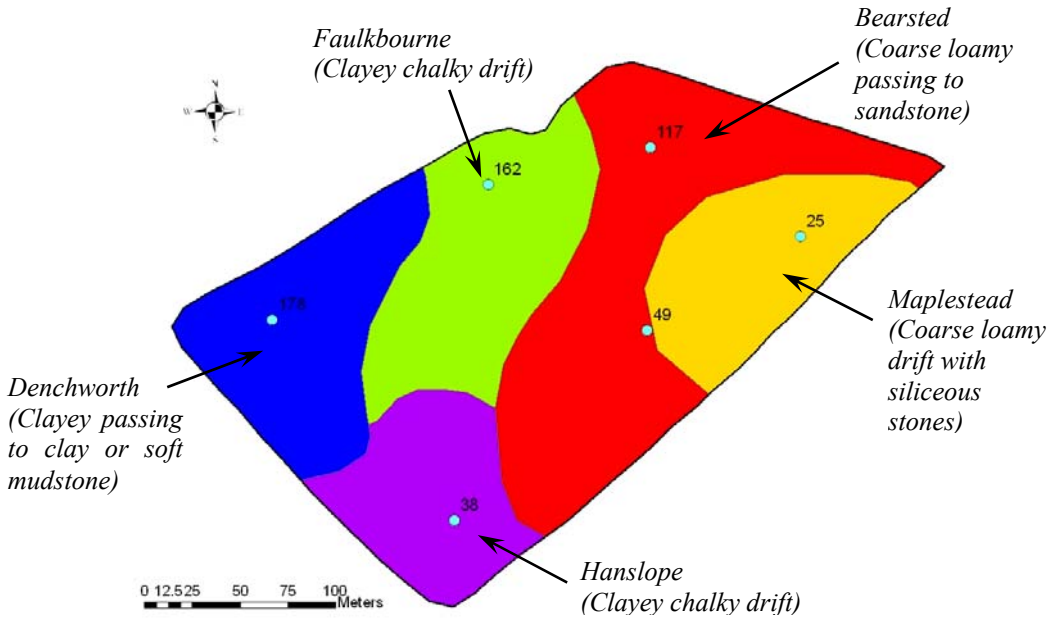

Figure 4.2 Soil series present within Downings field (Soil Data© Cranfield University (NSRI) 2007). Spots represent the sampling points.

4.4 Comparing the readings obtained from trafficked and non-trafficked areas

4.4.1 Methodology

In order to compare the potential differences between the readings obtained within the trafficked tramlines and between them, the sensors were pulled within the two neighbouring tramlines and the two adjacent non-trafficked areas as it is shown at the Figure 4.3. The operating speed of the Conductometer varied approximately from 1.0 $m.s^{-1}$ to 1.2 $m.s^{-1}$ and from 1.8 $m.s^{-1}$ to 2.0 $m.s^{-1}$ within trafficked and non-trafficked areas respectively. As the Conductometer was at that time equipped with the old processor which enables to log the readings every 5 seconds, the distance between two readings varied from 5 m to 6 m and from 9 m to 10 m within trafficked and non-trafficked areas respectively. The *EM38* obtained the readings every second and the distance between successive readings varied from 1.4 m to 1.7 m for both trafficked and non-trafficked areas.

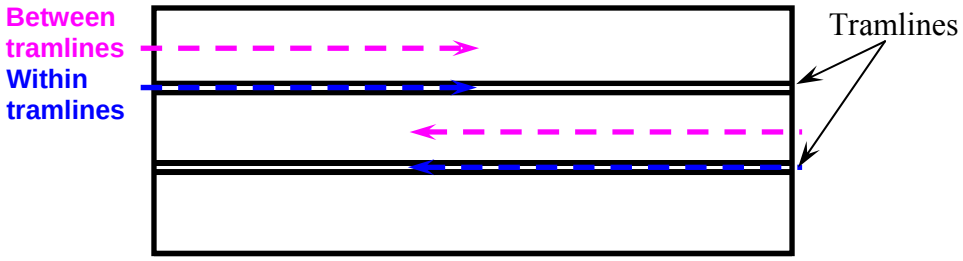

Figure 4.3 Layout of the experiment aimed at the investigation of the differences between the EC readings obtained from trafficked and non-trafficked areas.

Figure 4.4 Positions of the coulter disc electrodes while running within the tramline.

4.4.2 Results and discussion of results

The EC readings collected by the Conductometer within the first pair of runs (within and between tramlines) at both soil depth ranges (0-0.3 and 0-0.9 m) are shown in Figure 4.6 and Figure 4.7 respectively. It can be seen that the EC values representing soil profile of 0-0.3 m are mostly higher within trafficked (tramlines) than non-trafficked areas (between tramlines). This increase is possibly caused by the higher soil bulk density within the trafficked areas. However it was observed that the EC readings representing soil profile of 0-0.9 m are mostly lower within trafficked than non-trafficked areas. This is unexpected phenomenon which probably relates with the lesser contact between the soil and outer discs while running within tramlines. As it can be seen in the Figure 4.4 and Figure 4.5, the inner electrodes were placed between wheel marks whilst the outer ones run directly within wheel marks. Because of the absence of the crop and higher soil bulk density within wheel marks, the soil surface

dried sooner within these areas. The lower water content caused decrease soil adhesion and thus the contact between outer discs and soil. This phenomenon is clearly visible in the Figure 4.5. The wetter soil stuck on the discs and was drawn out of the soil surface (B) but the soil which was more dry did not stick and only negligible cut left in the soil surface (A).

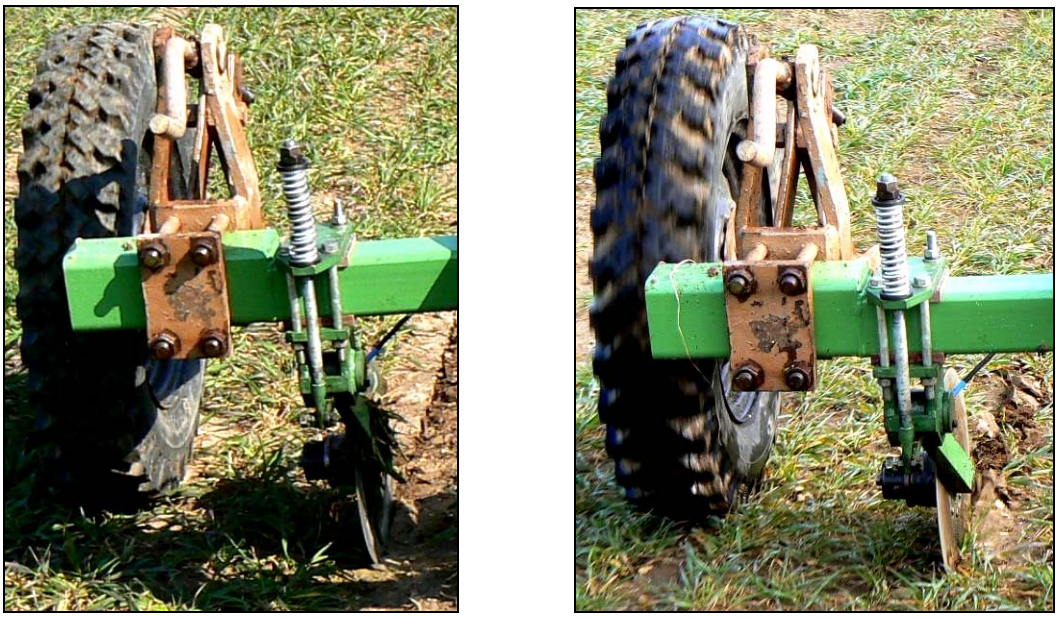

A **B**

Figure 4.5 Coulter disc electrodes within wheel mark (A) and in non-trafficked soil (B).

The data obtained from both trafficked and non-trafficked areas were subsequently analysed using the t-test which compared the significance of the differences between the means. The t-test was performed for both pairs of runs but non-significant difference was found out for data collected within trafficked and non-trafficked areas at both depth ranges (see Table 4.1 or Table V.1 – Table V.4 in Appendix V). This phenomenon is most likely caused by little difference between means and high variability of individual datasets. Therefore the differences between shallow (0-0.3 m) and deep (0-0.9 m) EC readings (Figure 4.8) obtained from trafficked areas were compared with the differences from non-trafficked areas using t-test. Performed analysis showed significant (for first pair of runs even high significant) difference between differences (EC30-EC90) between trafficked and non-trafficked areas (see Table 4.1 or Table V.5 and Table V.6 in Appendix V). The compaction along

tramlines was examined and further investigation was done by running perpendicularly (see Chapter 4.6).

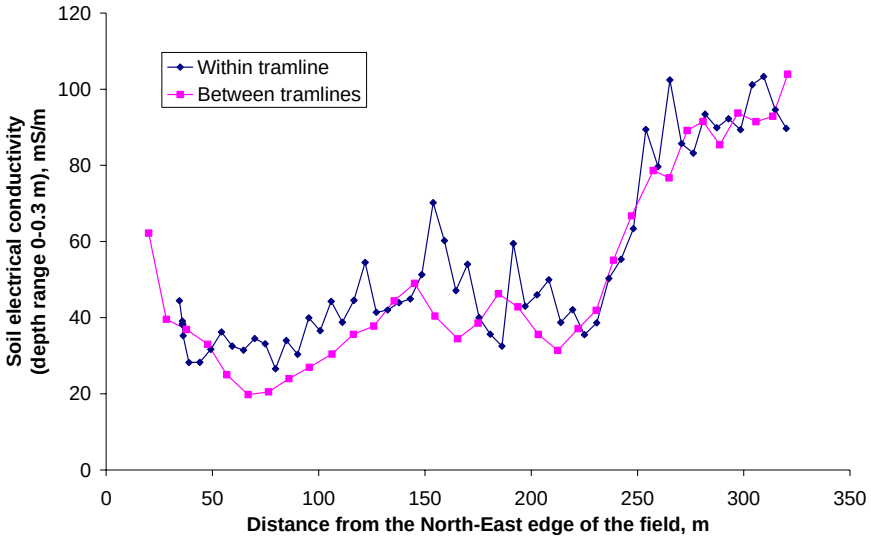

Figure 4.6 Soil EC readings collected at depth range of 0-0.3 m within and between the tramlines.

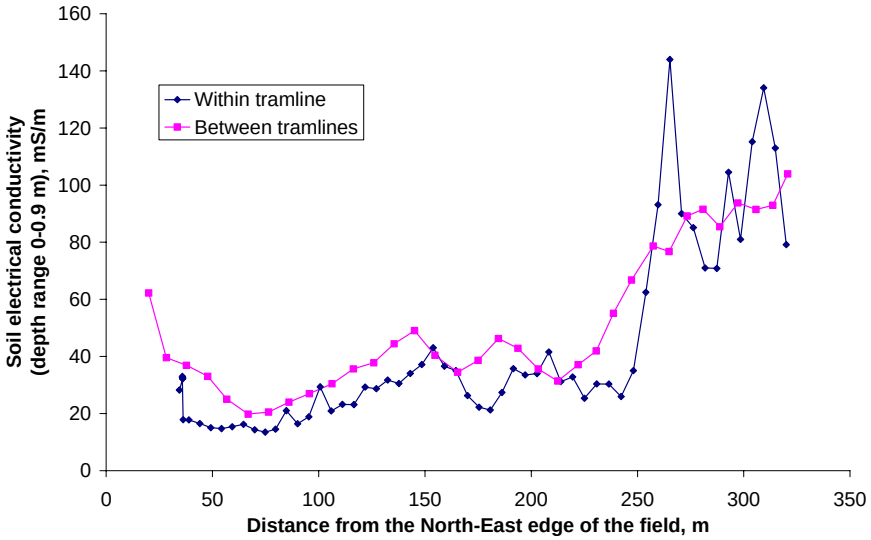

Figure 4.7 Soil EC readings collected at depth range of 0-0.9 m within and between the tramlines.

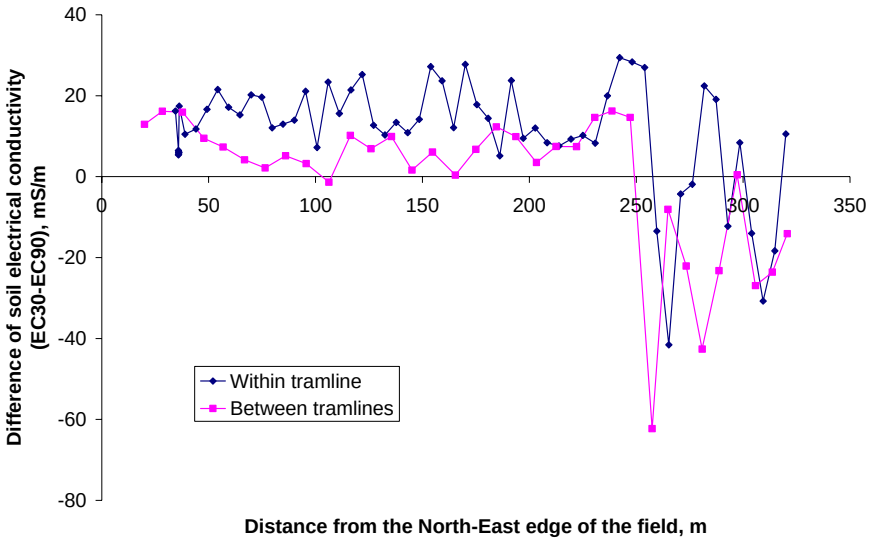

Figure 4.8 Difference of soil EC readings collected at depth range of 0-0.3 m and 0-0.9 m (EC30-EC90) within and between the tramlines.

The EC readings obtained by *EM38* were also analysed by t-test (see Figure 4.9, Table 4.1 or Table V.7 and Table V.8 in Appendix V). As the *EM38* works on the contact-less principle, it removes the disadvantage of the Conductometer and the EC data reaches slightly higher mean values within trafficked areas than within non-trafficked areas. However as the *EM38* operated in vertical mode scanned the deeper soil profile (up to 1.5 m) than the Conductometer, the increase of soil bulk density in top soil layer had much less contribution to the strength of electromagnetic signal than other soil parameters (e.g. soil water content, soil texture or porosity). That is the reason why no significant difference was found for the EC data collected within trafficked and non-trafficked areas. Sudduth et al. (2005) compared *Veris® 3100* with *EM38*. They found out similar findings and reported that the differences between both machines are caused by the differences between their response curves (see Figure 2.16 in Chapter 2.3.5).

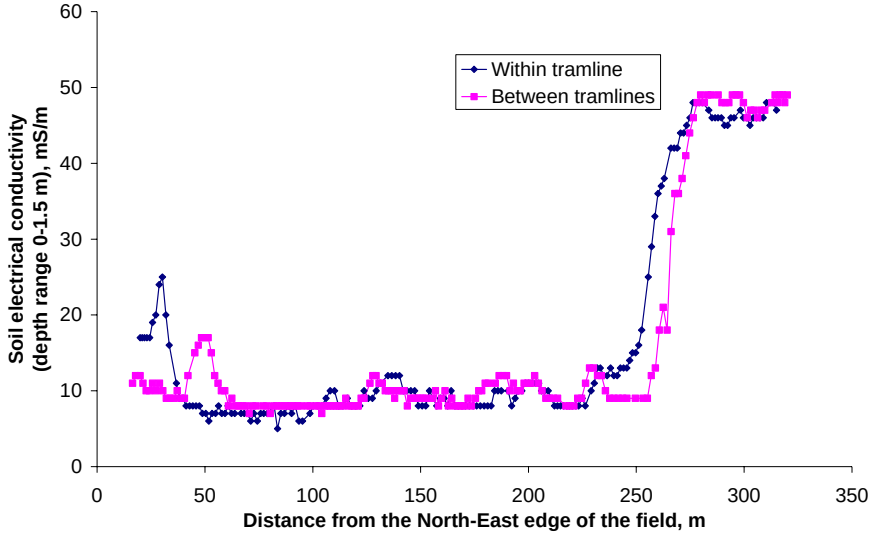

Figure 4.9 Soil EC readings collected at depth range of 0-1.5 m within and between the tramlines.

Table 4.1 Summary table of the t-tests showing the signification of differences of individual measurements performed within and between tramlines (* - significant difference at the confidence interval of 95%, ** - highly significant difference at the confidence interval of 99%, NS – non-significant difference).

Parameter, Instrument	Trafficked vv Non-Trafficked	
	1st run	2nd run
EC30 (Conductometer)	NS	NS
EC90 (Conductometer)	NS	NS
EC30-EC90 (Conductometer)	**	*
EC150 (*EM38* vertical mode)	NS	NS

4.5 Measurement performed in the same line at both directions

4.5.1 Methodology

The revision of the repeatability of the performed survey was the main purpose of this measurement. The EC readings were collected within the same line at both directions (1st run and 2nd run) using both contact and contact-less instruments as these were pulled from side to side (see Figure 4.10). The Conductometer which sensed two

depth ranges (0-0.3 m and 0-0.9 m) was drawn through the field at average operating speed of about 1.0 $m.s^{-1}$. It corresponds with the distance between successive readings of about 5 m. The *EM38* was attached to the non-metallic cart and pulled by a quad bike through the field. It collected the EC readings from the soil profile of 0-1.5 m in the mutual distance of successive points ranging from 1.6 m to 2.0 m at average speed ranging from 1.6 $m.s^{-1}$ to 2.0 $m.s^{-1}$.

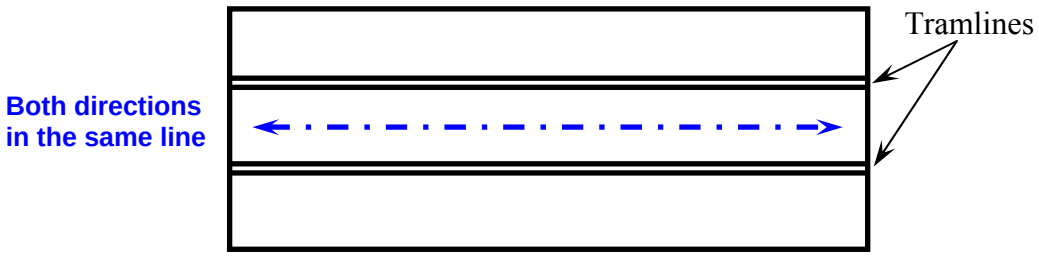

Figure 4.10 Layout of the experiment aimed at the investigation of the repeatability of the EC measurements.

4.5.2 Results and discussion of results

The Conductometer

Soil depth ranges of 0-0.3 m and 0-0.9 m were sensed by the Conductometer. The obtained readings are plotted on Figure 4.11 and Figure 4.12 respectively. It can be seen that most of the readings collected in 2nd run are lower than the values collected in 1st run. The statistical analyse shows that for the confidence interval of 95 % there is a significant difference between the means of EC readings obtained in 1st and 2nd run at the depth range of 0-0.3 m (see Table 4.2 or Table VI.1 in Appendix VI) but there is not a significant difference at depth range of 0-0.9 m (see Table 4.2 or Table VI.2 in Appendix VI). During the 2nd run the higher impact on the data collected within the shallow layer (0-0.3 m) was most likely caused by the reduced contact between the electrodes and the soil matter, resulting from the grooves (slits) created in the 1st run (see Figure 4.13). In other words the creation of the grooves caused the disturbance in the soil surface, increased the amount of the air in this area and reduced the physical contact surface between the coulter disc electrodes and the soil. The combination of all these factors caused the reduction of the values obtained

in the 2nd run which had a higher effect on the data obtained from the shallow soil profile. Doerge et al. (2001) reported that the good contact between the electrodes and the soil as a necessary condition for obtaining a reliable data but no one reported that such a small disturbance of a soil surface caused by previous run can affect the readings.

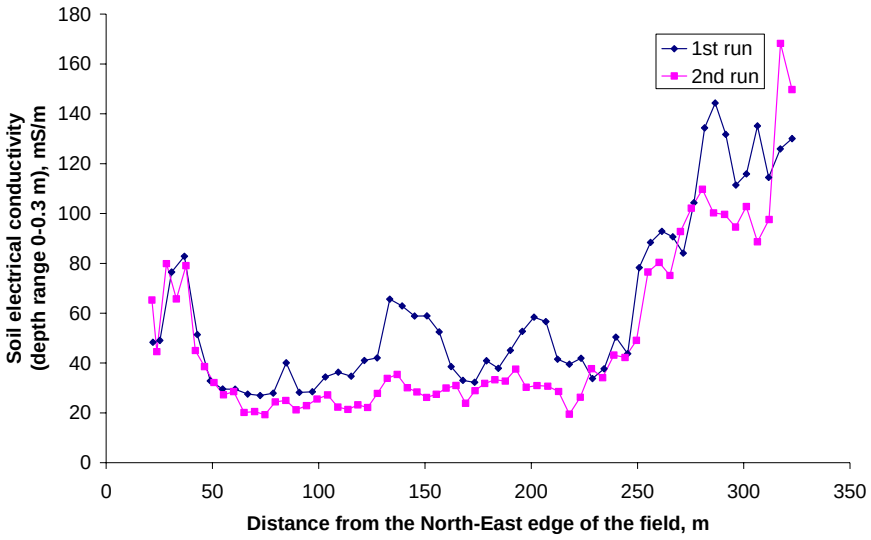

Figure 4.11 Soil EC readings collected in the same line in both directions (1st run and 2nd run) in depth range of 0-0.3 m.

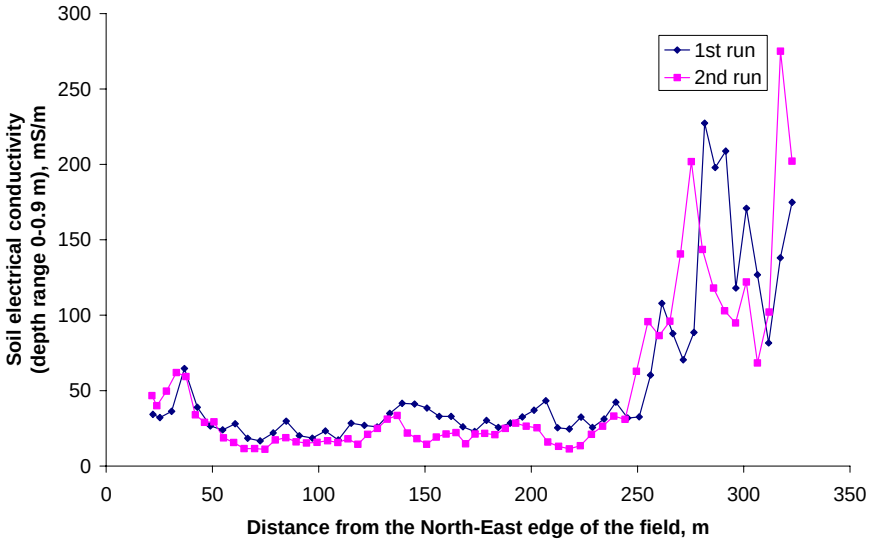

Figure 4.12 Soil EC readings collected in the same line in both directions (1st run and 2nd run) in depth range of 0-0.9 m.

Figure 4.13 Detail view of the disc running in the groove created during the 1st run.

The *EM38* operated in vertical mode

The measurement following the above procedure was performed also using the contact-less instrument (*EM38* operated in vertical mode) within the same site. The readings collected in this mode reflect the variations within the soil depth of 0-1.5 m. The data collected in the 1st and the 2nd run is shown in Figure 4.14 and it appears to be identical. This appearance was subsequently confirmed statistically. Both datasets were compared using the t-test within the confidence interval of 95 % (Table VI.3 in Appendix VI). It was found out that the means of both datasets (16.387 $mS.m^{-1}$ and 15.714 $mS.m^{-1}$) are not significantly different (see Table 4.2). This finding matches well with the result from previous experiment and confirms the advantage of contact-less method consist in the stability and repeatability of performed measurement.

Table 4.2 Summary table of the t-tests showing the signification of differences of individual measurements performed within the same line in both directions (* - significant difference at the confidence interval of 95%, ** - highly significant difference at the confidence interval of 99%, NS – non-significant difference).

Parameter, Instrument	1st run vv 2nd run
EC30 (Conductometer)	*
EC90 (Conductometer)	NS
EC150 (*EM38* vertical mode)	NS

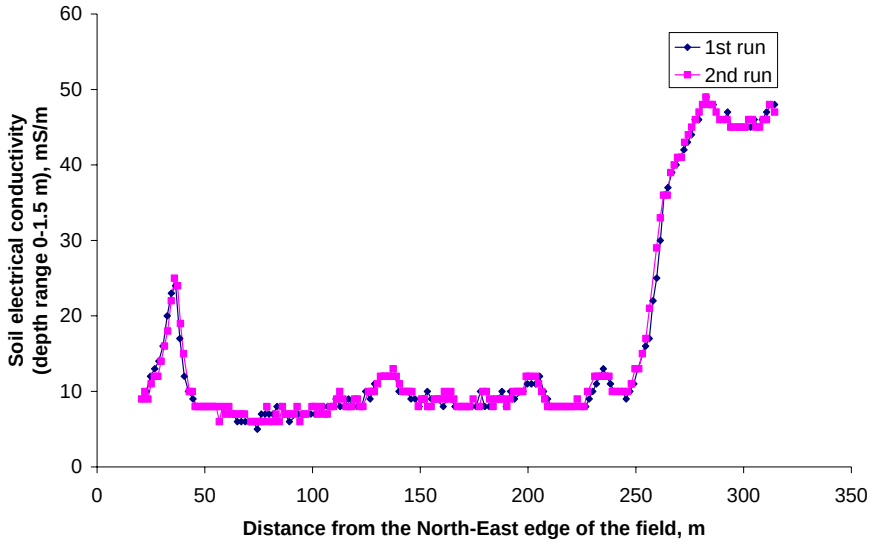

Figure 4.14 Soil EC readings collected in the same line in both directions (1st run and 2nd run) in depth range of 0-1.5 m.

4.6 Localization of the trafficked areas using the perpendicular EC survey

4.6.1 Methodology

In this case the both sensors were drawn perpendicularly across the tramlines. The positions of all tramlines were measured by measuring the distance from the field edge to each of the tramlines by measuring wheel. The tramlines were subsequently drawn in a map within GIS software.

The soil electrical conductivity readings were collected at four strips located at different soil conditions at four sites within the Downings field and each strip included four runs (see Figure 4.15 and Figure 4.16). The Conductometer collected the EC readings at speed of about 1 $m.s^{-1}$ at mutual distances of succeeding points about 5 m. The *EM38* moved at speed of about 1.3 $m.s^{-1}$ and the EC data has been collected about every 1.3 m.

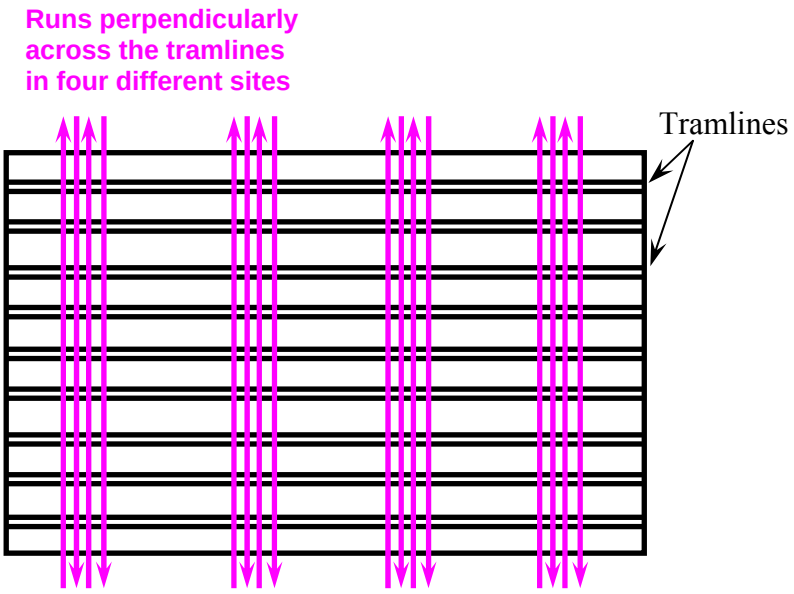

Figure 4.15 Layout of the experiment aimed at the localization of the tramlines using the EC readings.

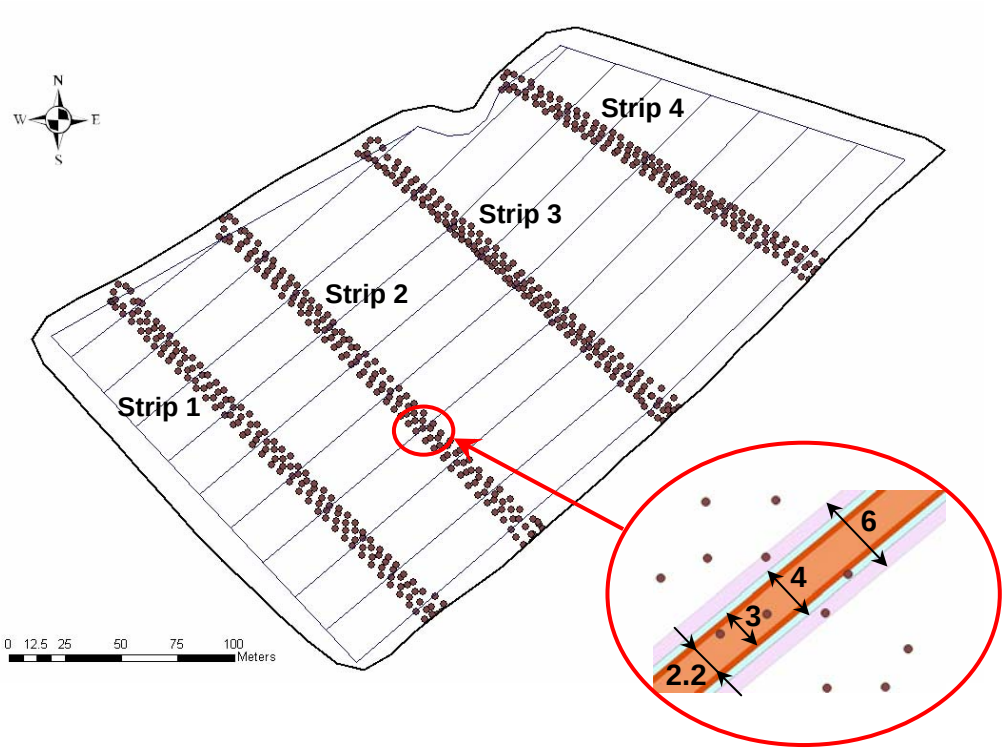

Figure 4.16 Soil EC readings collected within the Downings field perpendicularly across the tramlines. Detail shows the various widths along the tramlines dimensioned in meters that were used for data processing as it is described further.

4.6.2 Results and discussion of results

Statistical analyses

The data collected using both contact and contact-less instruments perpendicularly across the tramlines were plotted into the graph as well as the tramline positions (Figure 4.17 and Figure 4.18).

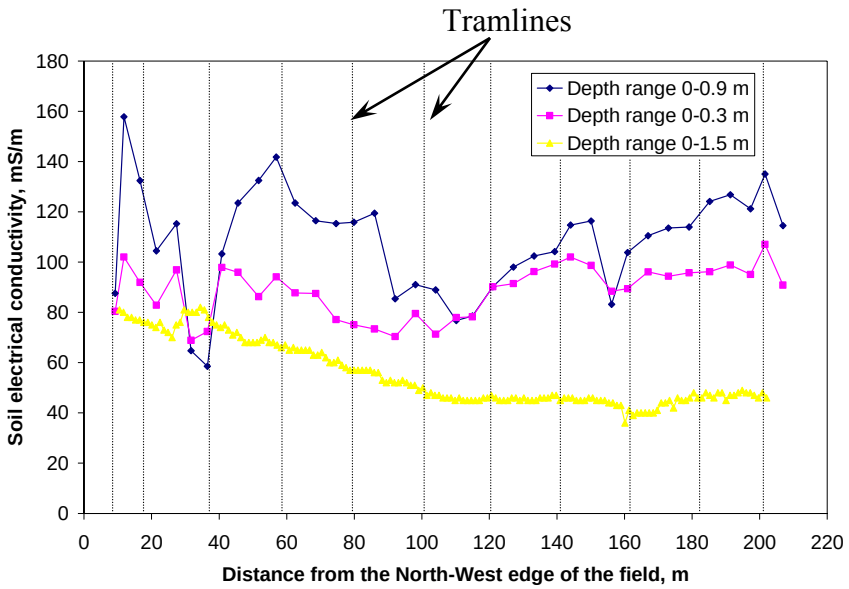

Figure 4.17 Soil EC readings collected perpendicularly across the tramlines (1st run within "Strip 1").

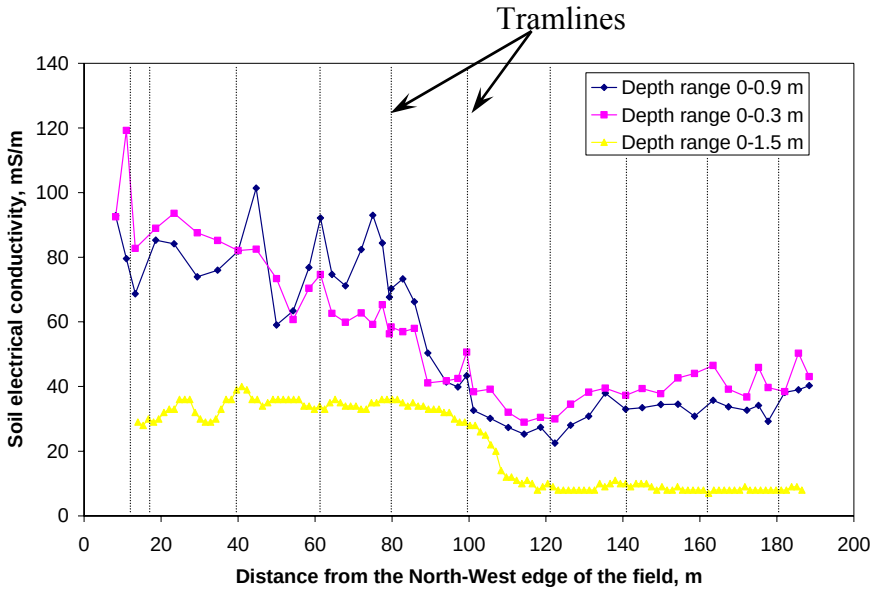

Figure 4.18 Soil EC readings collected perpendicularly across the tramlines (1st run within "Strip 3").

It can be seen that there is some major factor that affected the main shape of the curves in both above Figures. The influence of this major factor is easily seen in the readings collected by *EM38* at the depth of 1.5 m, but it also influences the readings collected by the Conductometer in both soil measured profiles (Figure 4.18). Therefore the EC data was compared with the results of soil analyses done by Wolharn (2001). He collected soil samples from soil profile by digging soil pits in many locations within Downings field. On the base of his results and using the EC readings collected in individual soil profiles the cross-section sketch of the Downings field along "Strip 3" was created (Figure 4.19).

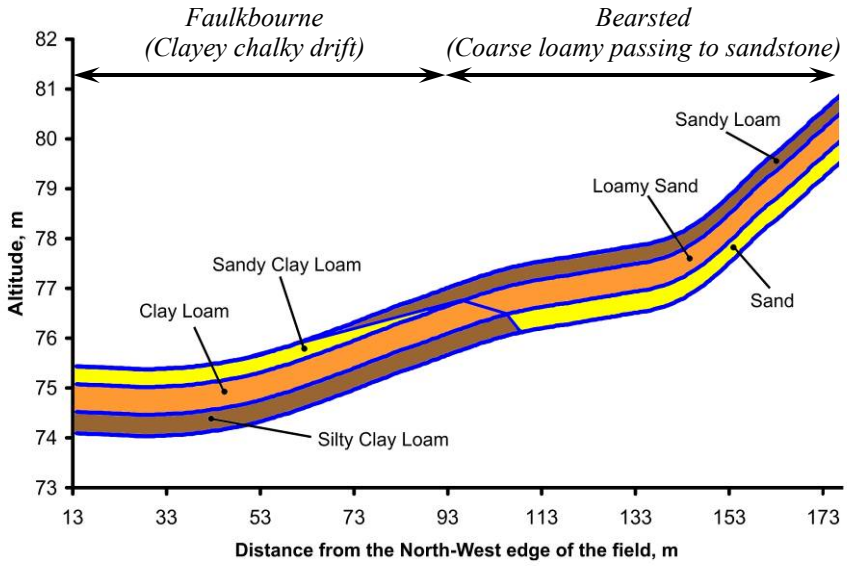

Figure 4.19 Sketch of Downings field cross-section along "Strip 3" showing different soil layering.

It can be clearly seen that the EC readings collected in the North-West part of the "Strip 3" (left hand of the sketch) are higher because of the higher content of clayey particles in soil matter. The readings collected within South-East half of the "Strip 3" (right half of the sketch) are lower because of higher proportion of sand and lower proportion of clay. Distribution of soil particles within the field has been affected by soil-forming process. In this case the fine clayey particles have been drift by water from the places with a higher altitude (South-East edge) to the areas with lower altitude (North-West edge) where they have settled. The move of soil particles has not been identical in all surveyed soil profiles. The EC readings collected at top 0.3 m continuously decrease from North-West towards the middle of the field and then stabilize. The EC readings collected at soil dept of 0-0.9 m change within much narrower zone. This change is affected by changing sandy clay loam and clay loam in North-West to the sandy loam and loamy sand in South-East within both upper soil profiles. The EC measured by *EM38* reflects the change in soil type within whole sensed profile by very sharp change of the curve. It is well known that the soil texture influences the soil water holding capacity and determines the direction of water flow within the soil pores. While the sandy soils are not able to hold water properly and the water drains into the soil by acting of gravitation force, the clayey soils have many

fine pores filled with the water and enable water to flow upwards by acting of capillary forces. Although the field survey was performed in early spring when the soil was saturated by water, the water from sandy soils already evaporated and flowed into deeper soil layers (see Table 4.4 and compare with Figure 4.2) and contributed to decrease the EC readings within such areas. The effect of soil texture and moisture is also clearly visible in previously mentioned Figures (Figure 4.6-Figure 4.9, Figure 4.11, Figure 4.12 and Figure 4.14).

In addition to the above mentioned influence of soil texture, the EC readings collected by the Conductometer are also affected by soil bulk density. It can be seen that within some sites the EC readings collected using the Conductometer reach the higher values near by the tramlines. Therefore the data located along the tramlines was cut out in the GIS environment and statistically compared with the rest of the data. In order to test the significance of the differences between both datasets in several widths along the tramlines, the data were cut out in strips wide 6, 4, 3 and 2.2 meters (the real width of tramlines) along the axes of individual tramlines (see detail in Figure 4.16). The individual datasets were compared by t-test. It was found out that the means of EC readings collected by the Conductometer within trafficked and non-trafficked areas within both shallow and deep soil layers are significantly different within the confidence interval of 95 %. These findings are valid for all investigated widths along the tramline axes (6, 4, 3 and 2.2 meters) (see Table 4.3 or Table VII.1-Table VII.8 in Appendix VII). Inverted results were obtained for the data collected by *EM38* operated in vertical mode. The means of such a data collected from trafficked and non-trafficked areas are not significantly different within the confidence interval of 95 % in no one of investigated widths (see Table 4.3 or Table VII.9-Table VII.12 in Appendix VII). It can be seen that there is no significant relationship between the EC readings collected by *EM38* operated in vertical mode and the tramline pattern. It means that the data collected by *EM38* operated in vertical mode are more significantly affected by the soil texture than soil bulk density (see Figure 4.17 and Figure 4.18).

Table 4.3 Summary table of the t-tests showing the signification of differences of individual measurements performed within trafficked and non-trafficked areas and evaluated within different widths along the tramline axes (* - significant difference at the confidence interval of 95%, ** - highly significant difference at the confidence interval of 99%, NS – non-significant difference).

Parameter, Instrument	Trafficked vv Non-Trafficked areas (width of evaluation)			
	2.2 m	3 m	4 m	6 m
EC30 (Conductometer)	*	*	*	*
EC90 (Conductometer)	*	*	*	*
EC150 (*EM38* vertical mode)	NS	NS	NS	NS

Geostatistical evaluation

EC data was also evaluated geostatistically following the procedure given by Carr (1982). He reported that there can be three components present in the plotted EC data collected across the field. One of them is the trend which can be caused by an influence of soil particle size. The second component is caused by the possible periodicity within the field and can result from fertilization, ploughing or compaction. The last component is caused by random events like lack of disc contact, any kind of surface noise and measurement error. As it was desirable to identify the periodical pattern of areas with higher soil bulk density under the tramlines using soil EC measurement, it was necessary to remove the global trend from the dataset. This was done using Genstat statistical package. The residuals of EC data were then used for assessing spatial dependency, modelling the variogram, fitting the optimal model and kriging the data. The output form Genstat was then imported to the GIS software and displayed as a map. The EC data collected within each of four measured strips was individually divided into intervals using "natural breaks (Jenks)" classification. This classification allows to divide the data into classes based on the natural groupings inherent in the data. The boundaries of individual classes are set where are relatively big jumps in the readings. It can be seen that the pattern of the tramlines (increased soil bulk density) is partly visible in the maps of the EC residuals created for three depth ranges within four surveyed strips (see Figure 4.20 - Figure 4.22).

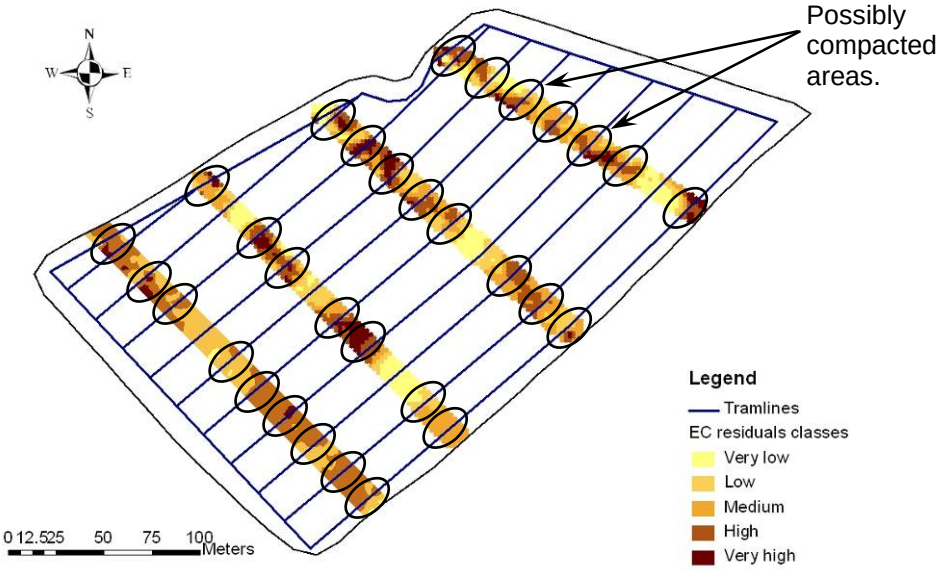

Figure 4.20 Natural break intervals of residuals of the soil EC readings measured by the Conductometer within the depth range 0-0.3 m.

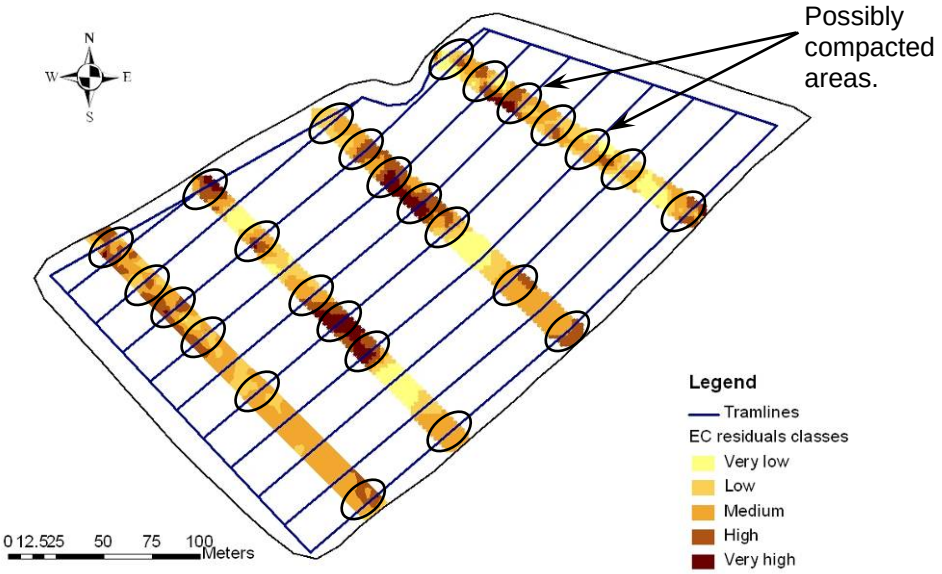

Figure 4.21 Natural break intervals of residuals of the soil EC readings measured by the Conductometer within the depth range 0-0.9 m.

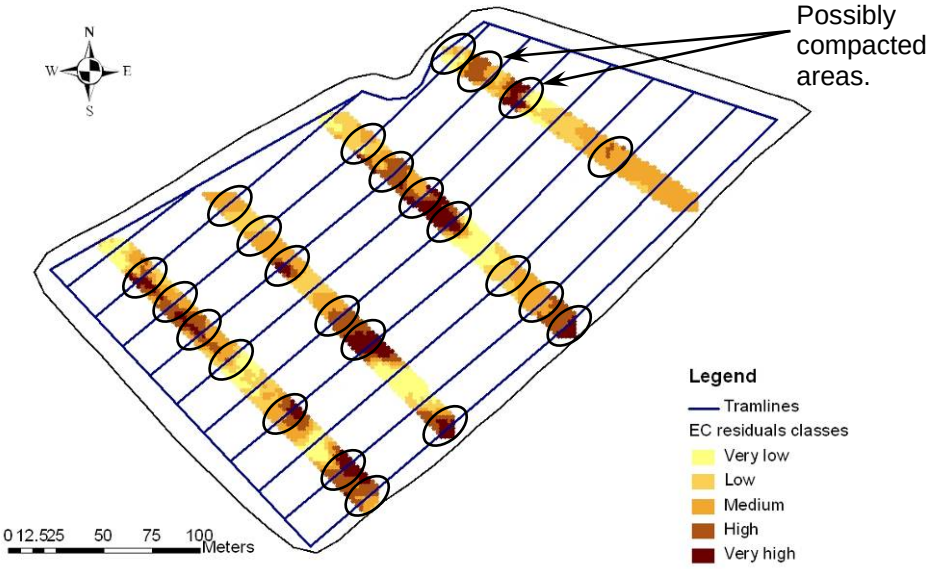

Figure 4.22 Natural break intervals of residuals of the soil EC readings measured by the *EM38* within the depth range 0-1.5 m.

Surveying of such a variable parameter as soil compaction would demand densely collected data. It is supposed that the sufficient amount of the EC data which would be collected in higher sampling frequency (e.g. 20-30 Hz) would improve the spatial pattern and the precision of the map of soil compaction.

The EC readings collected within the whole field were used for delineating soil texture boundaries (James et al., 2000). The EC readings were processed by the procedure mentioned above but the global trend remained in the data. The kriged readings were manually divided into four intervals while the division was performed for purpose of matching the EC data with the results of soil particle size analysis performed by Wolharn (2001). It can be clearly seen that the EC readings collected at different soil depth ranges are able do describe the soil environment and refine the soil type boundaries at particular depths (Figure 4.23 - Figure 4.25). It is obvious that the area of clayey soils at western part of the field increases with the depth of sensing likewise the sandy area in eastern and central part of the field.

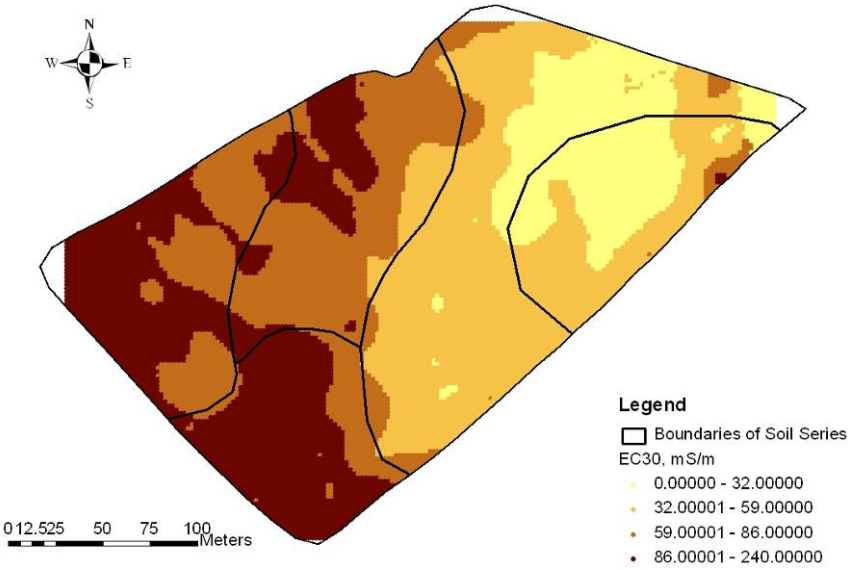

Figure 4.23 Soil electrical conductivity measured by the Conductometer within the depth range 0-0.3 m used to delineate soil texture boundaries.

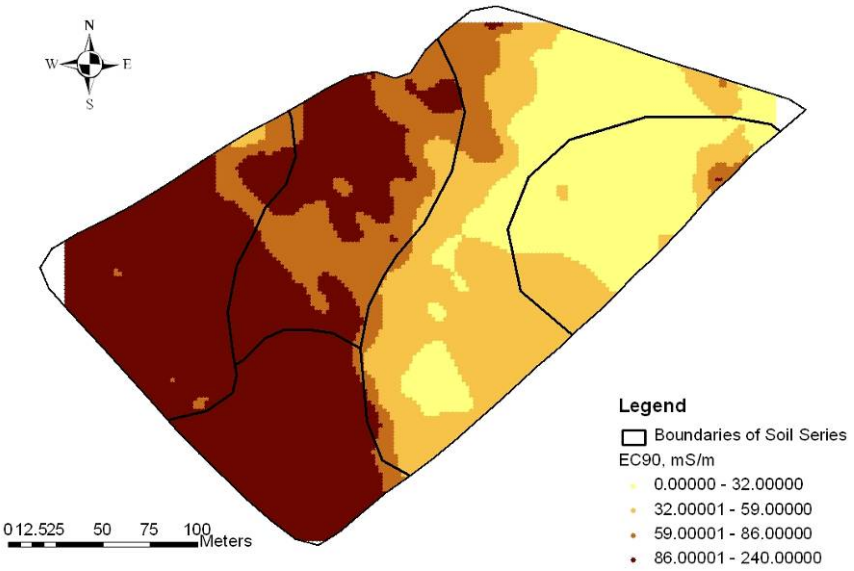

Figure 4.24 Soil electrical conductivity measured by the Conductometer within the depth range 0-0.9 m used to delineate soil texture boundaries.

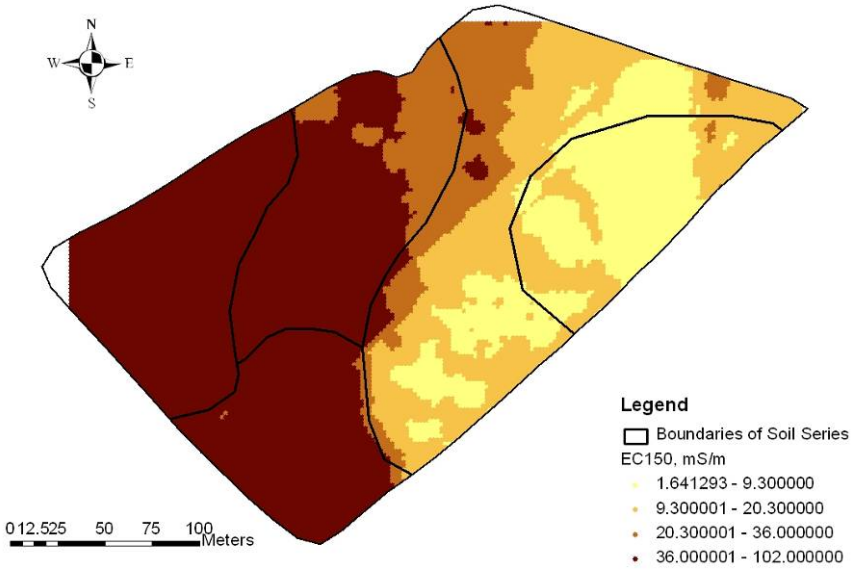

Figure 4.25 Soil electrical conductivity measured by the *EM38* within the depth range 0-1.5 m used to delineate soil texture boundaries.

4.7 Soil sampling

4.7.1 Methodology

The soil samples were collected from the sites shown in the Figure 4.2 (Chapter 4.3) one day after field survey using a soil auger. Positions of the individual sampling points were targeted on the base of soil series map and the trajectories of both EC sensors. The samples were collected from two depth ranges (0-0.3 m and 0-0.6 m). Soil samples for soil moisture by weight determination were collected into metal tins, immediately weighted, dried in the oven set at 105°C for 48 hours and re-weighted. The soil moisture by weight was subsequently determined by the formula:

$$w = \frac{m_W - m_D}{m_D} \times 100 \qquad \textbf{Equation 3}$$

where w – soil moisture by weight (%),

m_w – mass of wet soil (g),

m_D – mass of dry soil (g).

The rest of soil samples collected were intended for determination of pH, soil organic matter (loss on ignition method) and electrical conductivity by saturated paste. They were air-dried, grated and sieved using a 2 mm sieve. The laboratory analyses were conducted following the methodology given by British standards (see Appendix VIII).

4.7.2 Results and discussion of results

The soil moisture analysed in both soil profiles (0-0.3 m and 0.3-0.6 m) (Table 4.4) raises from the coarse loamy soils towards heavier clayey soils that have better water holding capacity (Figure 4.2). As the survey was performed in early spring the soil moisture content within clayey soils reached relatively high values (more than 35 %) whilst the coarsely textured soils were markedly less moist (about 15 %). The soil moisture decreased also with the raising depth within the soil profile.

Table 4.4Soil moisture by weight (%).

Sampling point	Depth	
	0-0.3 m	0.3-0.6 m
25	12.70	8.10
38	32.36	24.43
49	17.78	14.64
117	16.97	13.35
162	27.76	20.10
178	36.32	25.55

The clayey soils were well supplied by organic matter however its content within loamy soils was under averaged (Table 4.5). It is recommended to increase the portion of soil organic matter within loamy textured areas. The soil organic matter content (loss on ignition method) reached very low values at deeper soil profile (0.3-0.6 m) as expected.

Table 4.5 Soil organic matter content (Loss on ignition) (%).

Sampling point	Depth	
	0-0.3 m	0.3-0.6 m
25	4.0	2.1
38	7.0	3.9
49	4.4	2.2
117	3.4	2.1
162	6.1	3.6
178	6.3	3.4

The electrical conductivity by saturated paste is the main criterion for assessing the soil salinity (Table 4.6). As the measured values are very low (below 200 $mS.m^{-1}$), the

soils within Downings field were assessed as non-saline and no other analyses for determination of mineral elements were performed.

Table 4.6 Electrical conductivity by saturated paste (ECe, reported in mS.m^{-1}).

Sampling point	Depth	
	0-0.3 m	0.3-0.6 m
25	115.9	24.2
38	76.5	47.5
49	79.5	41.3
117	45.6	35.6
162	100.4	45.6
178	82.3	41.7

The soil pH ranged from 7.0 to 8.5 (Table 4.7) and the soil reaction was assessed as neutral (6.6-7.5) and weakly basic (7.6-9.5).

Table 4.7 Soil pH.

Sampling point	Depth	
	0-0.3 m	0.3-0.6 m
25	7.4	7.5
38	7.9	8.4
49	7.7	7.3
117	7.0	7.0
162	8.2	8.5
178	7.4	8.0

Soil texture within the Downings field was determined by Wolharn (2001). He dug several pits across the field, collected soil samples and determined the soil texture at soil profile up to 1.2 m. The results of his analyses from the pits situated closest to recent sampling points are listed in Table 4.8. They were used for visual comparison with the soil map showed in Figure 4.2 and with the above soil electrical conductivity maps and graphs.

Table 4.8 Soil texture (after Wolharn, 2001).

Sampling point	Depth range	Soil type
38	0-0.3 m	Clay
	0.3-0.6 m	Clay
	0.6-1.2 m	Clay
49	0-0.3 m	Sandy loam
	0.3-0.8 m	Loamy sand
	0.8-1.2 m	Sand
162	0-0.3 m	Sandy clay loam
	0.3-0.8 m	Clay loam
	0.8-1.2 m	Silty clay loam
178	0-0.3 m	Clay
	0.3-0.6 m	Clay
	0.6-1.2 m	Clay

4.8 Conclusions of initial field experiments

The repeatability of EC readings was tested by collecting data in two directions over the same strip of field. EC data collected by *EM38* at depth range of 0-1.5 m and by the Conductometer at depth range of 0-0.9 m showed high repeatability of performed measurement. EC collected by the Conductometer resulted in a significant difference between the first and second passes at 0-0.3 m sensing depth caused by reduced soil contact of disc coulters running in the slit created in the first run. This supports the findings of Doerge et al. (2001) in that good contact between the electrodes and the soil as a necessary condition for obtaining a reliable data but no one reported that such a small disturbance of a soil surface caused by previous run can affect the readings.

Proper contact between coulter disc electrodes and soil is an important condition for obtaining correct EC readings by the Conductometer. The lack of contact caused by lower moisture content within wheel marks or by disturbance of soil surface in repeated measurement decreased EC readings.

The EC readings of both sensors at all three surveyed depths were most affected by soil texture and moisture. This influence strongest affected the data collected by *EM38* at depth range of 0-1.5 m while the influence of the higher soil bulk density within wheel marks was negligible. The data collected by the Conductometer in both sensed profiles (0-0.3 m and 0-0.9 m) were affected by soil texture, moisture and compaction as well.

It was found out that the EC readings collected perpendicularly to the tramlines often rose nearby the location of the tramlines. This fact was confirmed by t-test and the significant difference was found for the data collected in 2.2, 3, 4 and 6 m wide strips along the tramlines whilst compared with the readings collected within the rest of the field.

The main trend in the EC data describes each soil profile and explains soil layering. Therefore the soil maps for different soil profiles and the cross-section diagram of the field can be created. It was found out that whilst the soil type in the top soil layer

changes little by little within the length of several tens of meters, the soil type at deeper layer changes suddenly within narrow area.

Removing the main trend from the initial dataset the residuals can be displayed in a map. Such a map shows some partial similarities with tramline locations. Higher degree of similarity could be probably reached by increasing the sampling frequency of the Conductometer. The sampling frequency of the original Conductometer configuration was too low (only 0.2 Hz) and the data represented the area along few meter long trajectory (5-6 m). Therefore it was not possible to rapidly collect enough readings to describe the differences within such a spatially variable parameter as soil bulk density at tramline wheelings.

Changes in the penetration depth of the coulter disc electrodes affected the EC readings in opposite way as the soil bulk density and the changes caused by the depth of electrodes were negligible in comparison with the changes involved by soil bulk density.

5 Randomized block design (RBD) experiment

5.1 Introduction

The results of the initial field experiments show the high variability of EC readings. The analyses of the data shown the EC readings were affected not only by variation of soil bulk density or soil compaction but probably also by others from whole range of soil properties that affect the soil EC (see Chapter 2.3.3). This was the most important reason which affected the location of the following experiment.

In order to investigate the dependency between soil EC and soil bulk density it was requested to exclude all other soil properties that can affect the soil EC. It was necessary to perform the experiment within an area with relatively homogeneous soil environment. Because of the above reasons part of the Avenue field was chosen as an experiment field.

5.2 Site characteristics

Following experiment was performed within a part of the Avenue field located in the North of Silsoe College Farm (see Figure 4.1 in Chapter 4.3). The Avenue field is characteristic by a presence of four different soil series (Figure 5.1). The soil is mostly loamy textured with a little of clay in Southern corner of the field. The area falling into Rivington soil series was chosen for placing the randomised block design experiment. The soil samples were collected in order to describe the soil properties within the experimental site. Monitored soil characteristics as pH, soil organic matter content (loss on ignition method), electrical conductivity by saturated paste and particle size distribution are described in detail in Chapter 5.5.2.

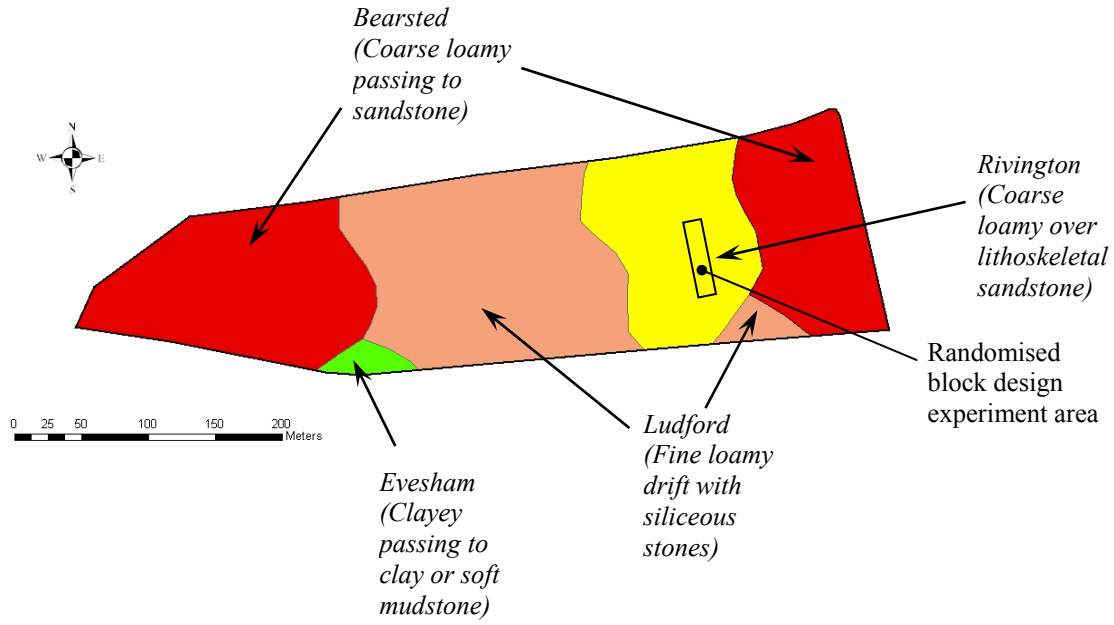

Figure 5.1 Soil series present within Avenue field (Soil Data© Cranfield University (NSRI) 2007).

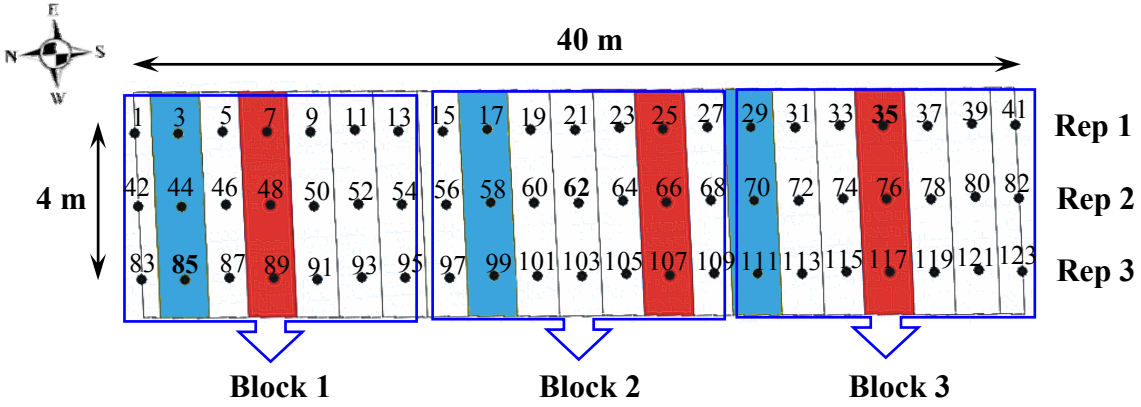

Figure 5.2 Layout of randomised block experiment performed within trial plot within Avenue field. Individual treatments were as follows: White – Compacted soil at whole profile, Blue – Soil compacted at depth of 0.6 m, and Red – Soil compacted at depth of 0.3 m. Soil core sampling points are labelled as 35, 62 and 85.

5.3 Methodology

The experiment was situated within Avenue field within Rivington soil series as shown in Figure 5.1. There were two important criterions that affected the selection of this area. One of them was the surface of the Avenue field which was flat and not grown by any cover crop. This was an advantage because the crop could potentially

affect the soil water content within the sensed profile as it was in experiment performed within Sports ground. Next, even more important criterion for selecting the Avenue field as an experimental field results from following: It is well known that it is much easier to change the soil bulk density by loosening a compacted soil than by attempting to compact a loose one. The soil within the selected part of Avenue field had already a higher soil bulk density raised by frequent field traffic.

In order to investigate the relationship between soil EC readings and soil compaction, and to control the soil conditions the layout of randomised block design experiment was chosen. The area of 40 m x 4 m was chosen as a trial plot (Figure 5.2). It was divided into three blocks with three replications. Each block contained 5 control treatments with compacted soil at whole profile, one treatment soil strip that was compacted below the depth of 0.3 m and one treatment with a compacted layer below the depth of 0.6 m. The initially compacted soil in the top layers of the two treatment strips were loosened using a Cousin V-form winged subsoiler with 5 legs at 0.5 m spacing. The trial plot was surveyed using the Conductometer, *EM38*, penetrometer and soil compaction sensor before and after treatment applying. All measurements were performed either in or within very close range around each of 63 measuring points regularly distributed across the trial plot. The Conductometer was used for EC data collecting in both stationary and dynamic mode. EC readings were logged for time of 1 minute while operated in stationary mode. Two different speeds (0.05 $m.s^{-1}$ and 1 $m.s^{-1}$) were tested while the instrument operated in dynamic mode. The average of EC readings collected within the radius of 0.5 m from each measuring point was used for further evaluation.

The EC data were obtained also using the *EM38* operated stationary in both vertical and horizontal mode. However because of the shortage of time the horizontal sensing mode was used only after treatment application. Data was logged about 30 seconds in each point using *Farm Works Software*® running in PDA. The averages from each point were used for the further evaluation.

Penetration resistance readings were collected using the Eijkelkamp penetrologger described in Chapter 3.1. Three penetrations to depth of 0.5 m were done in each

measuring point. Because of different cone base cross section area and the different strength action during the countersinking, the readings at depth range of 0-0.1 m were not taken into account. The rest of the data was averaged for each measuring within two depth intervals 0.1-0.3 m and 0.1-0.5 m. Such data was used in statistical analyses and compared with other datasets.

The soil strength was sensed by soil compaction sensor which was drawn across the trial plot by tractor at speed about 0.25 $m.s^{-1}$. The soil compaction sensor had to be attached on the frame of subsoiler equipped with two V-forms that helped to get the instrumented tine into the soil and keep lateral stability. As the V-forms loosen the soil within the whole trial plot, this device was used only after treatment application as the last measurement. The soil strength acting on the wedges of an instrumented tine induced a bending moment which was recorded at four depth ranges from 0.2 m to 0.4 m divided into 50 mm intervals. Average from whole sensed profile was used in ANOVA. The averages from individual depths were used for regression analysis with the soil penetration resistance readings obtained within related depths.

5.4 Results and discussion of results

5.4.1 Conductometer compaction measurements - stationary and dynamic

The EC readings were obtained using the Conductometer operated in both stationary and dynamic mode before and after soil loosening. The readings obtained before treatment applying are characterized by uniformity in that they vary negligibly across the field. The slight increase was reported within the third block and it was probably caused by slightly higher amount of the clay in deeper soil layers (see Chapter 5.4.7). The overall view on the EC data collected in dynamic mode is similar to the pattern obtained in stationary mode (Figure 5.3 - Figure 5.6). However the dynamically collected EC readings were more variable what was caused by constantly varying circumstances like the presence of stones on the soil surface and unlevelled surface and the lack of electrical contact in some locations. This finding is supported by Doerge et al. (2001) who says that the good contact between the soil and sensing electrodes is a necessary condition for obtaining a reliable data. The effect of lower

soil bulk density or soil loosening caused the decreasing of EC. This change is more visible in the soil with higher clay content (Block 3) where the initial EC readings reached higher values and the readings after soil loosening decreased more obviously.

The different depths of soil compacted layer presence are not reflected equally in all datasets. The readings collected by the Conductometer in shallow soil depth are most sensitive to the changes of soil bulk density. The lower bulk density in topsoil layer and the presence of compacted layer in both shallow and deeper soil profile are expressed by the similar decreasing measured values (Figure 5.4 and Figure 5.6).

The EC readings related to the deeper soil profile (0-0.9 m) are obviously affected by the lower soil bulk density appearing within the larger soil depth range (0-0.6 m) (Figure 5.4 and Figure 5.6). The soil with the compacted layer presented at shallow depth (0.3 m) shows the similar results as the soil compacted within whole profile. It means that by utilisation of EC readings related to both shallow (0-0.3 m) and deep (0-0.9 m) soil profiles the user might be able to identify and distinguish the areas with no compaction above 0.3 m, areas with no compaction above 0.6 m and areas compacted within whole soil profile.

Next evaluation was performed by comparing the ratios of the readings obtained before and after treatment applying (within compacted and loosened soil). The ratio was preferred to compare relative differences instead of comparing the absolute differences that might be more affected by soil moisture. The ratio of EC readings obtained by the Conductometer operated in stationary mode was highly significantly different between compacted and treated (loosened) areas. However non-significant difference was found out between the treatments containing the compacted layer in deeper and shallower soil profile (Table 5.1). The overall review of ANOVA results for all evaluated datasets is listed in Table 5.1 and in Appendix IX.

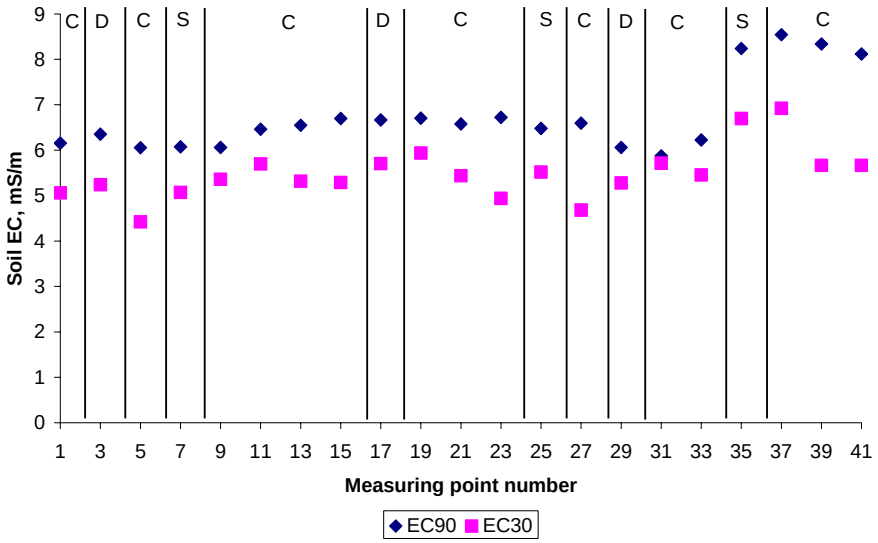

Figure 5.3 EC readings obtained by the Conductometer operated in stationary mode from the trial plot at both depth ranges 0-0.3 m and 0-0.9 m before treatment applying. C-Control (Compacted), D-Deep compaction (0.6m), S-Shallow compaction (0.3m).

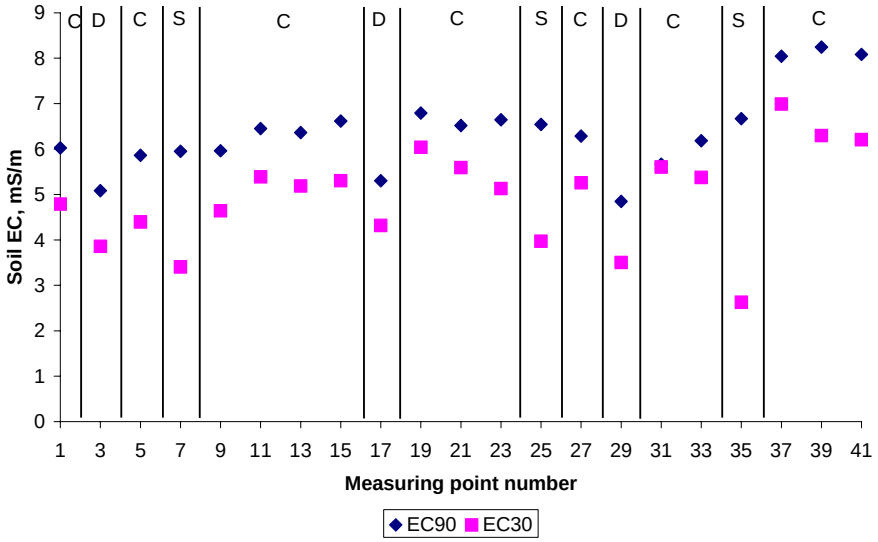

Figure 5.4 EC readings obtained by the Conductometer operated in stationary mode from the trial plot at both depth ranges 0-0.3 m and 0-0.9 m after treatment applying. C-Control (Compacted), D-Deep compaction (0.6m), S-Shallow compaction (0.3m).

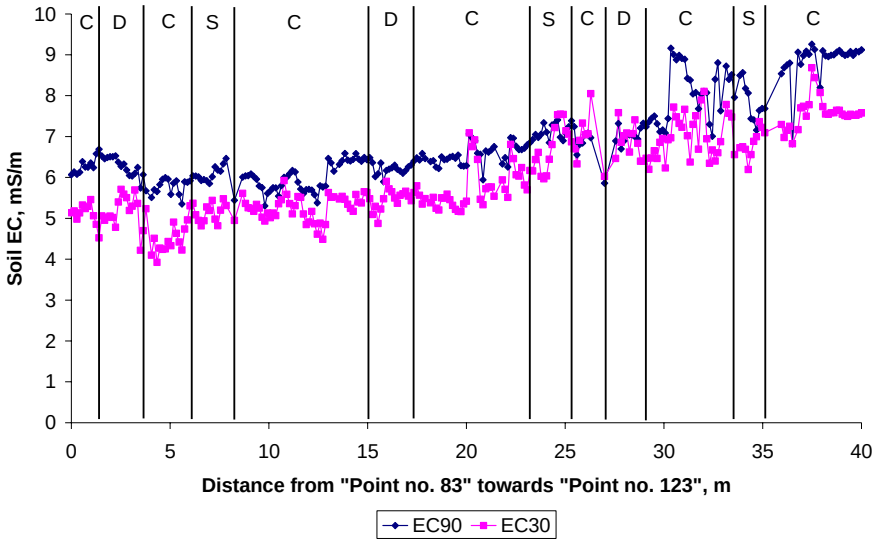

Figure 5.5 EC readings obtained by the Conductometer operated in dynamic mode (at speed of 0.05 m.s^{-1}) from the trial plot at both depth ranges 0-0.3 m and 0-0.9 m before treatment applying. C-Control (Compacted), D-Deep compaction (0.6m), S-Shallow compaction (0.3m).

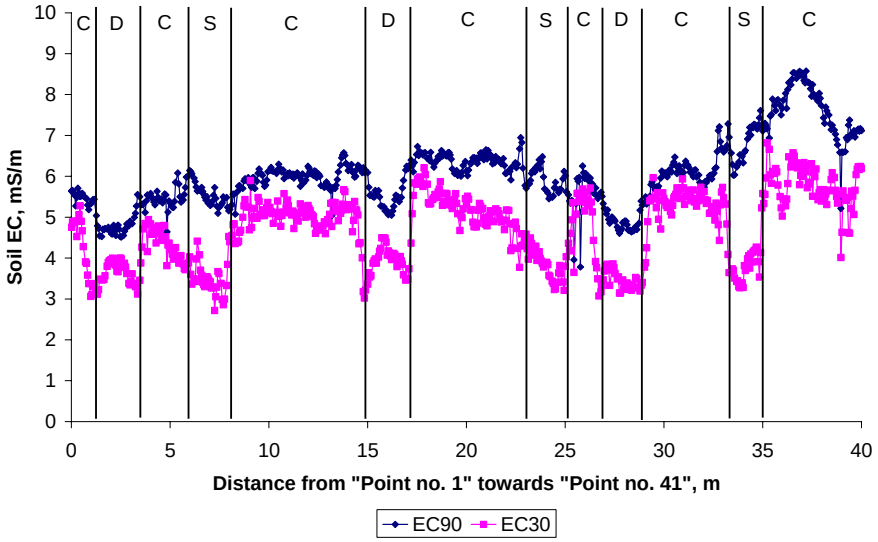

Figure 5.6 EC readings obtained by the Conductometer operated in dynamic mode (at speed of 0.05 m.s^{-1}) from the trial plot at both depth ranges 0-0.3 m and 0-0.9 m after treatment applying. C-Control (Compacted), D-Deep compaction (0.6m), S-Shallow compaction (0.3m).

EC data collected by the Conductometer in both stationary and dynamic mode (at speed of 0.05 m.s^{-1}) were plotted to scatter plot. The coefficient of regression (R^2) was equal to 0.89 and 0.92 for soil depth ranges of 0-0.3 m and 0-0.9 m respectively (Figure 5.7 and Figure 5.8).

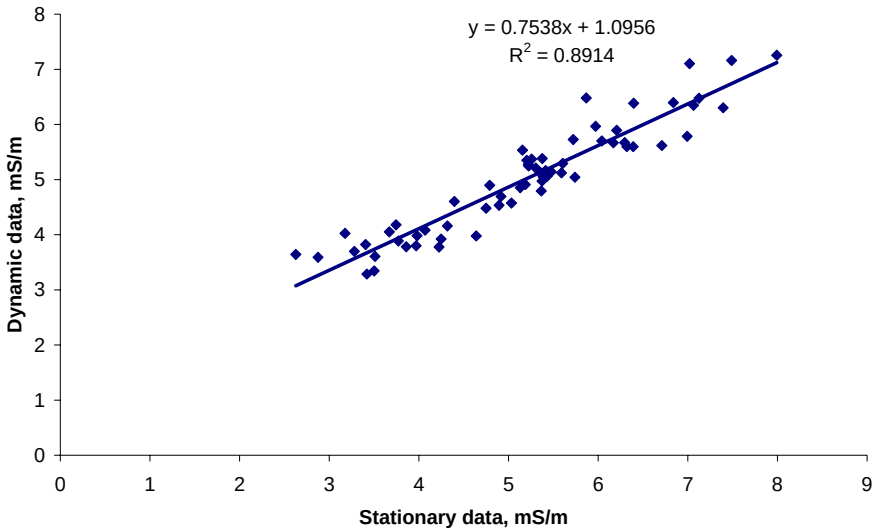

Figure 5.7 Scatter plot of EC readings collected by the Conductometer at depth of 0-0.3 m in stationary and dynamic mode (at speed of 0.05 m.s^{-1}).

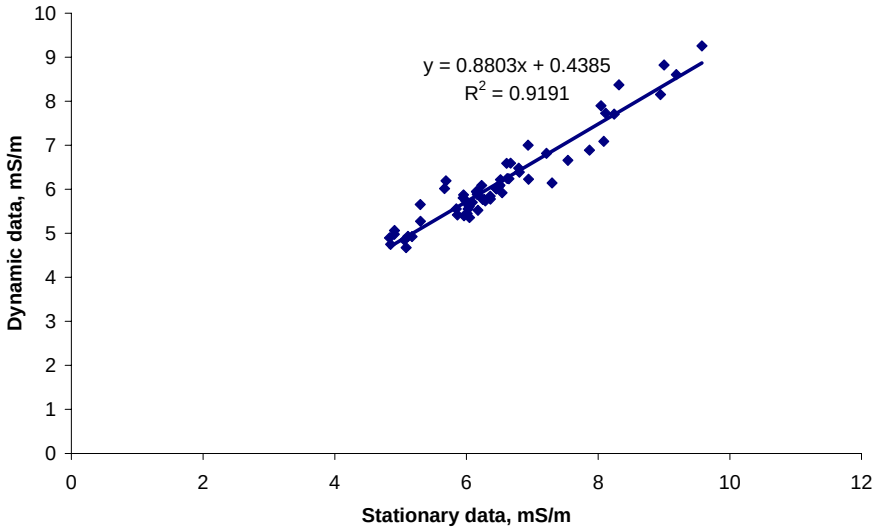

Figure 5.8 Scatter plot of EC readings collected by the Conductometer at depth of 0-0.9 m in stationary and dynamic mode (at speed of 0.05 m.s^{-1}).

5.4.2 Compaction treatment maps using Conductometer EC data

The EC readings collected stationary during the time of 1 minute in every measuring point were averaged. As the overall number of measuring points is too low for using kriging, the maps of EC spatial variability were created using "inverse distance weighting" (IDW) method under "spatial analyst" within ArcGIS software package (Figure 5.9 and Figure 5.11). The EC intervals for both datasets obtained in the particular depth before and after treatment applying were set manually with the aid of ANOVA results. Using the same intervals the differences between both maps (created before and after soil loosening) are clearly visible. The targeted application of soil loosening can be suggested either on the base of visual comparison both maps, or using simple ratio.

Visual comparison of EC maps related to the both sensed depth ranges (0-0.3 m and 0-0.9 m) obtained after treatement application enables user to distinguish the areas with three different depths of soil compaction. Map of EC30 is able to distinguish the areas with no compaction above 0.3 m from those compacted within whole profile. EC90 allows to distinguish the areas with no compaction above 0.6 m from the rest of the field. Using and comparing both maps the areas with no compaction above 0.3 m, areas with no compaction above 0.6 m and areas compacted within whole soil profile can be identified.

The relationship between EC maps related to the particular soil depth ranges obtained before and after soil loosening was calculated as a ratio with a view to minimize the influence of other factors (e.g. soil moisture) affecting the EC readings. Such application maps created using simple ratio are shown in Figure 5.10 and Figure 5.12. Figure 5.10 was created as a ratio of EC30 measured before treatment applying and after treatment application. The yellow areas represent the zones of the soil compacted within whole profile. Figure 5.12 shows the application map created similarly on the base of the EC readings collected at depth range of 0-0.9 m. The yellow and orange areas represent the areas compacted above the depth of 0.6 m. The error occurs in the southernmost strip displayed by dark brown. It is because the EC ratio reached higher values within this location. As this strip represents the area with the compacted layer

presented below 0.3 m, if it would be desirable to remove the compaction which occurs above 0.6 m, this zone would remain untreated. From this point of view it might be preferable to compare both maps (related to loosen soil and to potentially compacted soil) visually and subsequently manually propose the zones that should be treated.

The maps of EC readings collected in dynamic mode at speed of 0.05 $m.s^{-1}$ show similar patterns as the maps of EC readings collected stationary (see Figure XI.1 and Figure XI.3 in Appendix XI). However the application maps (Figure XI.2 and Figure XI.4 in Appendix XI) created on the base of dynamic data using simple ratio tool are less precise. It is supposed that the lower precision of application map is caused by possible shifts that could occur in georeferencing of the EC data. The GPS coordinates of the stationary and low speed collected EC readings were scattered around their real locations and had to be adjusted additionally during data processing on the base of known distance, time and positions of the first and last point (Figure XII.1 - Figure XII.3 in Appendix XII). For further collecting of stationary data it would be recommended to use either an averaging data logging system or a more accurate GPS (e.g. sub meter).

The EC data obtained in dynamic mode at speed of 1 $m.s^{-1}$ were collected very sparsely. Potential incorrect readings (caused e.g. by the lack of contact between the soil and the coulter disc electrodes) subsequently introduced the error into obtained dataset. This was confirmed by the analysis of variance (ANOVA) which showed significant difference only between EC30 obtained from control (compacted) and treated (loosened) areas but non-significant difference for the rest of measurements collected within different treatments. Therefore the EC readings collected at speed of 1 $m.s^{-1}$ were not used for creating of map of spatial variability.

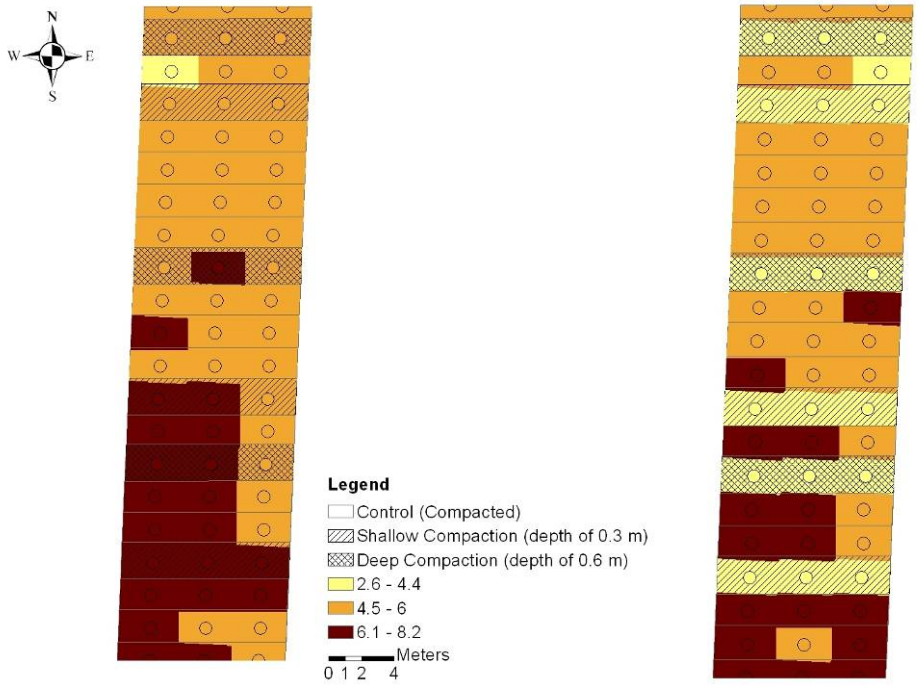

Figure 5.9 Map of EC readings obtained by the Conductometer operated in stationary mode from the trial plot at depth range of 0-0.3 m before (left) and after (right) treatment applying. EC values are displayed in mS.m^{-1}. Yellow areas (right) represent no compaction above 0.3 m.

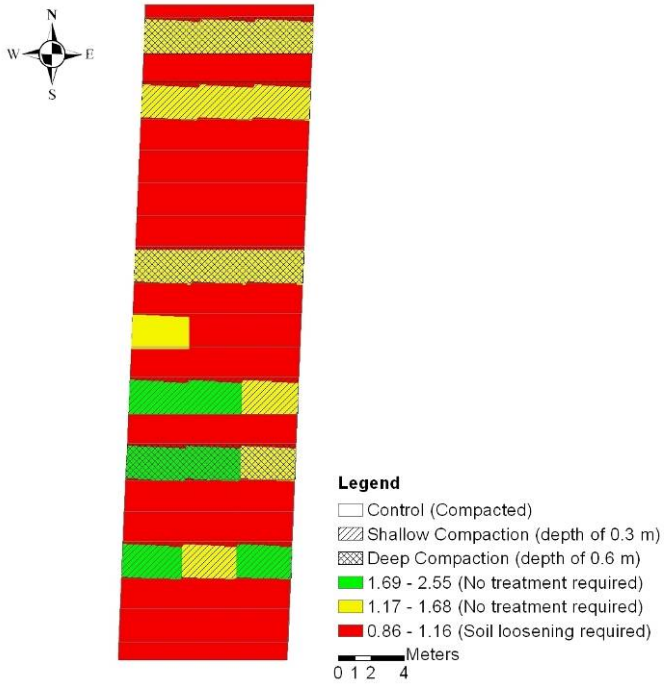

Figure 5.10 Application map created by "EC30 before treatment application / EC30 after treatment application" (simple ratio). The areas displayed by red are identified as being compacted within whole soil profile.

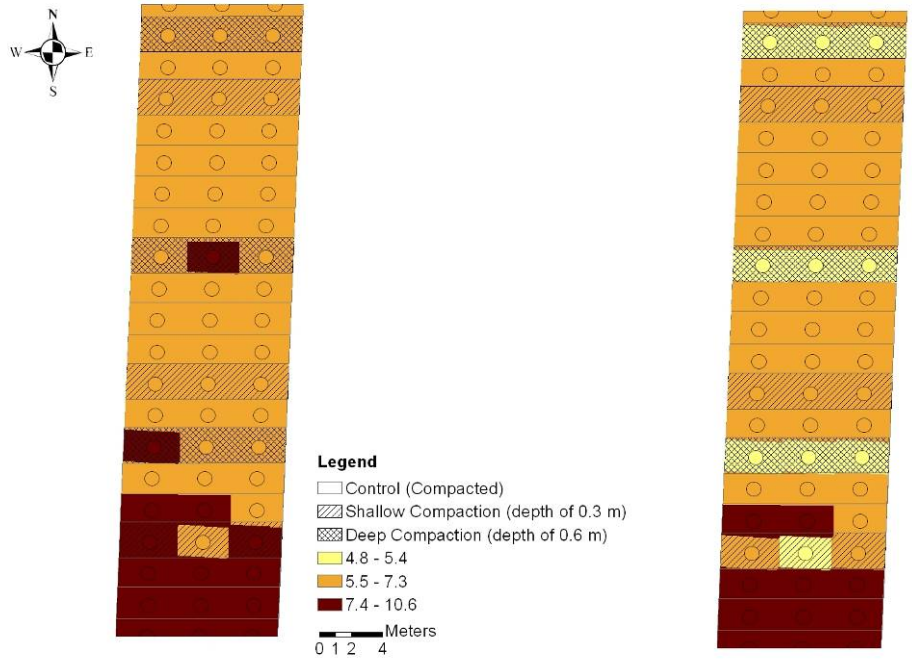

Figure 5.11 Map of EC readings obtained by the Conductometer operated in stationary mode from the trial plot at depth range of 0-0.9 m before (left) and after (right) treatment applying. EC values are displayed in mS.m^{-1}. Yellow areas (right) represent no compaction above 0.6 m.

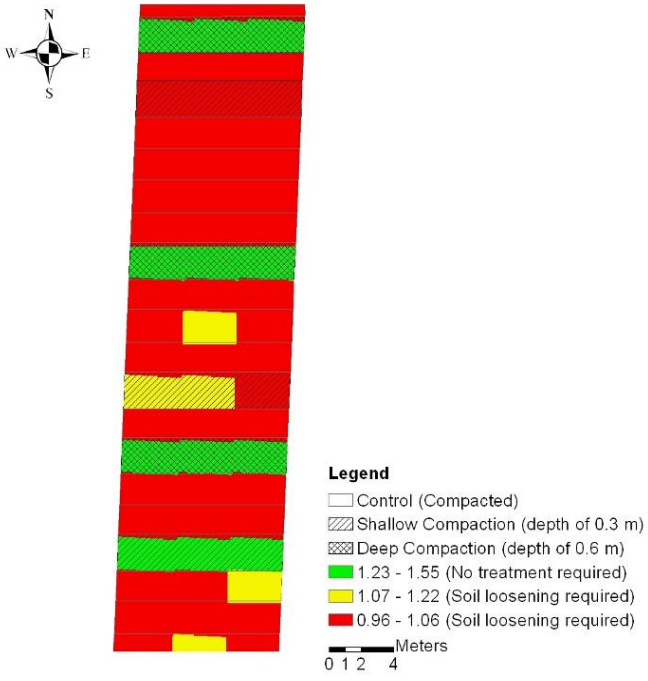

Figure 5.12 Application map created as "EC90 before treatment application / EC90 after treatment application" (simple ratio). The areas displayed by red and yellow are identified as being compacted above 0.6 m.

5.4.3 *EM38* compaction measurements

The EC readings obtained by the contact-less instrument *EM38* operated in vertical mode (depth of sensing 0-1.5 m) do not reflect the soil bulk density conditions. This can be seen either in the Figure 5.13 and Figure 5.14 or in the results of analyse of variance (ANOVA) which showed non-significant difference between any treatments (Table 5.1). It is supposed that some other soil properties have stronger contribution to the signal then the soil bulk density. However the EC readings obtained by the same instrument operated in horizontal mode (depth of sensing 0-0.75 m) are affected by soil bulk density. ANOVA showed highly significant difference between data collected within treated and compacted areas (Table 5.1). Map of spatial variability of EC readings obtained by *EM38* operated in horizontal mode is shown in Figure 5.16. In this case the yellow areas are identified as those with no compaction above 0.3 m. The error occurs in southernmost strip containing the compacted layer at depth of 0.3 m. The most of this strip is identified as a soil compacted within whole profile. Unfortunately, because of the shortage of the time, the *EM38* was not used in horizontal mode before treatment application. Therefore the map of an original condition and the application map could not be created.

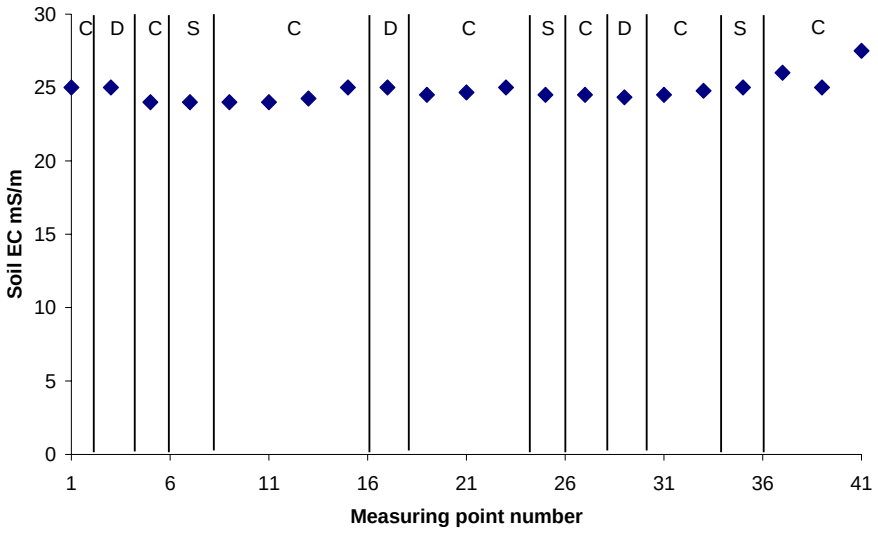

Figure 5.13 EC readings obtained by *EM38* operated in vertical mode from the trial plot at depth range 0-1.5 m before treatment applying. C-Control (Compacted), D-Deep compaction (0.6m), S-Shallow compaction (0.3m).

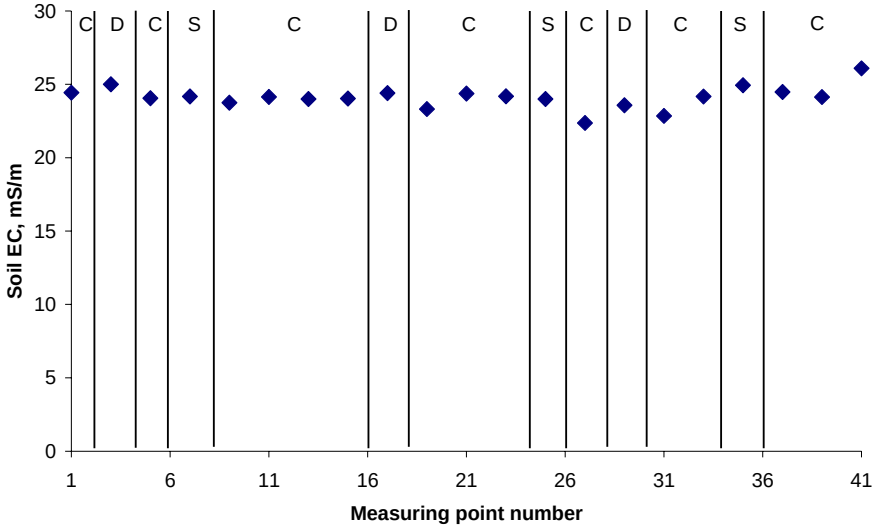

Figure 5.14 EC readings obtained by *EM38* operated in vertical mode from the trial plot at depth range 0-1.5 m after treatment applying. C-Control (Compacted), D-Deep compaction (0.6m), S-Shallow compaction (0.3m).

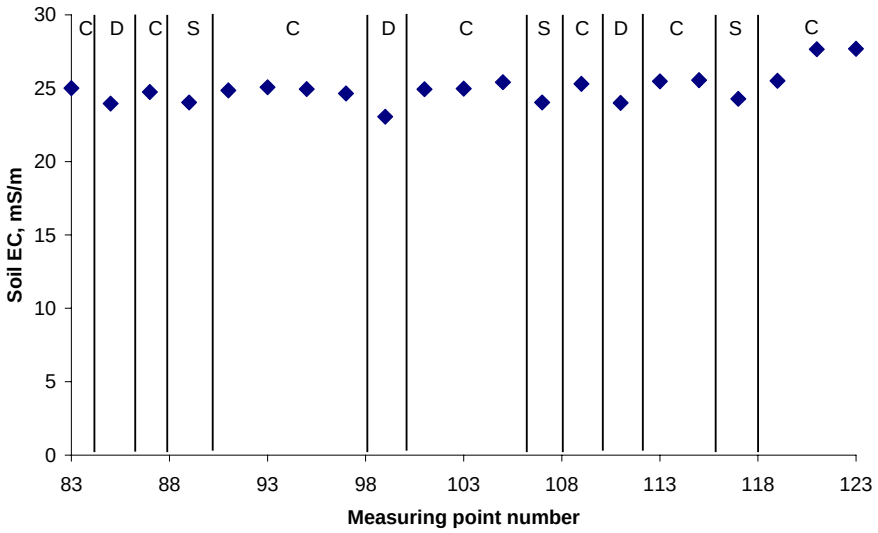

Figure 5.15 EC readings obtained by *EM38* operated in horizontal mode from the trial plot at depth range 0-0.75 m after treatment applying. C-Control (Compacted), D-Deep compaction (0.6m), S-Shallow compaction (0.3m).

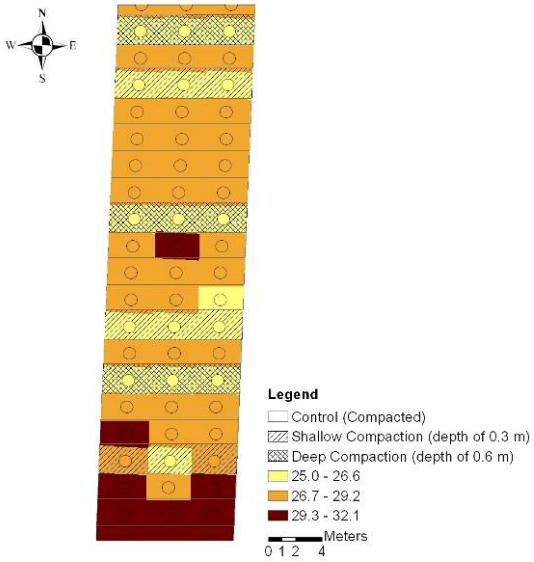

Figure 5.16 Map of EC readings obtained by the EM operated in horizontal mode from the trial plot at depth range of 0-0.75 m after treatment applying. EC values are displayed in $mS.m^{-1}$. Yellow areas represent no compaction above 0.3 m.

5.4.4 Penetrometer compaction measurements

Penetration resistance was measured to the depth of 0.5 m. The diagram of the penetration resistance readings obtained using the Eijkelkamp penetrologger within different treatments is shown in Figure 5.17. Because of the incorrect readings that may occur near the soil surface, the readings obtained within the depth range 0-0.1 m were not taken into account. The rest of the readings was averaged within two depth ranges (0.1-0.3 m and 0.1-0.5 m) and evaluated using the analysis of variance (ANOVA). The results of the analysis showed that the penetration resistance readings averaged within both examined soil profiles are highly significantly different between compacted and any of treated areas and also there are significant differences between areas containing compacted layer under the depth of 0.3 m and 0.6 m (Table 5.1, Figure 5.18 and Figure 5.19).

Averaged soil penetration resistance readings were used for creating the maps of spatial variability (Figure 5.20 and Figure 5.22). It can be clearly seen that the soil penetration resistance is the parameter most sensitive on the changes of soil bulk density among all investigated parameters. Subsequently the application maps (Figure 5.21 and Figure 5.23) were created following the same procedure as was used for

processing the soil electrical conductivity data based on ratio before and after application. However some errors again occur in the application maps created as a ratio of the readings collected before and after soil loosening. Therefore it would be recommended to compare maps visually.

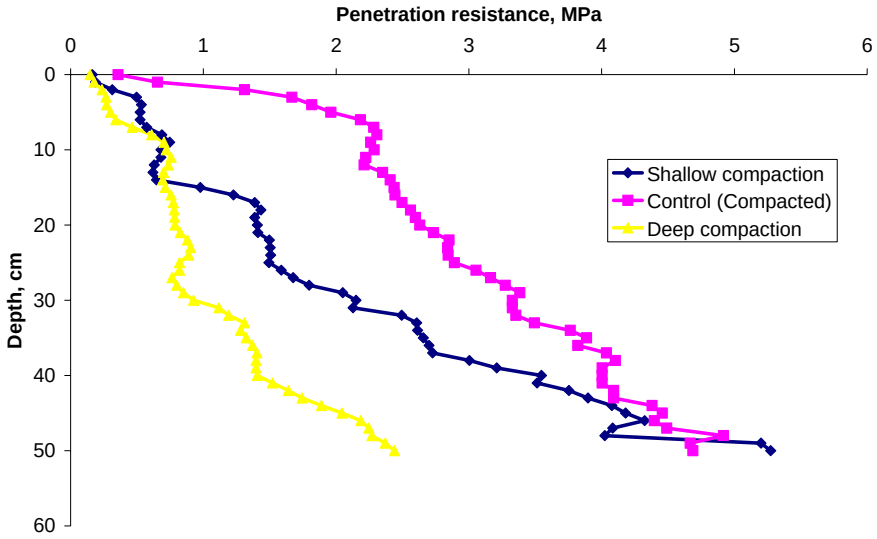

Figure 5.17 Diagram of soil penetration resistance measured within different treatments (Shallow compaction (0.3 m) – measuring point no. 35, Control (Compacted) – measuring point no. 62, Deep compaction (0.6 m) – measuring point no. 85).

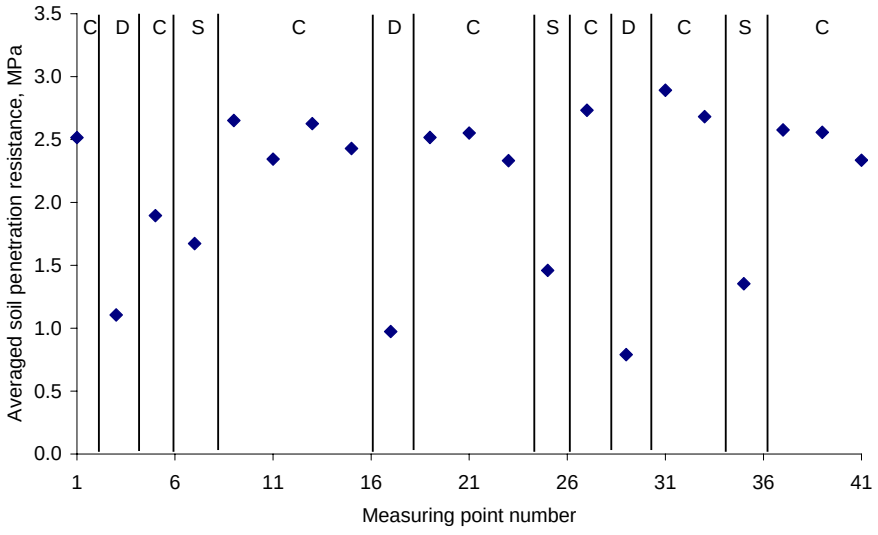

Figure 5.18 Soil penetration readings obtained from the trial plot after treatment applying and averaged at depth range 0.1-0.3 m. C-Control (Compacted), D-Deep compaction (0.6m), S-Shallow compaction (0.3m).

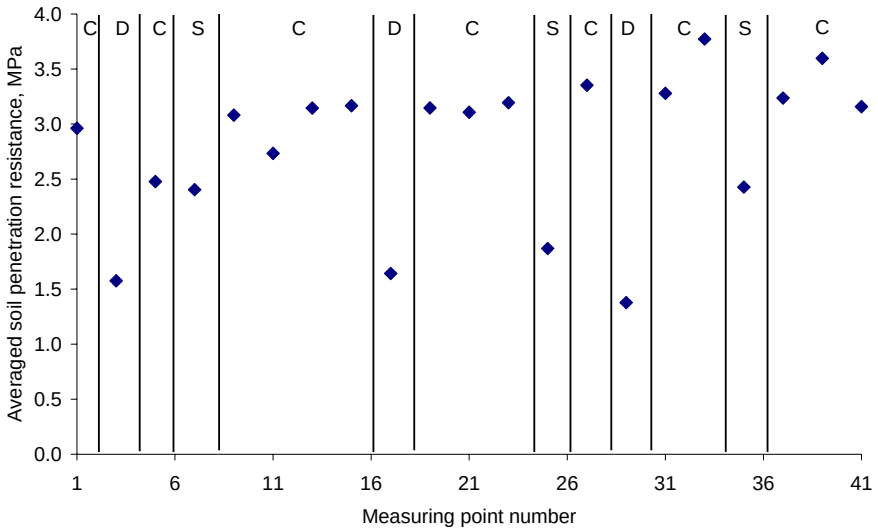

Figure 5.19 Soil penetration readings obtained from the trial plot after treatment applying and averaged at depth range 0.1-0.5 m. C-Control (Compacted), D-Deep compaction (0.6m), S-Shallow compaction (0.3m).

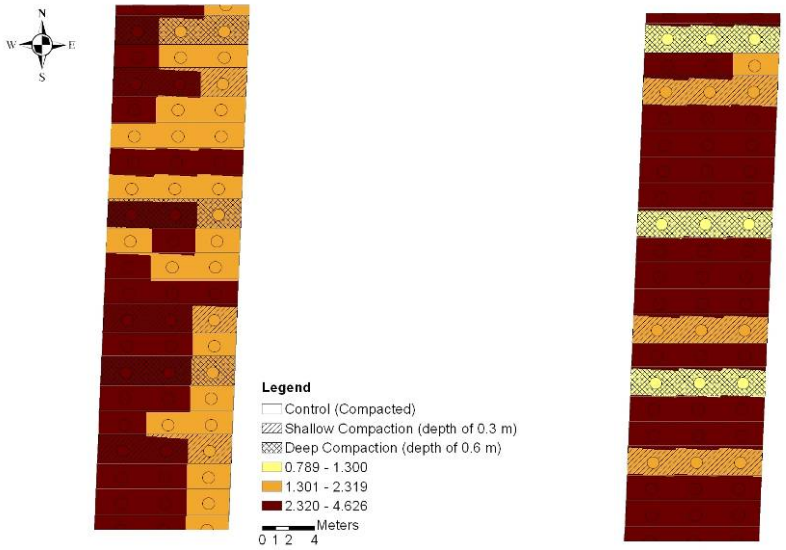

Figure 5.20 Map of soil penetration resistance readings obtained from the trial plot and averaged at depth range of 0-0.3 m before (left) and after (right) treatment applying. Values are displayed in MPa. Yellow areas (right) represent no compaction above 0.6 m, orange areas represent no compaction 0.3 m and brown areas represent soil compacted within whole profile.

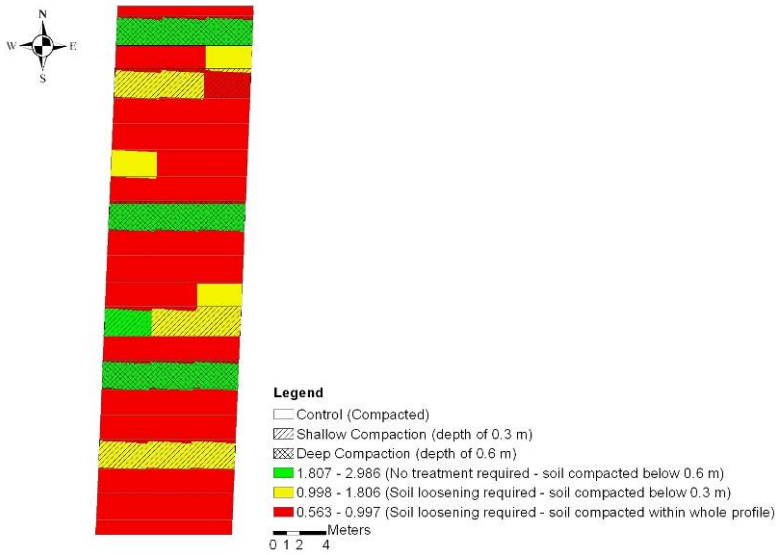

Figure 5.21 Application map created by "PR30 before treatment application / PR30 after treatment application" (simple ratio). Green areas - deep compaction (0.6 m); Yellow areas - shallow compaction (0.3 m); Red – soil compacted within whole profile.

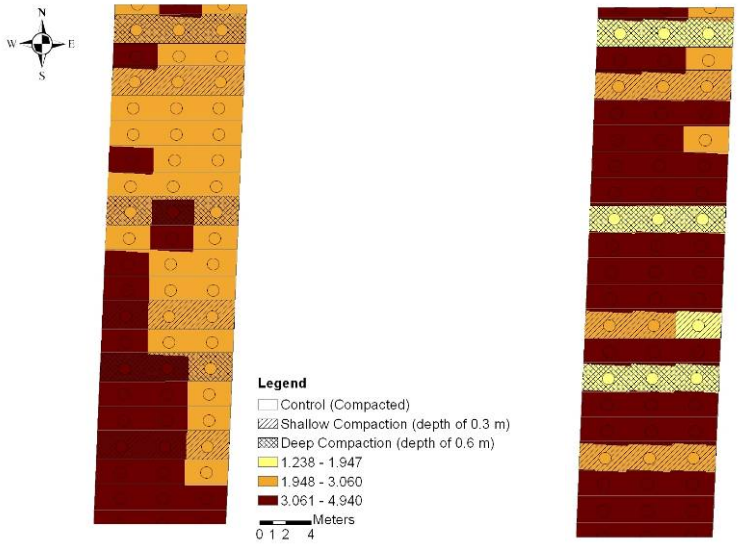

Figure 5.22 Map of soil penetration resistance readings obtained from the trial plot and averaged at depth range of 0-0.5 m before (left) and after (right) treatment applying. Values are displayed in MPa. Yellow areas (right) represent no compaction above 0.6 m, orange areas represent no compaction 0.3 m and brown areas represent soil compacted within whole profile.

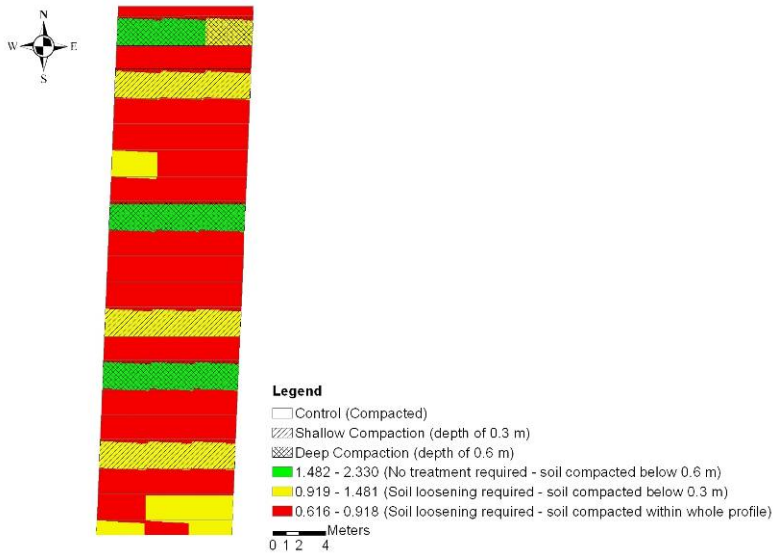

Figure 5.23 Application map created by "PR50 before treatment application / PR50 after treatment application" (simple ratio). Green areas - deep compaction (0.6 m); Yellow areas - shallow compaction (0.3 m); Red – soil compacted within whole profile.

5.4.5 Soil compaction sensor

A soil compaction sensor was used for measuring of bending moment which was introduced by soil strength acting on the wedges of an instrumented tine. The bending moment measured across the trial plot between measuring points number 1 and 41 is shown in Figure 5.24. It can be seen that the different treatments are clearly visible. The averages of the readings collected within individual treatments in all sensed depths were evaluated by ANOVA. The results confirmed the highly significant difference which can be found between both control and any of applied treatments and also between readings obtained from the areas containing deep and shallow compaction (Table 5.1). The averaged readings obtained by the soil compaction sensor from four depths were used for creating the map of spatial variability which is shown in Figure 5.25. The map of bending moment identifies the compacted areas well, but some errors occurred in southernmost part of the trial plot around the shallow compacted area. The absolute readings of bending moment obtained within this area are affected by the differences in soil texture which is slightly heavier and contains more clay particles (see Chapter 5.5.2).

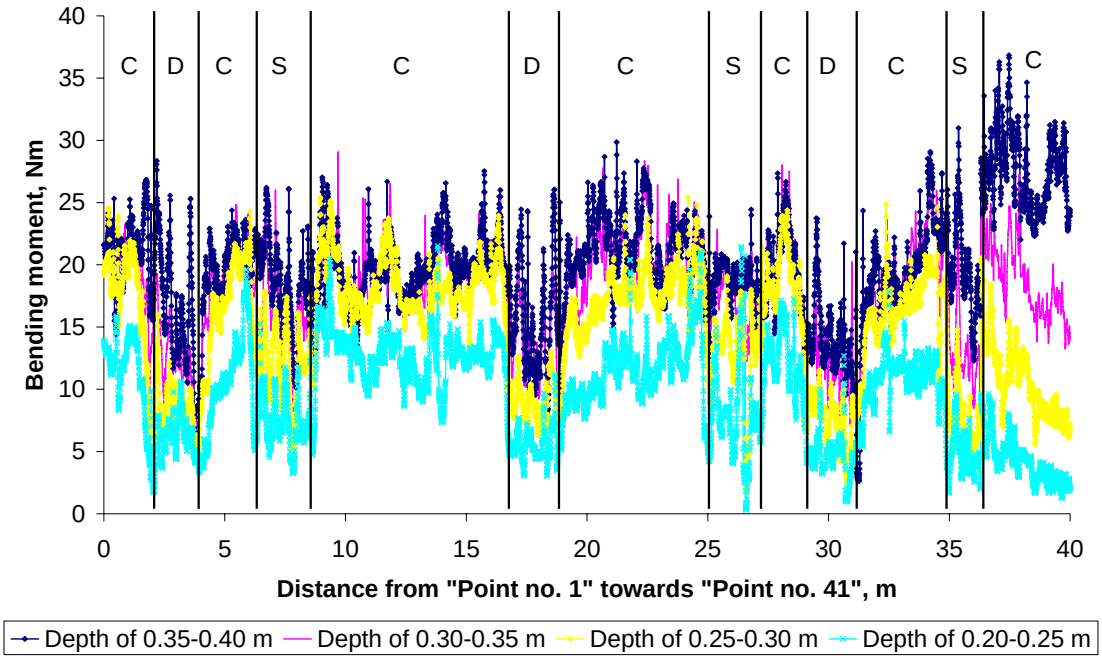

Figure 5.24 Bending moment measured by soil compaction sensor within the trial plot at multiple depth ranges. C-Control (Compacted), D-Deep compaction (0.6m), S-Shallow compaction (0.3m).

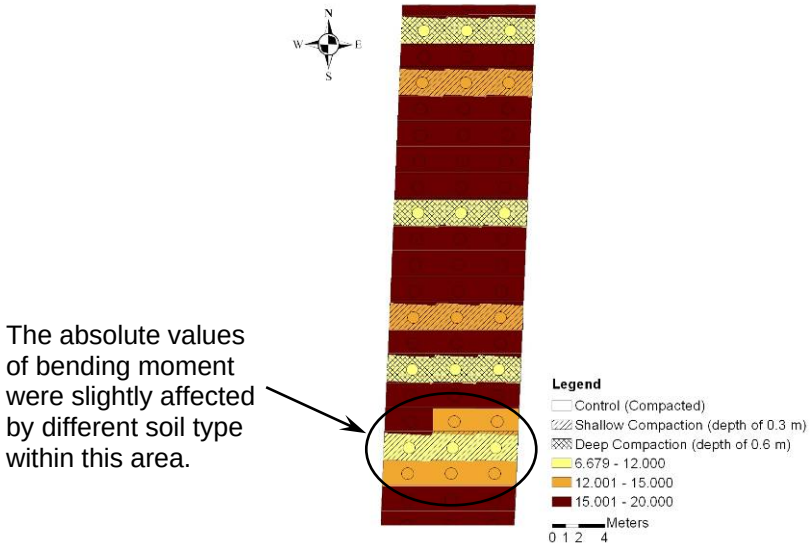

Figure 5.25 Map created on the base of the bending moment readings sensed by the soil compaction sensor obtained from the trial plot after treatment applying. The values are displayed in Nm. Yellow areas are identified as not being compacted above 0.6 m, orange areas as not being compacted above 0.3 m and brown areas as being compacted within whole soil profile.

5.4.6 Summary of ANOVA for RBD experiment

The overall summary of analysis of variance (ANOVA) which was performed for the data collected in this research are listed in Table 5.1. This table shows the signification of differences of individual measurements between different treatments.

Table 5.1 Summary table of the ANOVA showing the signification of differences of individual measurements performed within different treatments (* - significant difference at the confidence interval of 95%, ** - highly significant difference at the confidence interval of 99%, NS – non-significant difference).

Parameter, Conditions of measurement Instrument	Control vv Treatment	Deep vv Shallow
EC30 (stationary) Conductometer	**	NS
EC90 (stationary) Conductometer	*	NS
EC150 (stationary) *EM38* vertical mode	NS	NS
EC75 (stationary) *EM38* horizontal mode	**	NS
Penetration resistance PR30 (stationary) Cone penetrometer	**	*
Penetration resistance PR50 (stationary) Cone penetrometer	**	*
Bending moment (0.25 $m.s^{-1}$) Soil compaction sensor	**	**
EC30 (0.05 $m.s^{-1}$) Conductometer	**	NS
EC90 (0.05 $m.s^{-1}$) Conductometer	*	NS
EC30 (1 $m.s^{-1}$) Conductometer	*	NS
EC90 (1 $m.s^{-1}$) Conductometer	NS	NS
Ratio EC90 (stationary) Conductometer	**	NS

Continuing of Table 5.1.

Parameter, Conditions of measurement Instrument	Control vv Treatment	Deep vv Shallow
Ratio EC30 (stationary) Conductometer	**	NS
Ratio EC150 (stationary) *EM38* vertical mode	NS	NS
Ratio Penetration resistance PR30 (stationary) Cone penetrometer	**	*
Ratio Penetration resistance PR50 (stationary) Cone penetrometer	**	**
Ratio EC30 (0.05 $m.s^{-1}$) Conductometer	**	NS
Ratio EC90 (0.05 $m.s^{-1}$) Conductometer	**	**
Ratio EC30 (1 $m.s^{-1}$) Conductometer	*	NS
Ratio EC90 (1 $m.s^{-1}$) Conductometer	*	NS

5.4.7 Regression analysis

The regression analysis was performed for the EC readings, penetration resistance and bending moment obtained within different depths. The best relationship was found out for the EC30 versus PR30 and for EC30 versus PR50 (see Figure X.1 and Figure X.5 in Appendix X). The graphs plotted for the EC versus SCS and for PR versus SCS were more scattered (see Figure X.4, Figure X.9 - Figure X.12 and Figure X.14 - Figure X.17 in Appendix X). The dependency between PR and EC150 and also between SCS and EC150 was not correlated (see Figure X.3, Figure X.8 and Figure X.13 in Appendix X) and there was no significant difference to zero found. The graphs listed in Appendix X can be used as the calibration lines for future measurements but the measuring conditions have to be close to those mentioned in Chapter 5.5.2.

5.5 Soil sampling

5.5.1 Methodology

The soil samples were collected using a soil auger on 5th June 2007, just one day after first field survey. Location of each of three sampling points was targeted into different intended treatment within different blocks. The samples were collected from two depth ranges (0-0.3 m and 0-0.6 m). Soil samples for soil moisture by weight determination were collected after soil survey performed both before and after treatment application. Soil samples for determination pH, soil organic matter content (loss on ignition), electrical conductivity by saturated paste and soil particle size were collected only once after first field survey. The subsequent processing of soil samples was performed by methodology mentioned in Chapter 4.7.1 and in Appendix VIII.

5.5.2 Results and discussion of results

The soil environment within randomised block design trial plot was relatively homogenous. The soil moisture varied slightly around 15%. The variations were higher at deeper layer where it ranged from 13% to 17% (Table 5.2).

Table 5.2 Soil moisture by weight (%).

Point no.	Treatment	Depth			
		0-0.3 m		0.3-0.6 m	
		before	after	before	after
35	Shallow compaction 0.3 m	14.91	15.91	16.59	16.92
62	Control (Compacted)	14.12	14.45	13.15	13.96
85	Deep compaction 0.6 m	15.30	15.82	15.03	15.45

Soil organic matter content (loss on ignition method) was very low and it ranged from 3.1% to 3.6% in topsoil layer. In deeper soil layer (0.3-0.6 m) it reached even lower values and ranged from 1.7% to 2.8% (Table 5.3).

Table 5.3 Soil organic matter content (Loss on ignition) (%).

Sampling point no.	Treatment	Depth	
		0-0.3 m	0.3-0.6 m
35	Shallow compaction 0.3 m	3.6	2.8
62	Control (Compacted)	3.1	1.7
85	Deep compaction 0.6 m	3.3	2.2

Electrical conductivity by saturated paste reached low values and the soil was assessed as non-saline (below 200 $mS.m^{-1}$). However the conductivity within block no. 3 (sampling point no. 35) reached values above 60 $mS.m^{-1}$ whilst the values within the rest of the trial plot ranged from 47.6 $mS.m^{-1}$ to 55.1 $mS.m^{-1}$ (Table 5.4). This phenomenon could be caused by slightly higher amount of salts within block 3.

Table 5.4 Electrical conductivity by saturated paste (ECe, reported in $mS.m^{-1}$).

Sampling point no.	Treatment	Depth	
		0-0.3 m	0.3-0.6 m
35	Shallow compaction 0.3 m	67.3	60.8
62	Control (Compacted)	55.1	48.7
85	Deep compaction 0.6 m	47.6	49.1

Soil pH was well balanced and varied from 7.5 to 7.9 (Table 5.5). Soil reaction was assessed as neutral (6.6-7.5) and weakly basic (7.6-9.5).

Table 5.5 Soil pH.

Sampling point no.	Treatment	Depth	
		0-0.3 m	0.3-0.6 m
35	Shallow compaction 0.3 m	7.6	7.5
62	Control (Compacted)	7.9	7.9
85	Deep compaction 0.6 m	7.6	7.5

The analysis of particle size distribution was performed using pipette method. The soil type within the randomised block design trial plot was assessed as Sandy Loam only the deeper layer (0.3-0.6 m) within the block 3 contained slightly more of clay and was assessed as Sandy Clay Loam (Table 5.6).

Table 5.6 Soil particle size distribution.

Sampling point no.	Treatment	Depth	
		0-0.3 m	0.3-0.6 m
35	Shallow compaction 0.3 m	Sandy Loam	Sandy Clay Loam
62	Control (Compacted)	Sandy Loam	Sandy Loam
85	Deep compaction 0.6 m	Sandy Loam	Sandy Loam

Mentioned differences within block 3 (mainly the electrical conductivity by saturated paste, soil texture and soil moisture) introduced the trend which caused slightly increasing of soil electrical conductivity readings towards the block 3 (see Figure 5.3 - Figure 5.6).

5.6 Conclusions of randomized block design experiment

The EC readings collected stationary and dynamically (at speed of 0.05 $m.s^{-1}$) are similar and the coefficient of regression (R^2) was equal to 0.89 and 0.92 for soil depth of 0-0.3 m and 0-0.9 m respectively.

It was found out that the soil EC measured within the depth range of 0-0.3 m is able to distinguish the areas of soil with no compaction above 0.3 m from areas compacted in whole soil profile. Soil EC measured within the depth range of 0-0.9 m is able to distinguish the areas of soil with no compaction above 0.6 m from the rest of the field. Using both datasets the zones with no compaction above 0.3 m, zones with no compaction above 0.6 m and zones compacted within whole soil profile can be identified. Subsequently the targeted soil loosening can be applied within the zones identified.

As expected it was found out that the soil compaction sensor and the soil penetration resistance survey provides the most reliable data for determining different levels of soil compaction. However the absolute values obtained by soil compaction sensor are affected by changes in soil texture. The high labour and time requirements are the main disadvantages of the penetrometer measurements. The soil compaction sensor has to be attached on the frame of the subsoiler and although it provides precise values, it has higher energy requirements. The second best results for identifying different depths of soil compaction were obtained by the Conductometer which is able to collect data on-the-go with much lower power requirements. The soil EC data obtained from the depth range of 0-0.75 m using the contact-less instrument *EM38* operated in horizontal mode distinguished the areas with no compaction above 0.3 m from the compacted ones with the lower precision.

The application map showing the spatial pattern of the targeted soil loosening can be created either manually on the base of visual comparison or using simple ratio of the map related to the soil without any compaction (initial map) and the map related to possibly compacted soil. As the effect of soil moisture is not the same for different soil types, it would be desirable to compare the EC readings obtained in approximately same conditions.

It is necessary to increase the sampling speed of the Conductometer to 20 Hz – 30 Hz which is suitable for the practical utilisation of this surveying method.

6 Conclusions

The methodology of identification within-field variability of soil compaction using two different soil electrical conductivity sensors, soil compaction sensor and cone penetrometer was developed and the randomized block design experiment was conducted.

The data obtained was compared statistically and the spatial variability maps were created. By comparison of maps related to initially compacted soil and subsequently loosened one, the strategies for application of targeted soil loosening were suggested.

A geostatistical method for the removal of the overall trend from the data was investigated, it creates a map of the residuals which shows the possible periodicity in the data. If the periodicity is caused by the higher soil bulk density within the tramlines than the map identifies such areas. Some possible compacted areas around tramlines where identified, but increased spatial frequency of data collection is recommended before further investigation.

The similarity of the EC readings collected by the Conductometer in stationary and dynamic mode was confirmed by the analysis of regression. The coefficient of regression (R^2) was equal to 0.89 and to 0.92 for the readings measured within the soil depth range of 0-0.3 m and 0-0.9 m respectively. It is expected that increasing the data collection frequency might improve the correlation.

EC readings obtained by the Conductometer at depth range of 0-0.3 m are able to identify the areas without any compaction above 0.3 m and the soil compacted within whole profile. The readings collected at depth range of 0-0.9 m are able to distinguish the areas with no compaction above 0.6 m from the rest of the field. It means that using both datasets one should be able to identify three different environments within the field: one compacted within whole profile, one containing no compaction above 0.3 m and one containing no compaction above 0.6 m.

The key finding was the development of application maps for the targeted soil loosening based on soil electrical conductivity surveying. The practical utilization of

this method is based on the comparison of two maps. The map which will be used as a standard for further comparisons is necessary to be obtained in desirable soil loosened conditions. Further map will characterize the EC within the compacted field. It is recommended that the both maps would be obtained in similar moisture conditions to minimize the effect of soil water content. The application map of targeted soil loosening can be created either manually using visual comparison of both initial (loosened soil) and further map (compacted areas), or using an appropriate mathematical operation, in this case the ratio of the two maps. By comparing these maps from year to year zones of compacted soil can be used to determine a soil loosening strategies.

The sampling frequency of the Conductometer is too low. The Conductometer is able to collect the data either in frequency of 0.2 Hz by an old processor or in 0.833 Hz using a new processor. Such a sampling frequency matches to distance of 5 meters or 1.2 meters, respectively, moved in working speed of 1 $m.s^{-1}$. It would be desirable to collect the data at spatial resolution at least of 0.5 m to identify the compaction caused by vehicle tyres. As the working speed of the contact and contact-less sensors can be - and from the labour productivity point of view it is desired to be - higher, the sufficient sampling frequency has to be higher than 2 Hz. The recommended sampling frequency for the higher working speeds and sufficient amount of collected data is between 20 Hz and 30 Hz.

It was found out that the readings collected by the Conductometer at both depth ranges of 0-0.3 m and 0-0.9 m increase with increasing depth of coulter disc electrodes. However this increase is negligible in comparison with the differences caused by soil bulk density. As the soil bulk density decreases it allows the disc electrodes to penetrate soil deeper. Electrical conductivity should then decrease with the lower soil density and at the same time increase with the higher penetration depth. It was found out that the EC readings finally significantly decreased.

Proper contact between the soil and coulter disc electrodes is an important condition for obtaining the correct EC data by the direct contact method.

The soil compaction sensor and the soil penetration resistance have most sufficient sensitivity for compacted soil depth determination. However the absolute readings of soil compaction sensor were more affected by soil texture. The higher labour and time requirements are the main disadvantages of the cone penetrometer. The soil compaction sensor has high energy requirements. The second best results were provided by the EC readings collected by the Conductometer which is able to obtain readings on-the-go. The Conductometer was followed by contact-less device *EM38* operated in horizontal mode which is able to distinguish the areas with no compaction above 0.3 m with less precision. The *EM38* operated in vertical mode has not sufficient sensitivity to distinguish the soil with different bulk densities.

7 Recommendations

For practical utilization of EC readings for the purpose of soil compaction spatial variability identification it is recommended to perform an EC survey of the loosened soil within the field and create an initial EC map. Such a map will serve as a base for comparison of further maps created for the same area with possibly compacted soils. For avoiding of undesirable effect of the soil moisture it is recommended to obtain both maps in similar conditions. Subsequent comparison of an initial map and map created for possibly compacted soil may be done either visually or by calculating simple ratio of both maps. Other spatial data comparison techniques might provide better results than the ratio method tested here.

It is recommended to examine the above procedure within different soil conditions first at small scale and then conduct field scale trials of the methodology.

For obtaining the proper data using the direct contact method it is necessary to perform a good contact between the soil and coulter disc electrodes.

If the soil within the field is assumed to be compacted periodically (e.g. hidden or invisible tramlines), it is recommended to survey the field across assumed periodicity.

It is recommended to increase the sampling frequency of the Conductometer to at least 20 Hz which enables collecting the EC readings in sufficient spatial resolution to capture the spatial variability of soil compaction when used dynamically (on-the-go).

8 References

Adamchuk, V.I., Jasa, P.J. (2002). *On-the-go vehicle-based soil sensors*. University of Nebraska Cooperative Extension EC 02-178.

Allmaras, R.R., Black A.L. and Rickman, R.W. (1973). Tillage, soil environment and root growth, In: *Proc. Natl. Conserv. Til. Conf* Des Moines, Iowa, pp. 62–86

ASABE, (2004). *Soil Cone Penetrometer*. ASAE S313.3 FEB04, ASABE, 2950 Niles Road, St. Joseph, MI 49085-9659, USA.

Bajla, J., (1998). *Penetrometrické merania pôdnych vlastností*. Nitra: VES SPU

Brady, N. C., and R. R. Weil. (1999). *The nature and properties of soils*, 12th edition edition. Prentice Hall, Upper Saddle River, N.J.

Carr, C. (1982). *Handbook on Soil Resistivity Surveying*. Center for American Archeology Press, Evanston, Illinois.

Chukwu, E., Bowers, C.G., Jr. (2005). Instantaneous multiple-depth soil mechanical impedance sensing from a moving vehicle. *Transactions of the ASAE*, 48, 885–894.

Chung, S.O., Sudduth, K.A., and Hummel, J.W. (2006). Design and validation of an on-the-go soil strength profile sensor. *Transactions of the ASABE* 49(1):5-14.

Clark, R. L., D. E. Kissel, F. Chen, and W. Adkins. (2000). *Mapping soil hardpans with the penetrometer and soil electrical conductivity*. ASAE Paper No. 001042, ASAE, St. Joseph, MI.

Coder, K.D. (2000). *Causes of Soil Compaction*. University of Georgia School of Forest Resources, Athens, GA

Commission of the European Communities (2006). *Proposal for a Directive of the European Parliament and of the Council, establishing a framework for the protection of soil and amending Directive 2004/35/EC*, COM(2006) 232 final, Brussels.

Committee to Review the Scientific Evidence on the Polygraph, Division of Behavioral and Social Sciences and Education, National Research Council (2002). *The Polygraph and Lie Detection*. Washington, DC: The National Academies Press.

Corwin, D.L., Lesch, S.M. (2005a). Apparent soil electrical conductivity measurements in agriculture. *Computers and Electronics in Agriculture*, 46, p. 11-43.

Corwin, D.L., Lesch, S.M. (2005b). Characterizing soil spatial variability with apparent soil electrical conductivity: I. Survey Protocols. *Computers and Electronics in Agriculture*. 46:103-133.

Crop Technology. (N/A). *Soil Doctor® System…* (WWW document). http://www.soildoctor.com. (accessed 27th October 2006).

Davis, G., Kitchen, N.R., Sudduth, K.A. and Drummond, S.T. (1997). Using electromagnetic induction to characterize soils. *Better Crops*, 81(4), p. 6-8.

Davis, J. L., and Annan, A. P., (1989) Ground-penetrating radar for high-resolution mapping of soil and rock stratigraphy. *Geophysical Prospecting*, 37, p. 531-551.

Doerge, T., Kitchen, N.R. and Lund, E.D. (2001). *Soil Electrical Conductivity Mapping*. SSMG-30. Site-Specific Management Guidelines. Potash & Phosphate Institute (PPI).

Doolittle, J.A., Indorante, S.J., Potter, D.K., Hefner, S.G., McCauley, W.M. (2002). Comparing three geophysical tools for locating sand blows in alluvial soils of southeast Missouri. *J. Soil Water Conserv.* 57, p. 175–182.

Duiker, S.W. (2004). *Effects of soil compaction*. The Pennsylvania State Univ., University Park.

Eijkelkamp (2007). *Operating instructions. 06.15.SA Penetrologger set* (WWW document). http://www.eijkelkamp.com/files/M1-0615SAe%20Penetrologger.pdf. (accessed 28th May 2007).

Flores, J., Navar, J. (2002) An Assessment of Stream Water Quality of the Rio San Juan, Nuevo Leon, México, 1995-1996. *J. Environ. Qual.*, 31, p. 1256-1265.

Gencer, N.G. and Tek, M.N. (1999) Electrical Conductivity Imaging via Contactless Measurements. *IEEE Transactions on Medical Imaging*, 18, p.617-627.

GeoModel, (2007). *Ground penetrating radar. Basic operating principles*. (WWW document). http://www.geomodel.com/gprtext.htm. (accessed 15th May 2007).

Geonics limited (2001). *EM38-DD Ground conductivity meter. Dual dipole version. Operating manual*.

Global Security. (N/A). *AN/PSS-12 Mine Detector* (WWW document). http://www.globalsecurity.org/military/systems/ground/an-pss-12.htm. (accessed 16th December 2006).

Hall, E., Raper, R.L. (2005). Development and concept evaluation of an on-the-go soil strength measurement system. *Transactions of the ASAE*. 48(2):469-477.

Hindický, M. (2007). *Elektrická vodivosť ako faktor produkčnej schopnosti pôdy* (unpublished MSc thesis). Slovak University of Agriculture in Nitra. Nitra. 82 p.

Infoterra Ltd and Bluesky©. (2007).

Jabro, J.D., Evans, R.G., Kim, Y., Stevens, W.B., Iversen, W.M. (2005). *Spatial variability of the apparent electrical conductivity and cone index as measured with sensing technologies: assessment and comparison*. ASABE Pacific Northwest Section Meeting, Lethbridge, Alberta, Canada, September 22-24, 2005. Paper PNW05-1017.

James, I. T., Waine, T. W., Godwin, R. J. (2000). A Comparison between traditional methods and EMI scanning for determining soil textural boundaries. *EurAgEng* Paper No. 00-PA-013, AgEng2000 Warwick, UK.

Johnson, C.K., J.W. Doran, B. Eghball, R.A. Eigenberg, B.J. Wienhold, and B.L. Woodbury. (2003). Status of soil electrical conductivity studies by central state researchers. *Trans. ASAE*, 48(3), p. 979–989.

Jones, R., Spoor, G., Thomasson, A.J. (2003). Vulnerability of Subsoils in Europe to Compaction. A Preliminary Analysis. *Soil & Tillage Research*, 73, p. 131-143.

Malo, D.D., Lee, D.K., Lee, J.H., Christopherson, S.M., Cole, C.M., Kleinjan, J.L., Carlson, C.G., Clay, D.E., Chang, J., Reese, C.L., Clay, S.A., Ellsbury, M.M., and Kitchen, N.R. (2001a). Soil Moisture, Bulk Density, Soil Temperature, and Soil Sensor (Veris 3100® and Geonics EM38®) Relationships: Part 1 – Moody County Site, Progress report, South Dakota State University, Brookings.

Malo, D.D., Lee, D.K., Lee, J.H., Christopherson, S.M., Cole, C.M., Kleinjan, J.L., Carlson, C.G., Clay, D.E., Chang, J., Reese, C.L., Clay, S.A., Ellsbury, M.M., and Kitchen, N.R.

(2001b). Soil Moisture, Bulk Density, Soil Temperature, and Soil Sensor (Veris 3100® and Geonics EM38®) Relationships: Part 2- Brookings County Site, Progress report, South Dakota State University, Brookings.

Mašek, J. (2005). Technologie zpracování půdy. *Mechanizace zemědělství*, Vol. 54 (8): 50-55

McNeill, J. D. (1992). Rapid, accurate mapping of soil salinity by electromagnetic ground conductivity meters. Cited in: G.C. Topp, W. D. Reynolds and R. E. Green (eds.) Advances in measurement of soil physical properties: Bringing theory into practice. *SSSA Spec. Publ. 30. ASA, CSSA and SSSA*, Madison, WI., p. 209-229.

McNeill, J.D. (1980). *Electrical Conductivity of soils and rocks*. Technical Note TN-5. Geonics Ltd., Mississauga, ON, Canada, 22 p.

Milsom, J. (2003). *Field geophysics*. Third edition. John Wiley & Sons Ltd, Chichester, England, 232 pp., ISBN 0-470-84347-0

OKM Ortungstechnik GmbH. (N/A). *Manufacturer of metal detector, Magnetometer, Ground Penetrating Radar and geophysical instrument* (WWW document). http://www.futuretreasure.com. (accessed 21st October 2006).

Oxford reference. (1992). *A concise dictionary of physics*. Oxford

Pires, S.M.G.M. (2004). *Proximal remote sensing of soil physical conditions and water availability for precision farming* (unpublished Ph.D thesis). Cranfield University. Cranfield.

Rhoades, J. D., Chanduvi, F., Lesch, S. (1999). Soil salinity assessment: methods and interpretation of electrical conductivity measurements. *FAO irrigation and drainage paper*, 57. Rome, Food and Agriculture Organization of the United Nations. ISSN 0254-5284

Rhoades, J.D., (1992). Instrumental field methods of salinity appraisal. In: Topp, G.C., Reynolds, W.D., Green, R.E. (eds.), Advances in Measurement of Soil Physical Properties: Bring Theory into Practice. *SSSA Special Publication No. 30*. Soil Science Society of America, Madison, WI, USA, p. 231– 248.

Rhoades, J.D., (1993). Electrical conductivity methods for measuring and mapping soil salinity. In: Sparks, D.L. (Ed.), *Advances in Agronomy*, 49. Academic Press, San Diego, CA, USA, p. 201–251.

Rhoades, J.D., Raats, P.A.C., and Prather, R.J. (1976). Effects of liquid-phase electrical conductivity, water content, and surface conductivity on bulk soil electrical conductivity. *Soil Sci. Soc. Am. J.* 40, p. 651-655.

Rhoades, J.M., Chanduvi, F., Lesch, S.M., (1999). *Soil salinity assessment. Methods and interpretation of electrical conductivity measurements*. FAO Irrigation and Drainage Paper 57. FAO, Rome, 150pp.

Samouëlian, A., Cousin, I., Richard, G., Tabbagh, A. and Bruand, A. (2003). Electrical resistivity imaging for detecting soil cracking at the centimetric scale. *Soil Science Society of America Journal*, 67, 1319–1326.

Šařec, P., Prošek, V., Digrín, P. Univerzální měřící systém a jeho aplikace. (Multi-purpose measuring system and its applications). In: *Trendy vo výskume a vývoji poľnohospodárskych strojov a technológií v ekosystéme kultúrnej krajiny*, Dudince 2nd – 3rd Jun 2005. [CD-ROM]. Nitra: SUA in Nitra, p. 378-383. ISBN 80-8069-523-7.

Sharifi, A. (2004). *Development of a soil compaction profile sensor* (unpublished Ph.D thesis). Cranfield University. Cranfield.

Sharifi, A., Godwin, R.J., O`Dogherty M.J., Dresser, M.L. (2007). Evaluating the performance of a soil compaction profile sensor under laboratory and field conditions. *Soil Use and Management* 23 (2), 171-177.

Smith, J. (2001). Soil electrical conductivity mapping and interpretations. *In-field mapping of soil and crop factors*. 23rd January. SCI London.

Soil Data© Cranfield University (NSRI). (2007).

Srinivasan, A., (2006). *Handbook of Precision Agriculture. Principles and Applications*, Binghamton, NY.

Sudduth K.A, Kitchen N.R, Wiebold W.J, et al. (2005). Relating Apparent Electrical Conductivity to Soil Properties across the North-Central USA. *Computers and Electronics in Agriculture*, 46(1-3): 263-283.

Sudduth, K.A., Hummel, J.W., Drummond, S.T. (2004). Comparison of the Veris Profiler 3000 to an ASAE-standard penetrometer. *Applied Engineering in Agriculture*. 20(5):535-541.

Sudduth, K.A., Kitchen, N.R., Drummond, S.T. (1998). Soil conductivity sensing on claypan soils: Comparison of electromagnetic induction and direct methods. In: *Proc. of the 4th International Conference on Precision Agriculture*, St. Paul, Minnesota, 19-22 July 1998, p. 979-990.

Sudduth, K.A., Kitchen, N.R., Drummond, S.T. (2001). Accuracy issues in electromagnetic induction sensing of soil electrical conductivity for precision agriculture. *Computer and Electronics in Agriculture*, 31, p. 239-264.

Taylor, H.M., Roberson, G.M. and Parker Jr., J.J. (1966). Soil strength-root penetration relations for medium- to coarse-textured soil materials. *Soil Sci.* 102:18-22.

Tekeste, M.Z., Grift, T.E. and Raper, R.L. (2002). Acoustic Compaction Layer Detection. *ASAE Paper 02-1089*, St. Joseph, MI.

Thomson, S.J., Ross, B.B. (1996). *Using Soil Moisture Sensors for Making Irrigation Management Decisions in Virginia*. Virginia Cooperative Extension, Publication Number 442-024. Virginia State University.

University of Minnesota. (2001). *Soil Compaction: Causes, Effects, and Control* (WWW document).
http://www.extension.umn.edu/distribution/cropsystems/components/3115s01.html. (accessed 12th November 2006).

Veris Technologies. (2003). *Frequently Asked Questions about Soil Electrical Conductivity (EC)…* (WWW document) http://www.veristech.com/faqs/about_soil_ec.htm. (accessed 14th October 2006).

Waine, T.W. (1999). *Non-invasive soil property measurement for precision farming* (unpublished Eng.D thesis). Cranfield University. Cranfield.

Wenner, F. (1916). A method of measuring earth resistivity. *U.S. Dept. Com. Cur. Of Stand. Sci.*, Paper 258.

Williams, B. G. and G. C. Baker. (1982). An electromagnetic induction technique for reconnaissance surveys of soil salinity hazards. *Aust. J. Soil Research*, 20, p. 107-118.

Wolharn, S. (2001). *The practical application of precision farming techniques* (unpublished M.Phil thesis). Cranfield University. Cranfield.

Appendices

Appendix I. *EM38* operating instructions

The battery should be removed from the instrument if there is an assumption of its low voltage. The battery voltage is possible to check as following: the range switch is necessary to be set in 1.000 mS/m and battery test switch to BATT. If the displayed readings fall into the range from -1.500 to -720 then the battery is good. If the displayed readings are not from the above range the battery is wrong and has to be changed.

Because of high sensitivity of the *EM38* it is recommended to remove all metal objects from the body of an operator (from the wrists, fingers, neck and pockets before the calibration) and to avoid any metal objects in the distance at least of 1.5 m. The sensitivity of the instrument is highest near the coils situated in both edges.

Calibration procedure

Turn on the instrument by setting the ON/OFF/BATT switch in "ON".

1. Put the *EM38* operated in vertical mode on the ground and set the mode switch in Q/P (Quad phase). Set the zero using the zero control button knob (Q/P).
2. Set the switch in I/P (In phase) position and set the reading to zero using the coarse and fine knobs. Go back to previous step and ensure that the instrument still displays zero in Q/P mode.
3. Set the mode switch into Q/P and using the zero setting knob set the value of 50 mS/m.
4. Set the mode switch back to I/P and using the coarse and the fine knobs set the reading at 50 mS/m.
5. Set the mode switch again into Q/P and ensure that it displays 50 mS/m. If the displayed reading is not equal to 50 mS/m then set the Phase control so that the Q/P reading is 50 mS/m (+/- 1 mS/m).
6. Again set the zero for the Q/P and I/P as it is described in step 1 and 2.

Lift the instrument to the height of about 1.5 m.

7. When the *EM38* is in the air in the horizontal mode, set the Q/P and I/P to zero as in step 1 and 2.
8. Remain the instrument in horizontal position and set the mode switch to Q/P. Turning the zero setting knob set the arbitrary value (i.e. HR = 10 mS/m). Turn the instrument into vertical position and note the reading (i.e. VR = 16 mS/m). Subtract the value measured in horizontal mode from the value measured in vertical mode (VR – HR = 6 mS/m).
9. Finally, while the mode switch is still in Q/P position and the instrument is in horizontal mode, using the zero setting knob set the value calculated in step 8. In this example it is 6 mS/m. If the instrument is subsequently turned to vertical position, it should display the value of 12 mS/m.

If the instrument is at least 1.5 m above the ground, the Q/P or conductivity value should always satisfy the following equation:

$$VR = 2HR \qquad \textbf{Equation 4}$$

where VR = reading obtained in vertical mode, and
HR = reading obtained in horizontal mode.

Appendix II. Time stability of EC readings

Table II.1 Descriptive statistics of the EC readings collected at depth range of 0-0.3 m in time of 10 minutes.

EC (depth range 0-0.3 m), mS/m	
Mean	17.529
Standard error	0.009
Median	17.549
Mode	17.549
Standard deviation	0.099
Sample Variance	0.010
Coefficient of Variation	0.006
Kurtosis	3.371
Skewness	-0.026
Range	0.639
Minimum	17.263
Maximum	17.903
Sum	2103.425
Count	120
Confidence level (95.0%)	0.018

Table II.2 Descriptive statistics of the EC readings collected at depth range of 0-0.9 m in time of 10 minutes.

EC (depth range 0-0.9 m), mS/m	
Mean	80.486
Standard error	0.094
Median	80.202
Mode	80.194
Standard deviation	1.030
Sample Variance	1.060
Coefficient of Variation	0.013
Kurtosis	12.847
Skewness	3.288
Range	6.671
Minimum	79.365
Maximum	86.036
Sum	9658.308
Count	120
Confidence level (95.0%)	0.186

Table II.3 Descriptive statistics of the EC readings collected at depth range of 0-0.3 m in time of 1 minute.

EC (depth range 0-0.3 m), mS/m	
Mean	17.614
Standard error	0.052
Median	17.566
Mode	Not available
Standard deviation	0.180
Sample Variance	0.032
Coefficient of Variation	0.010
Kurtosis	-1.021
Skewness	0.328
Range	0.544
Minimum	17.358
Maximum	17.903
Sum	211.373
Count	12
Confidence level (95.0%)	0.114

Table II.4 Descriptive statistics of the EC readings collected at depth range of 0-0.9 m in time of 1 minute.

EC (depth range 0-0.9 m), mS/m	
Mean	82.936
Standard error	0.490
Median	82.672
Mode	82.672
Standard deviation	1.698
Sample Variance	2.882
Coefficient of Variation	0.020
Kurtosis	-0.355
Skewness	0.556
Range	5.596
Minimum	80.440
Maximum	86.036
Sum	995.236
Count	12
Confidence level (95.0%)	1.079

Table II.5 Descriptive statistics of the EC readings collected in dynamic mode at depth range of 0-0.3 m characterizing one of the measuring points within randomised design experiment.

EC (depth range 0-0.3 m), mS/m	
Mean	4.853
Standard error	0.082
Median	4.903
Mode	Not available
Standard deviation	0.306
Sample Variance	0.093
Coefficient of Variation	0.063
Kurtosis	1.346
Skewness	-1.320
Range	0.996
Minimum	4.182
Maximum	5.178
Sum	67.946
Count	14
Confidence level (95.0%)	0.176

Table II.6 Descriptive statistics of the EC readings collected in dynamic mode at depth range of 0-0.9 m characterizing one of the measuring points within randomised design experiment.

EC (depth range 0-0.9 m), mS/m	
Mean	6.239
Standard error	0.041
Median	6.264
Mode	Not available
Standard deviation	0.155
Sample Variance	0.024
Coefficient of Variation	0.025
Kurtosis	-0.282
Skewness	-0.607
Range	0.524
Minimum	5.912
Maximum	6.436
Sum	87.350
Count	14
Confidence level (95.0%)	0.090

Appendix III. Weather data

Table III.1 Weather data for Silsoe area collected by the Met station.

Date	Tmax °C	Tmin °C	RH %	Sun hr	Solar MJ/m2	Net MJ/m2	Wind km/d	ET mm/d	Rain mm/d
1.5.2007	19.8	6.8	57	8.5	19.1	10.19	176.3	3.7	0
2.5.2007	17.9	7.8	76	5	14.9	8.8	233.3	3.2	0
3.5.2007	11.8	7.9	78	0	8.4	6.01	185.7	2	0
4.5.2007	13.6	8.2	70	1.4	10.7	7	179	2.3	0
5.5.2007	14.6	4.3	81	0.8	10	6.78	130.5	1.8	0
6.5.2007	18.4	10.3	70	1.5	11	7.19	230.6	2.7	10.8
7.5.2007	17.6	9.3	89	1.1	10.5	7.11	234.1	2.2	5
8.5.2007	17.4	9.7	72	4.6	14.9	8.98	254	3.2	0.2
9.5.2007	14.7	9.4	88	1.3	10.9	7.33	285.3	1.7	4.8
10.5.2007	14.5	7.5	92	1	10.6	7.19	225.5	1.6	17.6
11.5.2007	15.4	9.7	88	1.7	11.5	7.65	251.3	2	8.4
12.5.2007	15.9	8.7	89	0.9	10.5	7.21	161.3	1.8	2.6
13.5.2007	13.6	9.3	98	0	3.9	3.96	155.5	0.8	11.4
14.5.2007	11.5	4.5	93	0	6.1	5.08	133.5	1.2	3
15.5.2007	15.5	10	95	0.1	9.8	6.89	144	1.3	3.2
16.5.2007	14.4	11.7	94	0	7.1	5.58	119.5	1.3	7
17.5.2007	17.2	12.6	93	2.4	12.6	8.42	157.4	1.8	0.2
18.5.2007	19.1	8.4	74	6	17.2	10.35	280.4	3.5	0.6
19.5.2007	16.2	5.4	65	7.1	18.7	10.92	175.1	3.3	0
20.5.2007	17.2	9.5	73	2.5	12.9	8.35	84.3	2.2	0
21.5.2007	16.7	8.1	80	0.6	10.6	7.33	87.5	2.1	0
22.5.2007	20.6	8.3	60	8.5	20.6	11.85	73.1	3.2	0
23.5.2007	22.4	15.1	72	7	18.7	11.44	60.5	2.9	0
24.5.2007	23.4	12.5	77	3	13.7	8.95	62.8	2.8	0
25.5.2007	18.7	9.7	94	0	7.6	5.92	110.6	2.1	0.4
26.5.2007	12.8	8.1	91	0	7.7	5.97	99.5	1.7	6
27.5.2007	10.8	5.8	100	0	3.9	4.04	304.4	0.7	43.8
28.5.2007	8.5	4.8	98	0	6.9	5.55	123.6	1	5.4
29.5.2007	12.6	2.9	79	2.6	13.4	8.75	84.5	1.8	1.6
30.5.2007	16.2	8.7	93	0.9	11.3	7.82	151.8	1.5	3.6
31.5.2007	18.5	6	73	4.9	16.4	10.21	79.8	2.6	0
Mean	**16.05**	**8.42**	**82.32**	**2.37**	**11.68**	**7.70**	**162.41**	**2.13**	**4.37**
Total				**73.40**	**362.10**	**238.82**	**5034.70**	**66.00**	**135.60**

Appendix IV. Relationship between the depth of the discs and the EC readings

Table IV.1 Regression analysis for the EC readings obtained within soil depth range of 0-0.3 m in various depths of discs.

Regression Statistics	
Multiple R	0.914
R Square	0.836
Adjusted R Square	0.827
Standard Error	0.303
Observations	21

	df	*SS*	*MS*	*F*	*Significance F*
Regression	1	8.909	8.909	96.797	6.836E-09
Residual	19	1.749	0.092		
Total	20	10.657			

	Coefficients	*Standard Error*	*t Stat*	*P-value*	*Lower 95%*	*Upper 95%*	*Lower 95.0%*	*Upper 95.0%*
Intercept	1.564	0.272	5.754	1.520E-05	0.995	2.133	0.995	2.133
Depth	0.032	0.003	9.839	6.836E-09	0.025	0.039	0.025	0.039

Table IV.2 Regression analysis for the EC readings obtained within soil depth range of 0-0.9 m in various depths of discs.

Regression Statistics	
Multiple R	0.784
R Square	0.615
Adjusted R Square	0.594
Standard Error	0.223
Observations	20

	df	*SS*	*MS*	*F*	*Significance F*
Regression	1	1.437	1.437	28.803	4.226E-05
Residual	18	0.898	0.050		
Total	19	2.334			

	Coefficients	*Standard Error*	*t Stat*	*P-value*	*Lower 95%*	*Upper 95%*	*Lower 95.0%*	*Upper 95.0%*
Intercept	4.119	0.215	19.131	2.07E-13	3.667	4.572	3.667	4.572
Depth	0.014	0.003	5.367	4.226E-05	0.008	0.019	0.008	0.019

Appendix V. Statistical analyse of the EC readings obtained from the trafficked and non-trafficked areas

The Conductometer

Depth of sensing 0-0.3 m

Table V.1 t-Test of the EC readings collected at depth range of 0-0.3 m at1st pair of runs.

	Within tramlines	*Between tramlines*
Mean	52.618	51.734
Variance	516.424	637.886
Observations	60	34
Pooled Variance	559.992	
Hypothesized Mean Difference	0	
df	92	
t Stat	0.174	
P(T<=t) one-tail	0.431	
t Critical one-tail	1.662	
P(T<=t) two-tail	0.862	
t Critical two-tail	1.986	

Table V.2 t-Test of the EC readings collected at depth range of 0-0.3 m at 2nd pair of runs.

	Within tramlines	*Between tramlines*
Mean	55.739	49.762
Variance	756.939	601.952
Observations	110	66
Hypothesized Mean Difference	0	
df	149	
t Stat	1.494	
P(T<=t) one-tail	0.069	
t Critical one-tail	1.655	
P(T<=t) two-tail	0.137	
t Critical two-tail	1.976	

Depth of sensing 0-0.9 m

Table V.3 t-Test of the EC readings collected at depth range of 0-0.9 m at 1st pair of runs.

	Within tramlines	*Between tramlines*
Mean	41.687	52.299
Variance	996.146	1554.098
Observations	60	34
Pooled Variance	1196.281	
Hypothesized Mean Difference	0	
df	92	
t Stat	-1.429	
P(T<=t) one-tail	0.078	
t Critical one-tail	1.662	
P(T<=t) two-tail	0.156	
t Critical two-tail	1.986	

Table V.4 t-Test of the EC readings collected at depth range of 0-0.9 m at 2nd pair of runs.

	Within tramlines	*Between tramlines*
Mean	48.524	52.807
Variance	1661.150	2382.228
Observations	50	32
Pooled Variance	1940.568	
Hypothesized Mean Difference	0	
df	80	
t Stat	-0.429	
P(T<=t) one-tail	0.334	
t Critical one-tail	1.664	
P(T<=t) two-tail	0.669	
t Critical two-tail	1.990	

Difference between shallow and deep EC readings

Table V.5 t-Test of the differences between shallow and deep EC (EC30-EC90) readings collected at 1st pair of runs.

	Within tramlines	*Between tramlines*
Mean	10.931	-0.565
Variance	184.649	319.383
Observations	60	34
Hypothesized Mean Difference	0	
df	55	
t Stat	3.255	
P(T<=t) one-tail	0.001	
t Critical one-tail	1.673	
P(T<=t) two-tail	0.002	
t Critical two-tail	2.004	

Table V.6 t-Test of the differences between shallow and deep EC (EC30-EC90) readings collected at 2nd pair of runs.

	Within tramlines	*Between tramlines*
Mean	10.961	-5.140
Variance	372.023	689.787
Observations	50	32
Hypothesized Mean Difference	0	
df	52	
t Stat	2.990	
P(T<=t) one-tail	0.002	
t Critical one-tail	1.675	
P(T<=t) two-tail	0.004	
t Critical two-tail	2.007	

The *EM38* operated in vertical mode

Table V.7 t-Test of the EC readings collected at depth range of 0-1.5 m at 1st pair of runs.

	Within tramlines	*Between tramlines*
Mean	17.217	15.454
Variance	203.280	186.948
Observations	203	207
Pooled Variance	195.034	
Hypothesized Mean Difference	0	
df	408	
t Stat	1.278	
P(T<=t) one-tail	0.101	
t Critical one-tail	1.649	
P(T<=t) two-tail	0.202	
t Critical two-tail	1.966	

Table V.8 t-Test of the EC readings collected at depth range of 0-1.5 m at 2nd pair of runs.

	Within tramlines	*Between tramlines*
Mean	17.239	16.575
Variance	212.217	207.088
Observations	176	179
Pooled Variance	209.631	
Hypothesized Mean Difference	0	
df	353	
t Stat	0.432	
P(T<=t) one-tail	0.333	
t Critical one-tail	1.649	
P(T<=t) two-tail	0.666	
t Critical two-tail	1.967	

Appendix VI. Statistical analyse of the EC readings obtained in the same line in both directions

The Conductometer

Table VI.1 t-Test of the EC readings collected at depth range of 0-0.3 m.

	1st run	*2nd run*
Mean	62.411	48.735
Variance	1193.512	1138.643
Observations	55	63
Pooled Variance	1164.185	
Hypothesized Mean Difference	0	
df	116	
t Stat	2.172	
P(T<=t) one-tail	0.016	
t Critical one-tail	1.658	
P(T<=t) two-tail	0.032	
t Critical two-tail	1.981	

Table VI.2 t-Test of the EC readings collected at depth range of 0-0.9 m.

	1st run	*2nd run*
Mean	56.483	48.517
Variance	2805.535	2845.792
Observations	55	63
Pooled Variance	2827.052	
Hypothesized Mean Difference	0	
df	116	
t Stat	0.812	
P(T<=t) one-tail	0.209	
t Critical one-tail	1.658	
P(T<=t) two-tail	0.419	
t Critical two-tail	1.981	

The *EM38* operated in vertical mode

Table VI.3 t-Test of the EC readings collected at depth range of 0-1.5 m.

	1st run	*2nd run*
Mean	16.387	15.714
Variance	199.742	184.597
Observations	150	185
Pooled Variance	191.374	
Hypothesized Mean Difference	0	
df	333	
t Stat	0.443	
P(T<=t) one-tail	0.329	
t Critical one-tail	1.649	
P(T<=t) two-tail	0.658	
t Critical two-tail	1.967	

Appendix VII. Statistical analyse of the EC readings obtained within and between tramlines

The Conductometer

Depth of sensing 0-0.3 m

Table VII.1 t-Test of the EC readings collected at depth range of 0-0.3 m within the 6 m wide strip along the tramline axes.

	Within Tramlines	*Between Tramlines*
Mean	66.548	59.177
Variance	703.357	681.397
Observations	193	461
Pooled Variance	687.863	
Hypothesized Mean Difference	0	
df	652	
t Stat	-3.278	
P(T<=t) one-tail	0.001	
t Critical one-tail	1.647	
P(T<=t) two-tail	0.001	
t Critical two-tail	1.964	

Table VII.2 t-Test of the EC readings collected at depth range of 0-0.3 m within the 4 m wide strip along the tramline axes.

	Within Tramlines	*Between Tramlines*
Mean	66.764	59.905
Variance	591.588	717.881
Observations	138	516
Pooled Variance	691.344	
Hypothesized Mean Difference	0	
df	652	
t Stat	-2.722	
P(T<=t) one-tail	0.003	
t Critical one-tail	1.647	
P(T<=t) two-tail	0.007	
t Critical two-tail	1.964	

Table VII.3 t-Test of the EC readings collected at depth range of 0-0.3 m within the 3 m wide strip along the tramline axes.

	Within Tramlines	*Between Tramlines*
Mean	68.016	59.976
Variance	570.890	714.433
Observations	112	542
Pooled Variance	689.996	
Hypothesized Mean Difference	0	
df	652	
t Stat	-2.949	
P(T<=t) one-tail	0.002	
t Critical one-tail	1.647	
P(T<=t) two-tail	0.003	
t Critical two-tail	1.964	

Table VII.4 t-Test of the EC readings collected at depth range of 0-0.3 m within the 2.2 m wide tramlines.

	Within Tramlines	*Between Tramlines*
Mean	68.800	60.164
Variance	533.211	715.158
Observations	90	564
Hypothesized Mean Difference	0	
df	130	
t Stat	-3.220	
P(T<=t) one-tail	0.001	
t Critical one-tail	1.657	
P(T<=t) two-tail	0.002	
t Critical two-tail	1.978	

Depth of sensing 0-0.9 m

Table VII.5 t-Test of the EC readings collected at depth range of 0-0.9 m within the 6 m wide strip along the tramline axes.

	Within Tramlines	*Between Tramlines*
Mean	72.809	62.586
Variance	1579.742	1400.595
Observations	193	461
Pooled Variance	1453.350	
Hypothesized Mean Difference	0	
df	652	
t Stat	-3.128	
P(T<=t) one-tail	0.001	
t Critical one-tail	1.647	
P(T<=t) two-tail	0.002	
t Critical two-tail	1.964	

Table VII.6 t-Test of the EC readings collected at depth range of 0-0.9 m within the 4 m wide strip along the tramline axes.

	Within Tramlines	*Between Tramlines*
Mean	71.241	64.095
Variance	1149.241	1551.061
Observations	138	516
Hypothesized Mean Difference	0	
df	245	
t Stat	-2.122	
P(T<=t) one-tail	0.017	
t Critical one-tail	1.651	
P(T<=t) two-tail	0.035	
t Critical two-tail	1.970	

Table VII.7 t-Test of the EC readings collected at depth range of 0-0.9 m within the 3 m wide strip along the tramline axes.

	Within Tramlines	*Between Tramlines*
Mean	72.358	64.207
Variance	1089.122	1542.964
Observations	112	542
Hypothesized Mean Difference	0	
df	182	
t Stat	-2.299	
P(T<=t) one-tail	0.011	
t Critical one-tail	1.653	
P(T<=t) two-tail	0.023	
t Critical two-tail	1.973	

Table VII.8 t-Test of the EC readings collected at depth range of 0-0.9 m within the 2.2 m wide tramlines.

	Within Tramlines	*Between Tramlines*
Mean	72.771	64.459
Variance	1000.932	1540.598
Observations	90	564
Hypothesized Mean Difference	0	
df	137	
t Stat	-2.233	
P(T<=t) one-tail	0.014	
t Critical one-tail	1.656	
P(T<=t) two-tail	0.027	
t Critical two-tail	1.977	

The *EM38* operated in vertical mode

Depth of sensing of 0-1.5 m

Table VII.9 t-Test of the EC readings collected at depth range of 0-1.5 m within the 6 m wide strip along the tramline axes.

	Within Tramlines	*Between Tramlines*
Mean	34.837	33.722
Variance	702.126	472.879
Observations	552	1511
Hypothesized Mean Difference	0	
df	837	
t Stat	-0.886	
P(T<=t) one-tail	0.188	
t Critical one-tail	1.647	
P(T<=t) two-tail	0.376	
t Critical two-tail	1.963	

Table VII.10 t-Test of the EC readings collected at depth range of 0-1.5 m within the 4 m wide strip along the tramline axes.

	Within Tramlines	*Between Tramlines*
Mean	34.639	33.881
Variance	779.988	479.149
Observations	379	1684
Hypothesized Mean Difference	0	
df	488	
t Stat	0.495	
P(T<=t) one-tail	0.310	
t Critical one-tail	1.648	
P(T<=t) two-tail	0.621	
t Critical two-tail	1.965	

Table VII.11 t-Test of the EC readings collected at depth range of 0-1.5 m within the 3 m wide strip along the tramline axes.

	Within Tramlines	*Between Tramlines*
Mean	34.763	33.898
Variance	846.119	483.264
Observations	291	1772
Hypothesized Mean Difference	0	
df	346	
t Stat	0.485	
P(T<=t) one-tail	0.314	
t Critical one-tail	1.649	
P(T<=t) two-tail	0.628	
t Critical two-tail	1.967	

Table VII.12 t-Test of the EC readings collected at depth range of 0-1.5 m within the 2.2 m wide tramlines.

	Within Tramlines	*Between Tramlines*
Mean	34.568	33.960
Variance	827.769	501.972
Observations	206	1857
Hypothesized Mean Difference	0	
df	233	
t Stat	-0.294	
P(T<=t) one-tail	0.385	
t Critical one-tail	1.651	
P(T<=t) two-tail	0.769	
t Critical two-tail	1.970	

Appendix VIII. Methodology of soil laboratory analyses

Particle size distribution

This methodology is based on the British Standard BS 7755 Section 5.4:1998 *Determination of particle size distribution in mineral soil material – Method by sieving and sedimentation* which is identical to ISO 11277:1998.

Procedure for removal of organic matter

1. Approximately 10 ml of air-dried soil samples with grains smaller than 2 mm was placed in a labelled polycarbonate bottle, using the 10 ml brass scoop.

2. It was added, by measuring cylinder, 30 ml ± 1 ml of water to each soil sample bottle, and 25 ml ± 2.5 ml, by dispenser, of 100 vol hydrogen peroxide solution.

3. The content was mixed by gently swirling and the bottles were placed onto cold hotplate in a fume cupboard and left there overnight (Figure VIII.1 Samples placed onto hotplate.Figure VIII.1).

4. The hotplate was switched on and the temperature was set to 100°C ± 2°C. The bottles stayed there for 2 hours.

Figure VIII.1 Samples placed onto hotplate.

Procedure for dispersal and wet sieving

1. Each bottle was balanced to 200 g ± 1 g by adding demineralised water. The content of bottles was shaken vigorously and the bottles were subsequently placed

into centrifuge and centrifuged at 2000 rpm ± 100 rpm for 20 min. Created supernatant was discarded.

2. 20 ml ± 2 ml of buffered sodium hexametaphosphate was added, by dispenser, to each bottle. Likewise 150 ml ± 2 ml of water was added, by measuring cylinder, to each bottle and the content was thoroughly shaken.

3. Subsequently the bottles were placed on the end-over-end shaker overnight for 18 hours.

4. 20 ml ± 2 ml of buffered sodium hexametaphosphate dispersing solution was added into glass bottle weighted to 4 decimal places. The bottle with the content was placed into the oven set at 105°C and dried overnight. Afterwards the bottle was cooled down in a desiccator and re-weighted.

5. The large plastic funnel was placed into 500 ml measuring cylinder. All content of bottle containing the soil sample was washed out onto the 0.063 mm sieve which was placed in the funnel. This procedure was performed for all bottles.

6. The residues on the sieve were carefully washed into the numbered drying tin and dried out in an oven set at 105°C ± 2°C.

Procedure for dry sieving the sand fraction

1. The content of each beaker was sieved through a nest of sieves (in reversed order) using the sieve shaker for 15 minutes.

2. The mass of each full sieve containing the sample was dared and recorded for 4 decimal places. Likewise just the sieves were dared.

3. Then the content of the receiver was returned to the measuring cylinder containing particular sample, and the volume was made up to 500 ml with deionised water.

Determination one silt and one clay fraction by pipette extraction

1. The measuring cylinders were placed into a water bath to equilibrate the sample temperatures to 25°C overnight (Figure VIII.2).

2. Two sets of the glass bottles were dared for 4 decimal places. One bottle set was later used for the samples containing the soil particles of size 0.002 mm – 0.063 mm. The other one later contained the soil particles of the size less than 0.002 mm.

3. The content of each cylinder was thoroughly mixed for approximately 30 seconds. At the end of stirring began timing. At a depth of 10 cm from the liquid surface 25 ml was pipetted into the bottle intended for the fraction of 0.002 mm - 0.063 mm, which contains silt and clay components. Then the samples were left to sediment for time of 6 hours and 23 minutes. After this time the second fraction containing the 0.002 mm particles (clay fraction) was pipetted at the depth of 9 cm from the new liquid surface into second set of the glass bottles.

4. Both sets of glass bottles were subsequently dried in the oven at 105°C ± 2°C for 24 hours.

5. The dried bottles were cooled down in a desiccator and re-dared.

Figure VIII.2 Measuring cylinders placed into a water bath.

Calculation of results

The individual soil particle size fractions were calculated using following equations:

$$D = \frac{d}{20}$$ **Equation 5**

$$F = S + ((Z - D) \times 20)$$ **Equation 6**

$$\% \text{ Sand} = \frac{\text{Mass of Particular Sand Fraction}}{\text{F}} \text{ x } 100$$ **Equation 7**

$$\% \text{ 0.002 mm} - \text{0.063 mm} = \frac{(Z - C) \times 20}{F} \times 100$$ **Equation 8**

$$\% < \text{0.002 mm} = \frac{(C - D) \times 20}{F} \times 100$$ **Equation 9**

Both the Dispersant Factor (D) and Factor (F) were calculated to 4 decimal places. The particle size fractions were calculated and reported to 2 decimal places as well as the final results. The soil texture was determined using the triangle shown in Figure VIII.3.

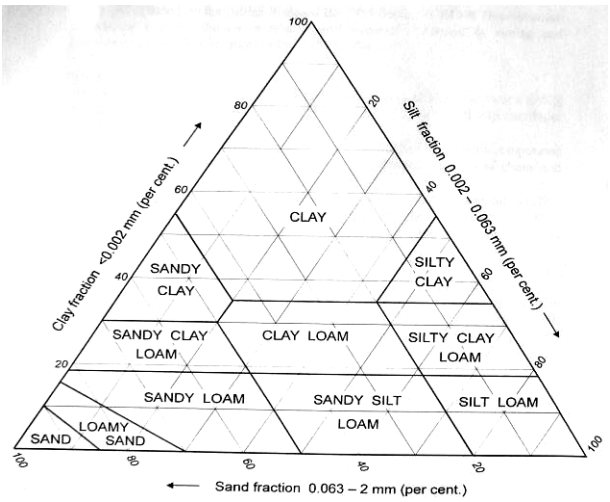

Figure VIII.3 Triangle for soil particle size distribution determination.

Electrical conductivity by saturated paste

The determination of electrical conductivity by saturated paste is based on the USDA Soil Survey Investigations Report (1996) *Soil Survey Laboratory Methods Manual*.

Procedure for preparation of saturated extract and own measurement

1. About 250 g of air-dried pre-treated soil sample was placed into plastic beaker and mixed with demineralised water until achieving of saturation point.

2. The paste was then left to stand for one hour and the saturation was rechecked. In some cases when it was necessary more water was added and the content of the beaker was remixed.

3. The saturated paste was subsequently filtered under vacuum using a Buchner funnel and the filtrate was used for analysis (Figure VIII.4 A).

4. The electrical conductivity of the prepared saturated extract was measured by immersion of 1 cm cell completely to the extract. The value of electrical conductivity was displayed on LCD display (Figure VIII.4 C).

5. After the measurement the cell was carefully rinsed by the deionised water.

A

B

C

Figure VIII.4 Procedure for preparation of saturated extract and own measurement: A-saturated extract obtaining, B-samples containing saturated extract, C-measurement.

Loss on ignition

Loss on ignition is based on the British Standard BS EN 13039:2000*Determination of the organic matter content and ash*. The air-dried pre-treated soil sample was used for this analysis.

Procedure for determination of loss on ignition

1. The mass of a silica dish (m_0) was dared with the accuracy to 4 decimal places. Approximately 5 g of sample was dared into the dish.

2. The soil with the dish was put into the oven set at 105°C ± 5°C and dried overnight.

3. The dish containing the sample was then cooled down in a desiccator and the mass (m_1) was again recorded to 4 decimal places.

4. Subsequently the dishes were placed into cool muffle furnace. The temperature was set at 450°C ± 10°C and the dishes stayed there for 4 hours ± 15 minutes.

5. Then the dishes containing the soil samples were cooled down in a desiccator and the mass (m_2) was determined to 4 decimal places (Figure VIII.5).

6. The loss on ignition was calculated using the following equation:

$$LOI = \frac{m_1 - m_2}{m_1 - m_0} \times 100$$ **Equation 10**

Figure VIII.5 Silica dishes placed in a desiccator.

Determination of soil pH

Determination of soil pH is based on the British Standard BS ISO 10390:2005 *Determination of pH*.

Procedure for preparation of the suspension

1. Using the brass scoop it was measured 10 ml of air-dried pre-treated soil sample into 100 ml glass bottle.

2. Using the dispenser it was subsequently added 50 ml of demineralised water into each bottle (Figure VIII.6 A).

3. The bottles were put onto the side-to-side shaker set at 300 min^{-1} and shaken for 60 minutes (Figure VIII.6 B).

4. The bottles were then allowed to stand for 1 hour but not longer then 3 hours and following the below steps the pH was measured.

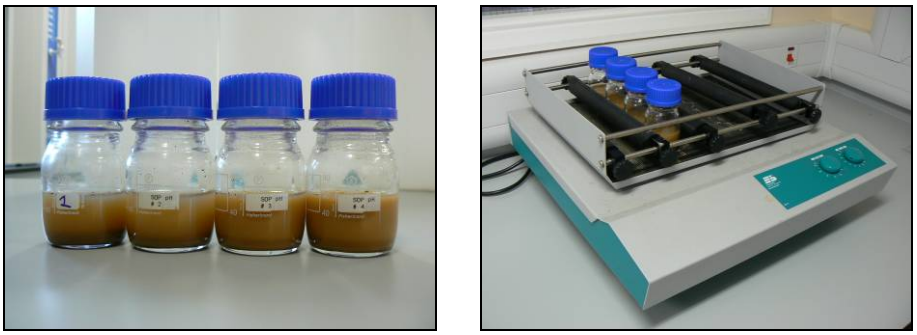

A **B**

Figure VIII.6 Procedure for preparation of the suspension: A-bottles containing samples, B-bottles placed onto side-to-side shaker.

Measurement of soil pH

1. Before own measurement, the pH meter was calibrated using pH 4.0, pH 7.0 and pH 10.0 solutions (Figure VIII.7 A).

2. Every sample was shaken thoroughly before measurement and then the pH was immediately measured by immersing a pH probe into the suspension (Figure VIII.7 B).

3. After the measurement of each sample the pH probe was rinsed with deionised water and dried to be prepared for further measurement.

A **B**

Figure VIII.7 Procedure for own measurement: A-calibration solutions, B-measurement of soil pH.

Appendix IX. Bar charts – graphical interpretation of ANOVA results

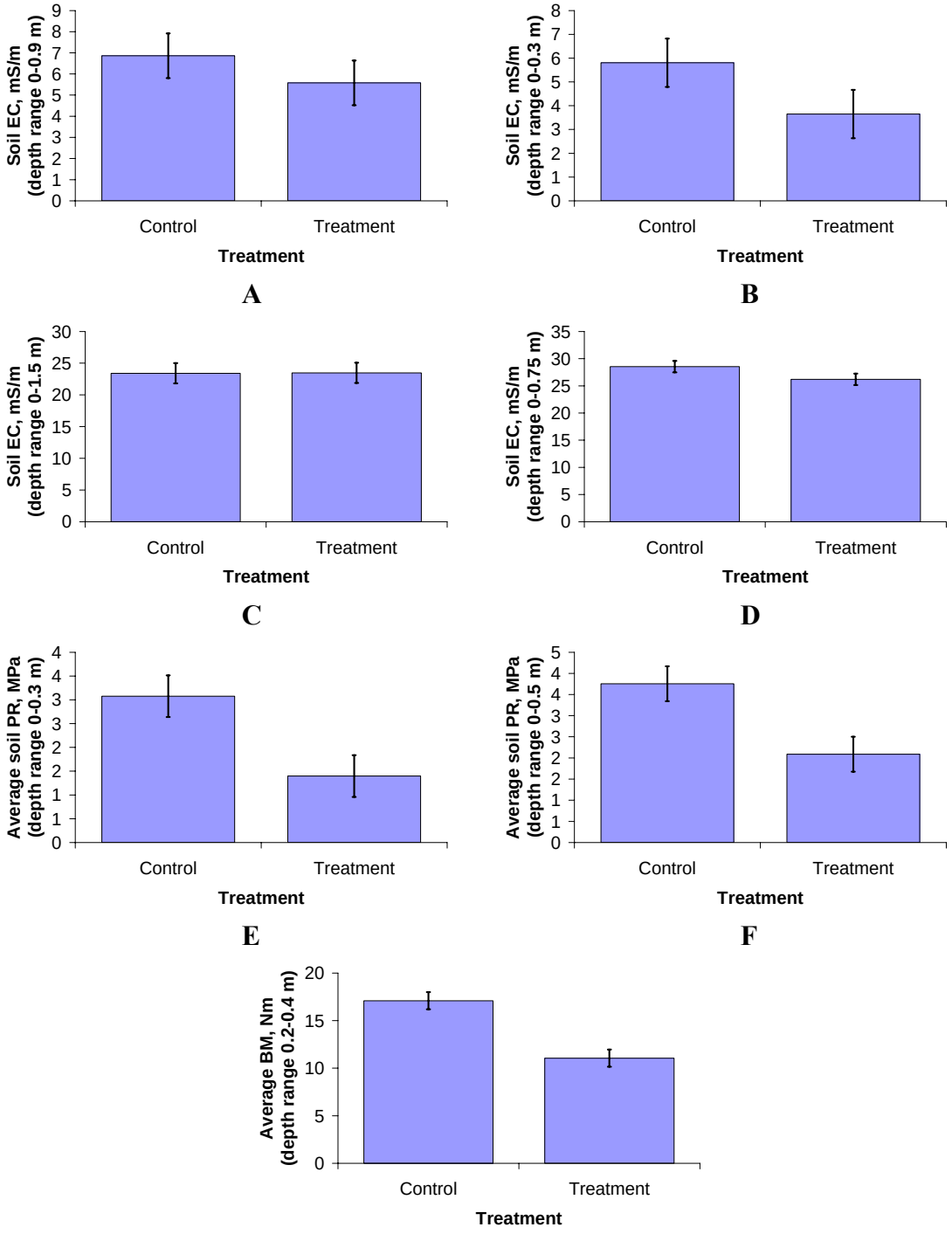

Figure IX.1 Stationary data obtained after treatment. Comparison is done between readings obtained within "Control" and averaged readings obtained within both "Treatment" areas. A –

EC90, B – EC30, C – EC150, D – EC75, E – PR30, F – PR50, G – BM averaged within soil profile. Error bars show LSDs.

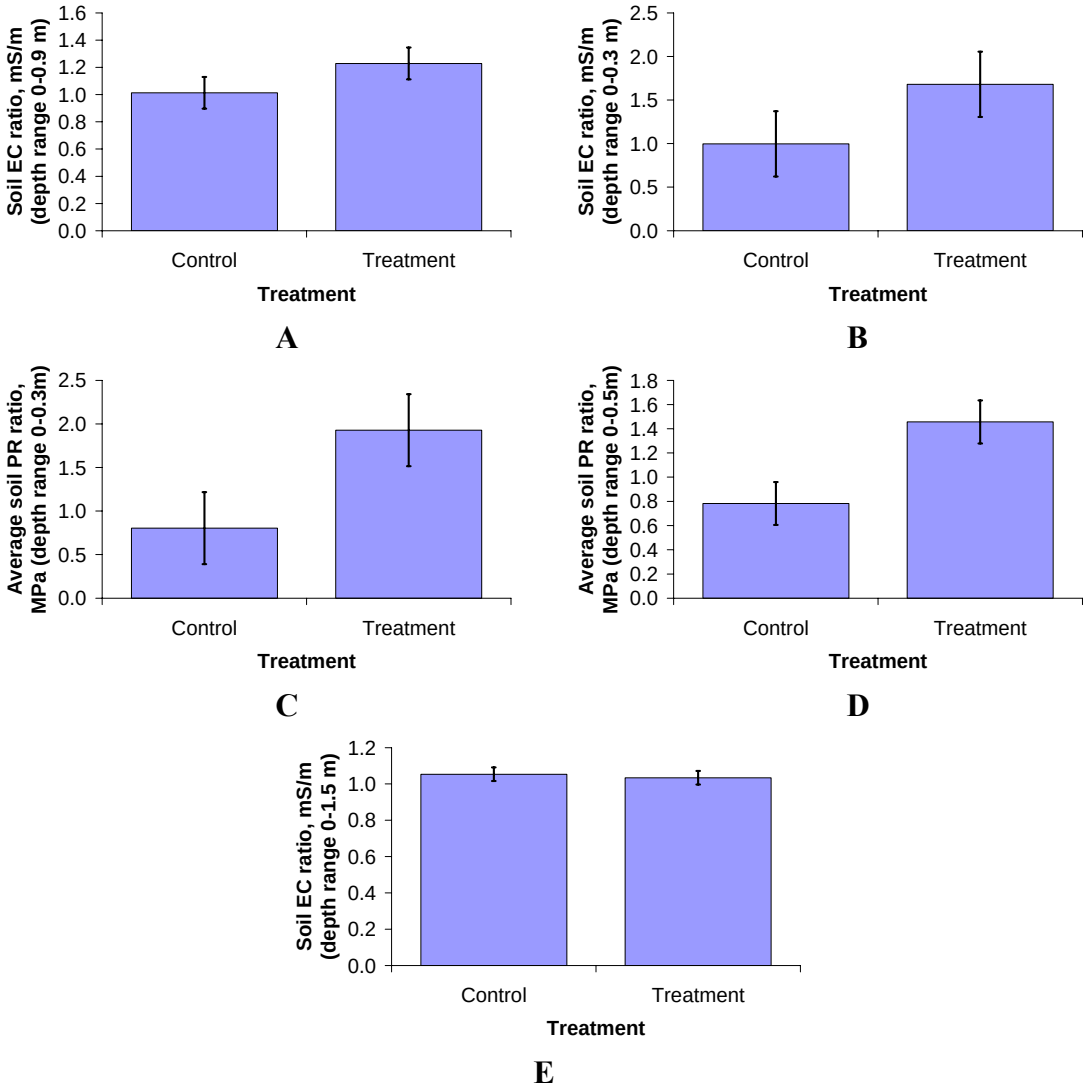

Figure IX.2 Ratio of the stationary data (before/after treatment). Comparison is done between readings obtained within "Control" and averaged readings obtained within both "Treatment" areas. A – EC90, B – EC30, C – PR30, D – PR50, E – EC150. Error bars show LSDs.

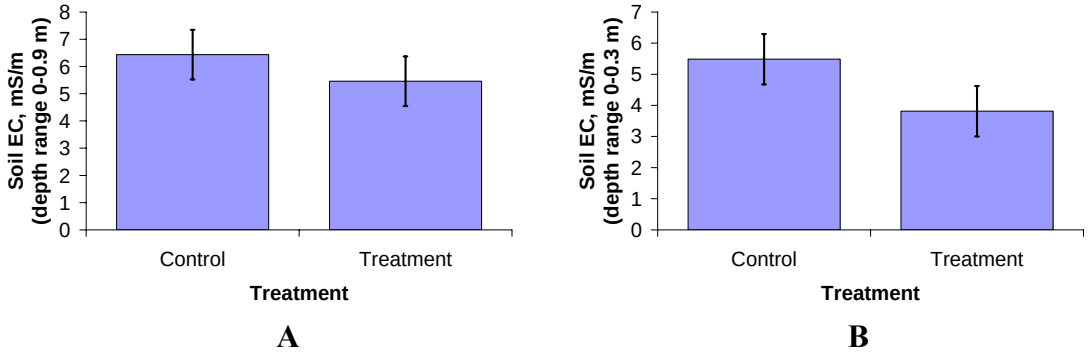

Figure IX.3 Dynamic (0.05 m.s^{-1}) EC data obtained after treatment. Comparison is done between readings obtained within "Control" and averaged readings obtained within both "Treatment" areas. A – EC90, B – EC30. Error bars show LSDs.

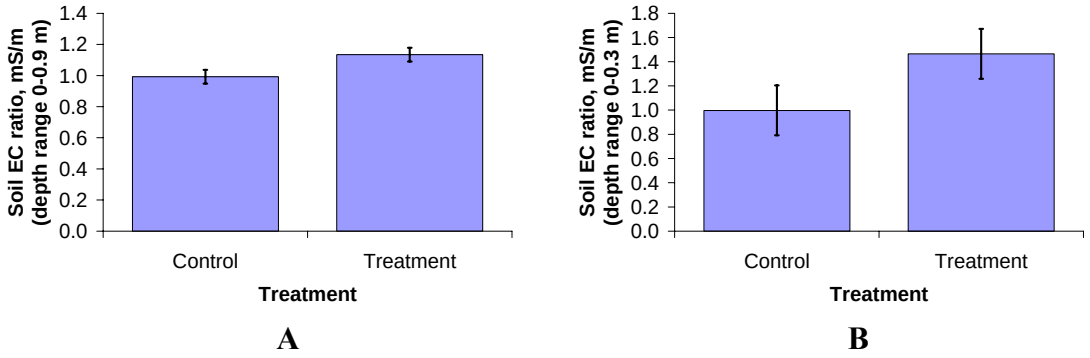

Figure IX.4 Ratio of the dynamic (0.05 m.s^{-1}) data (before/after treatment). Comparison is done between readings obtained within "Control" and averaged readings obtained within both "Treatment" areas. A – EC90, B – EC30. Error bars show LSDs.

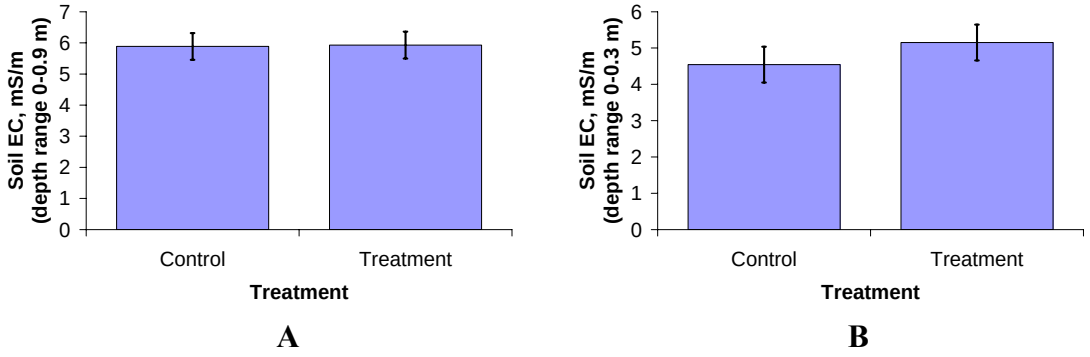

Figure IX.5 Dynamic (1 m.s^{-1}) EC data obtained after treatment. Comparison is done between readings obtained within "Control" and averaged readings obtained within both "Treatment" areas. A – EC90, B – EC30. Error bars show LSDs.

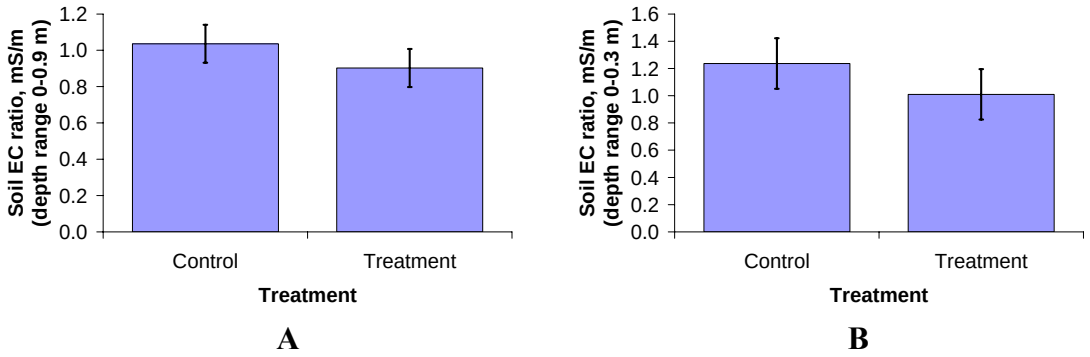

Figure IX.6 Ratio of the dynamic (1 m.s^{-1}) data (before/after treatment). Comparison is done between readings obtained within "Control" and averaged readings obtained within both "Treatment" areas. A – EC90, B – EC30. Error bars show LSDs.

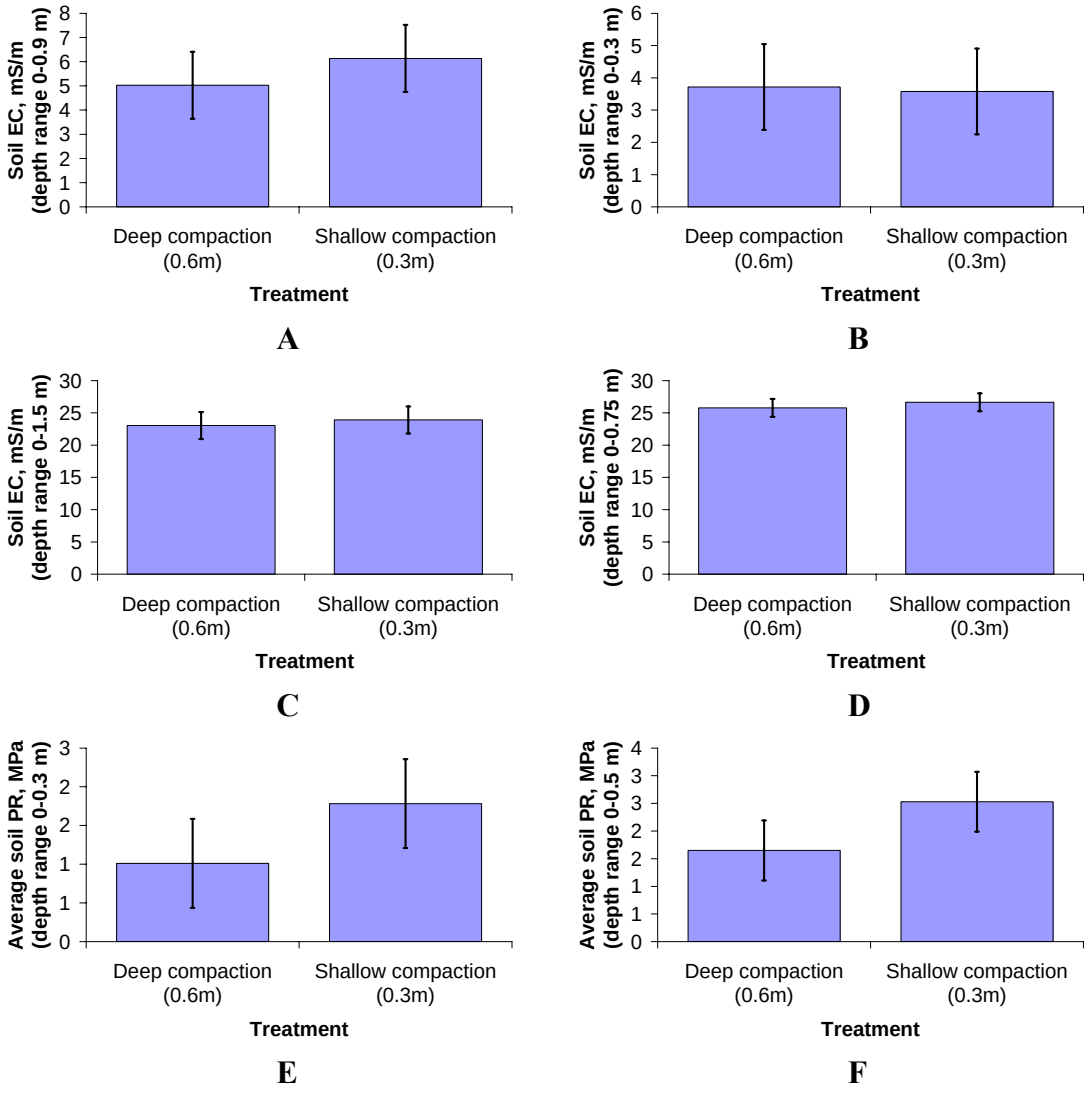

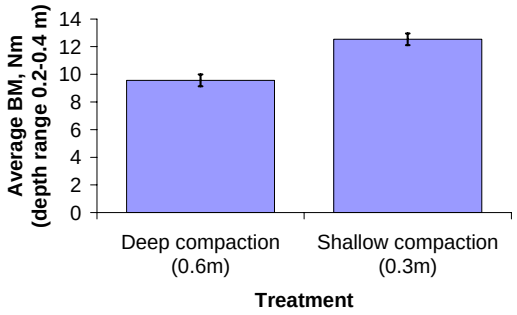

G

Figure IX.7 Stationary data obtained after treatment. Comparison is done between readings obtained within areas containing "Deep" and "Shallow" compaction. A – EC90, B – EC30, C – EC150, D – EC75, E – PR30, F – PR50, G – BM averaged within soil profile. Error bars show LSDs.

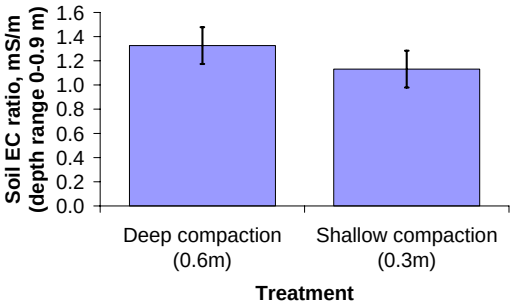

A

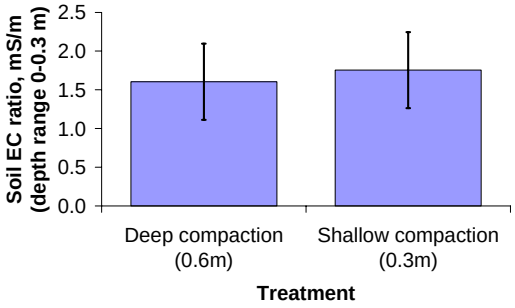

B

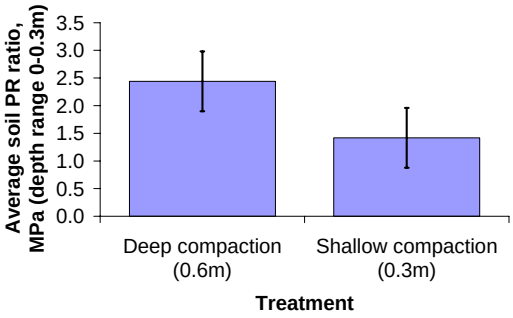

C

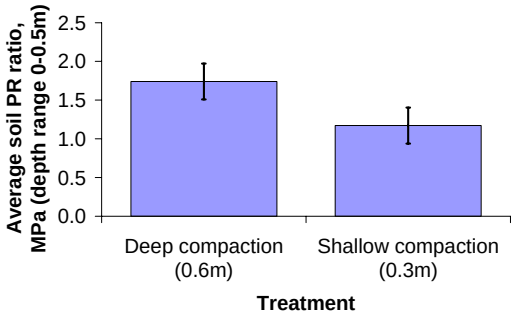

D

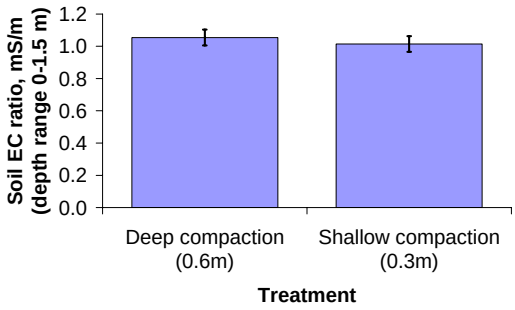

E

Figure IX.8 Ratio of the stationary data (before/after treatment). Comparison is done between readings obtained within areas containing "Deep" and "Shallow" compaction. A – EC90, B – EC30, C – PR30, D – PR50, E – EC150. Error bars show LSDs.

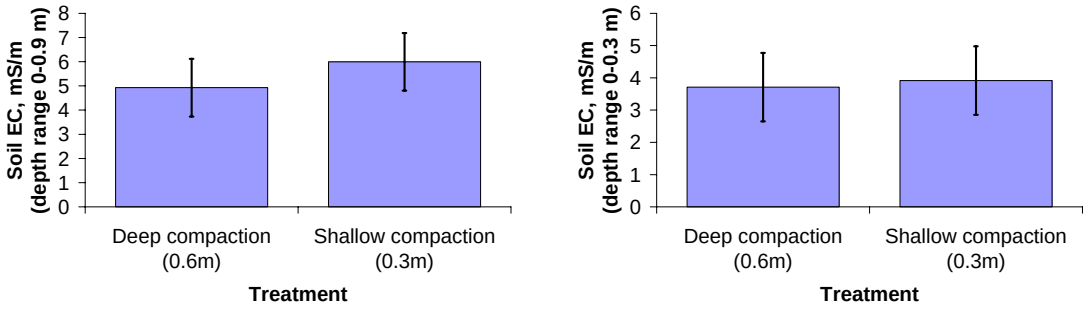

A **B**

Figure IX.9 Dynamic (0.05 m.s^{-1}) EC data obtained after treatment. Comparison is done between readings obtained within areas containing "Deep" and "Shallow" compaction. A – EC90, B – EC30. Error bars show LSDs.

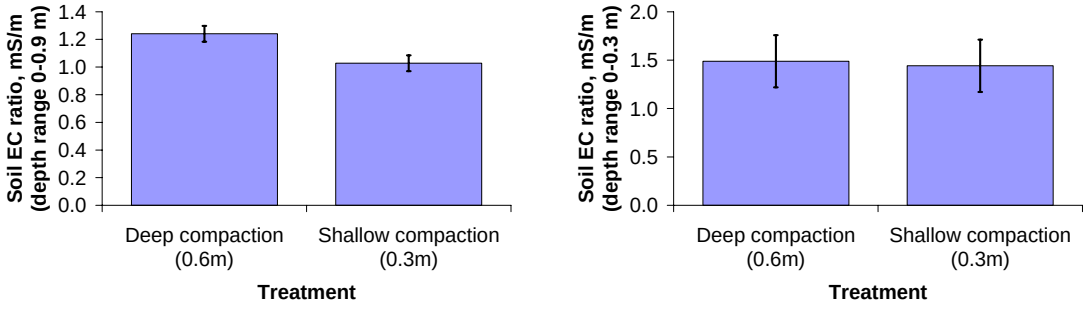

A **B**

Figure IX.10 Ratio of the dynamic (0.05 m.s^{-1}) data (before/after treatment). Comparison is done between readings obtained within areas containing "Deep" and "Shallow" compaction. A – EC90, B – EC30. Error bars show LSDs.

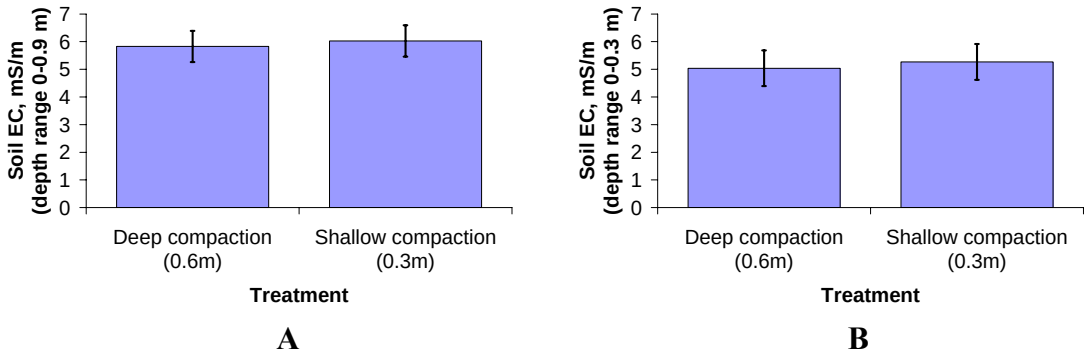

Figure IX.11 Dynamic (1 m.s^{-1}) EC data obtained after treatment. Comparison is done between readings obtained within areas containing "Deep" and "Shallow" compaction. A – EC90, B – EC30. Error bars show LSDs.

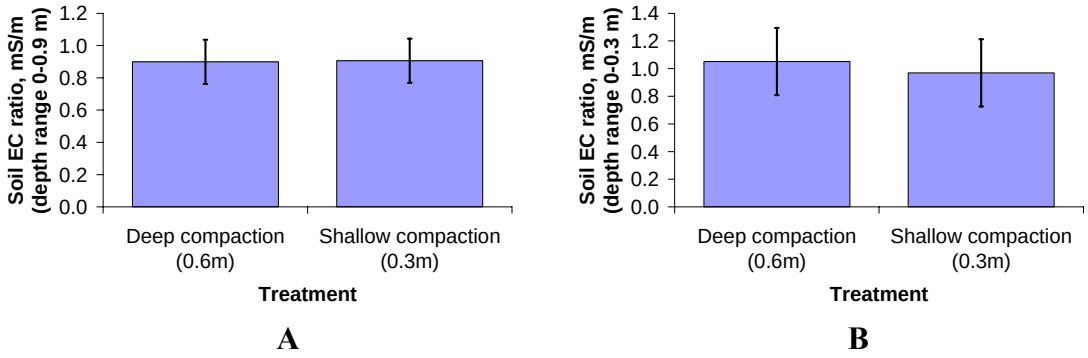

Figure IX.12 Ratio of the dynamic (1 m.s^{-1}) data (before/after treatment). Comparison is done between readings obtained within areas containing "Deep" and "Shallow" compaction. A – EC90, B – EC30. Error bars show LSDs.

Appendix X. Graphs of regression analyses

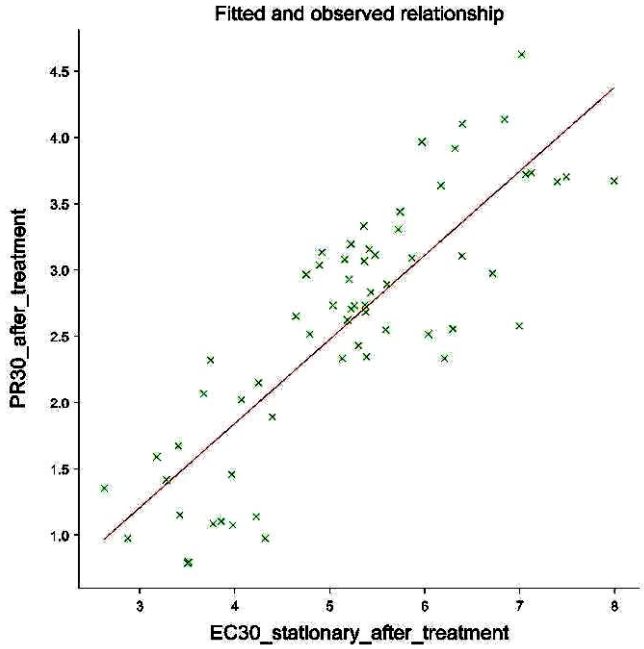

Figure X.1 Scatter plot of the soil electrical conductivity measured at stationary mode at depth range of 0-0.3 m and the penetration resistance averaged within the depth range of 0.1-0.3 m.

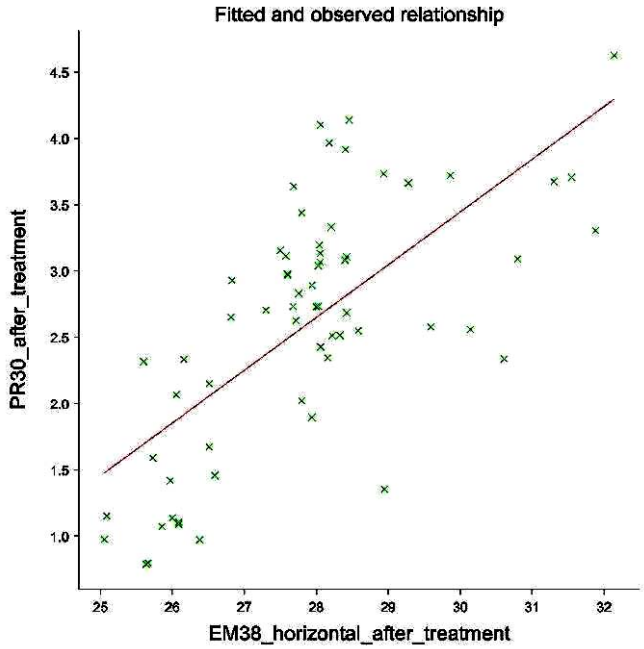

Figure X.2 Scatter plot of the soil electrical conductivity measured at stationary mode at depth range of 0-0.75 m and the penetration resistance averaged within the depth range of 0.1-0.3 m.

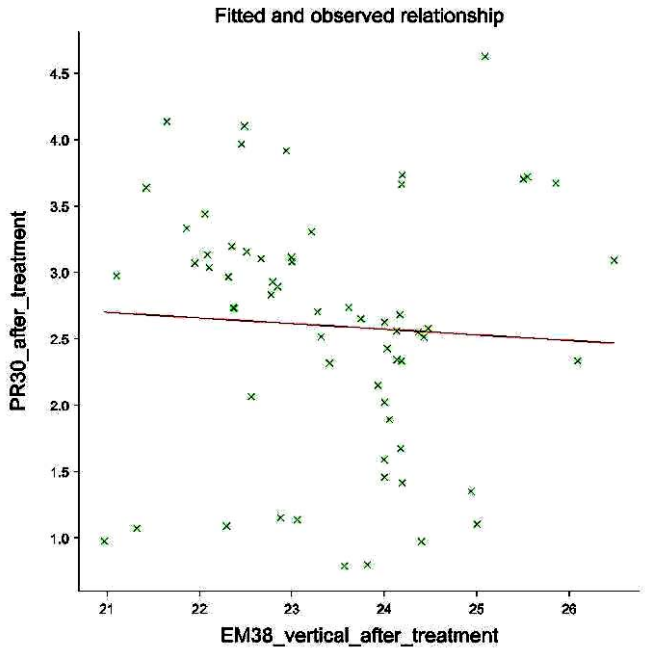

Figure X.3 Scatter plot of the soil electrical conductivity measured at stationary mode at depth range of 0-1.5 m and the penetration resistance averaged within the depth range of 0.1-0.3 m.

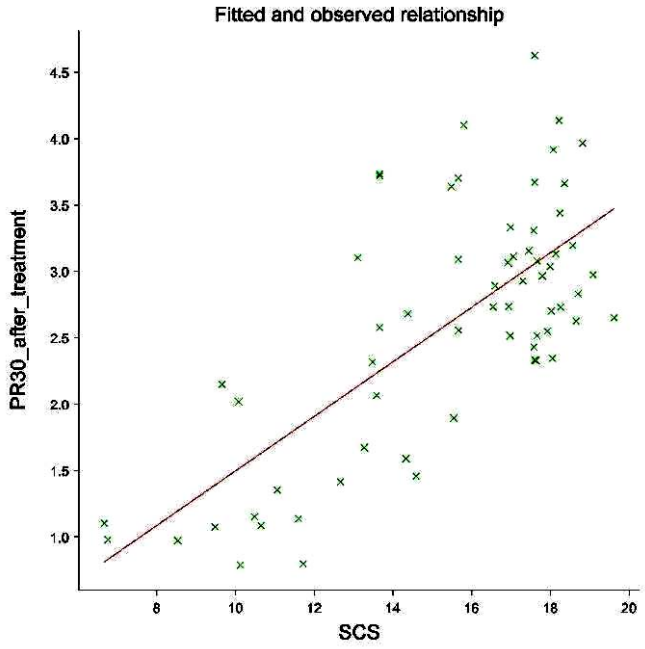

Figure X.4 Scatter plot of the bending moment measured by the soil strength sensor and averaged at depth range of 0.2-0.4 m and the penetration resistance averaged within the depth range of 0.1-0.3 m.

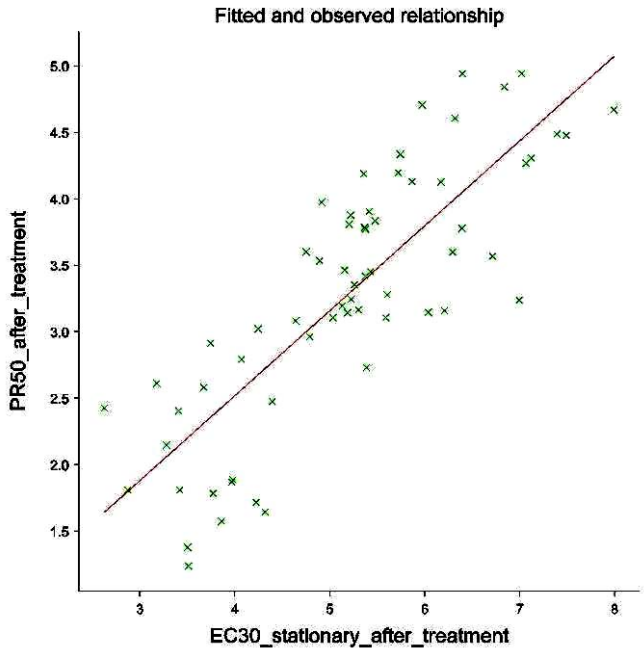

Figure X.5 Scatter plot of the soil electrical conductivity measured at stationary mode at depth range of 0-0.3 m and the penetration resistance averaged within the depth range of 0.1-0.5 m.

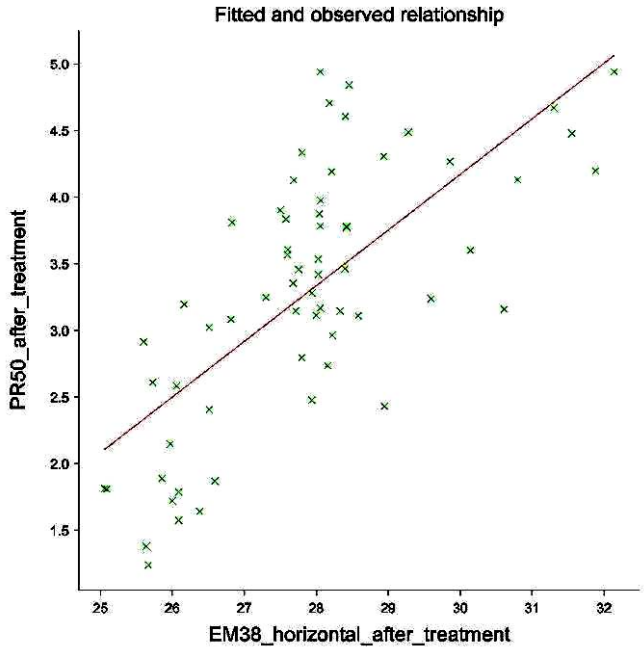

Figure X.6 Scatter plot of the soil electrical conductivity measured at stationary mode at depth range of 0-0.75 m and the penetration resistance averaged within the depth range of 0.1-0.5 m.

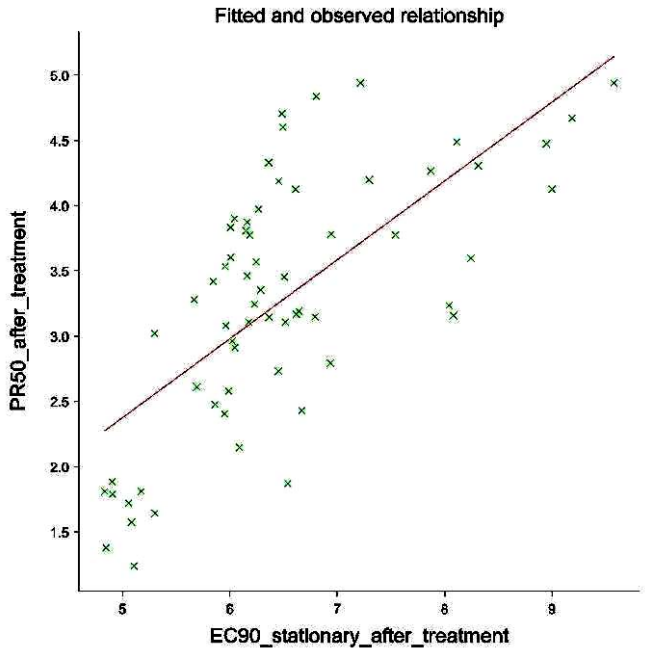

Figure X.7 Scatter plot of the soil electrical conductivity measured at stationary mode at depth range of 0-0.9 m and the penetration resistance averaged within the depth range of 0.1-0.5 m.

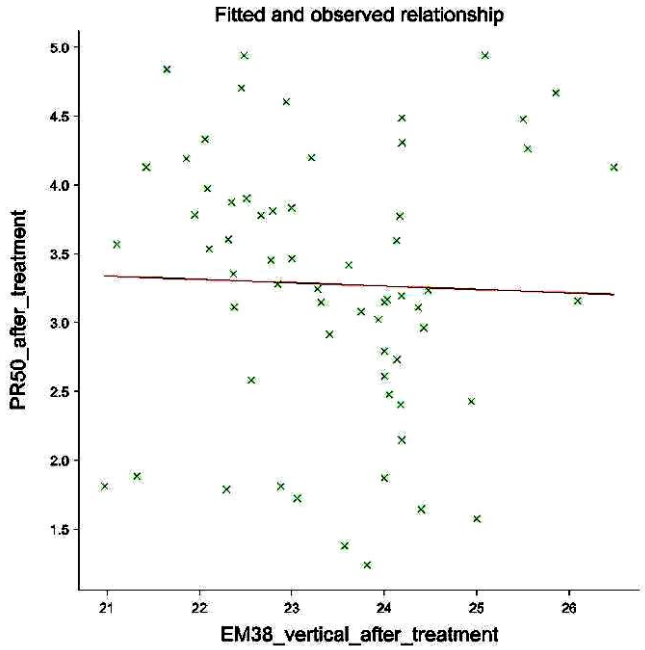

Figure X.8 Scatter plot of the soil electrical conductivity measured at stationary mode at depth range of 0-1.5 m and the penetration resistance averaged within the depth range of 0.1-0.5 m.

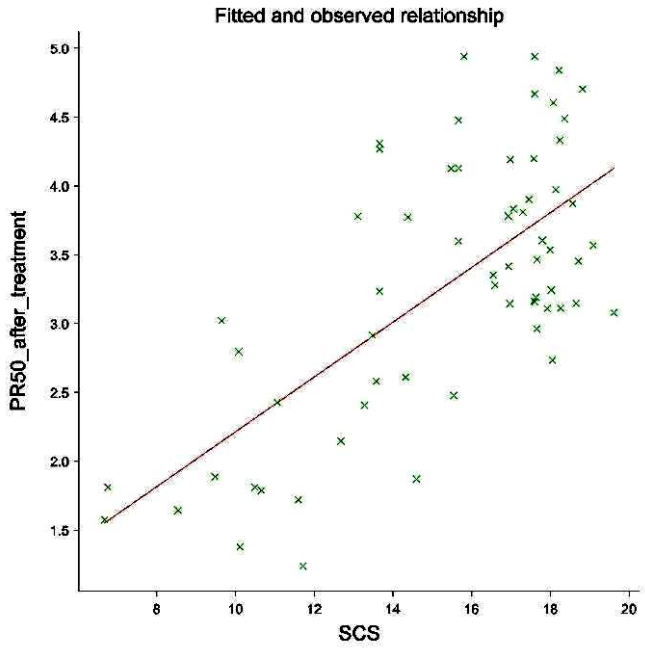

Figure X.9 Scatter plot of the bending moment measured by the soil strength sensor and averaged at depth range of 0.2-0.4 m and the penetration resistance averaged within the depth range of 0.1-0.5 m.

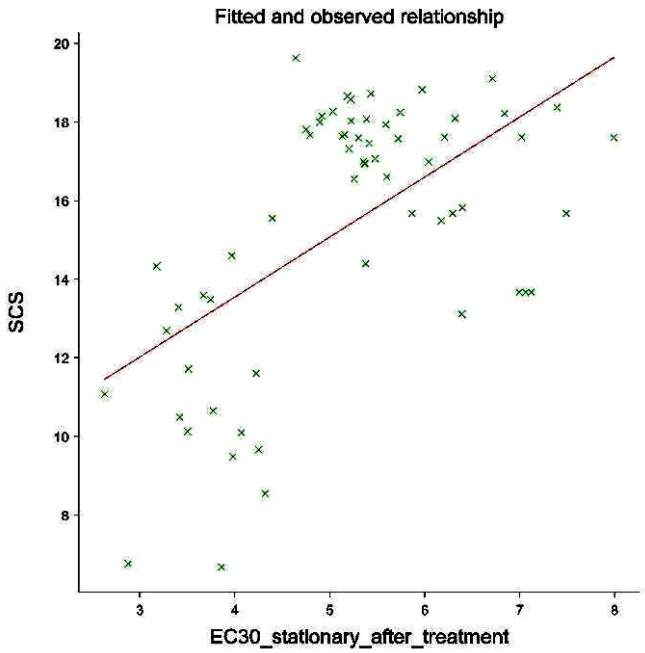

Figure X.10 Scatter plot of the bending moment measured by the soil strength sensor and averaged at depth range of 0.2-0.4 m and the soil EC readings measured within the depth range of 0-0.3 m.

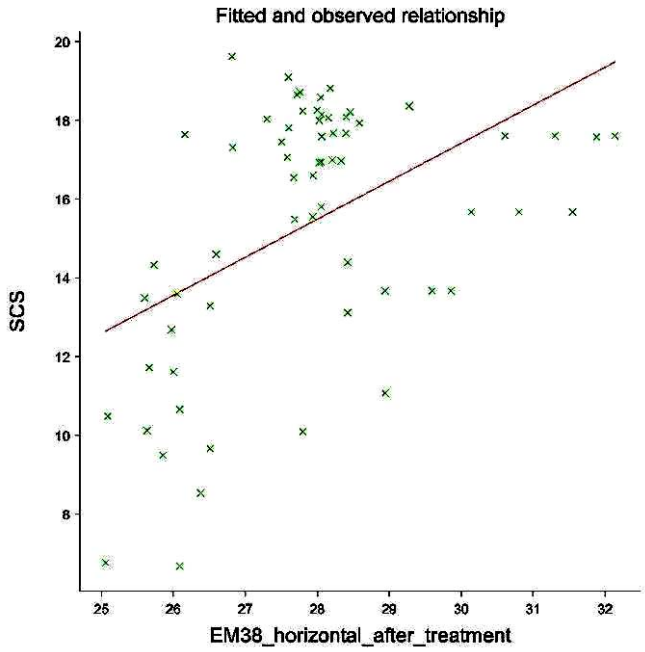

Figure X.11 Scatter plot of the bending moment measured by the soil strength sensor and averaged at depth range of 0.2-0.4 m and the soil EC readings measured within the depth range of 0-0.75 m.

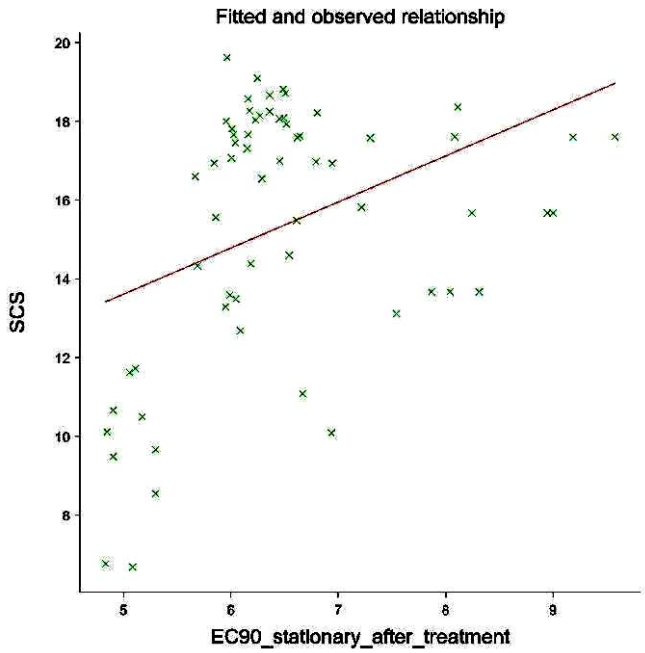

Figure X.12 Scatter plot of the bending moment measured by the soil strength sensor and averaged at depth range of 0.2-0.4 m and the soil EC readings measured within the depth range of 0-0.9 m.

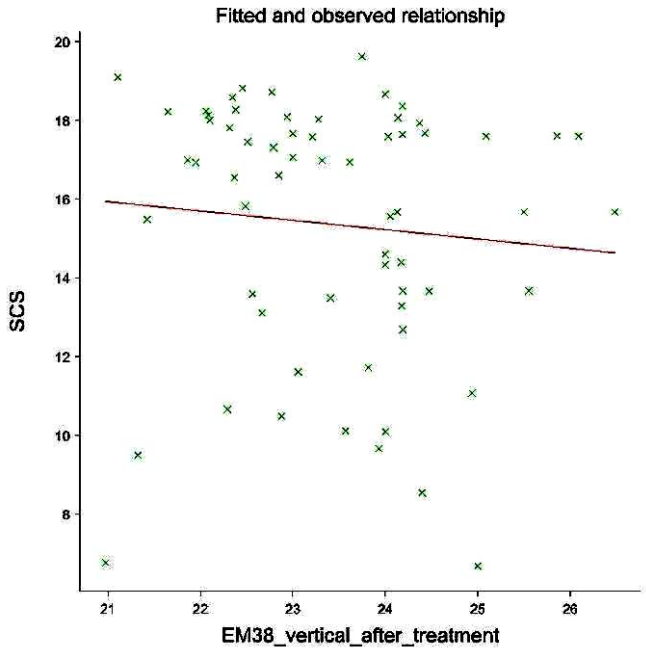

Figure X.13 Scatter plot of the bending moment measured by the soil strength sensor and averaged at depth range of 0.2-0.4 m and the soil EC readings measured within the depth range of 0-1.5 m.

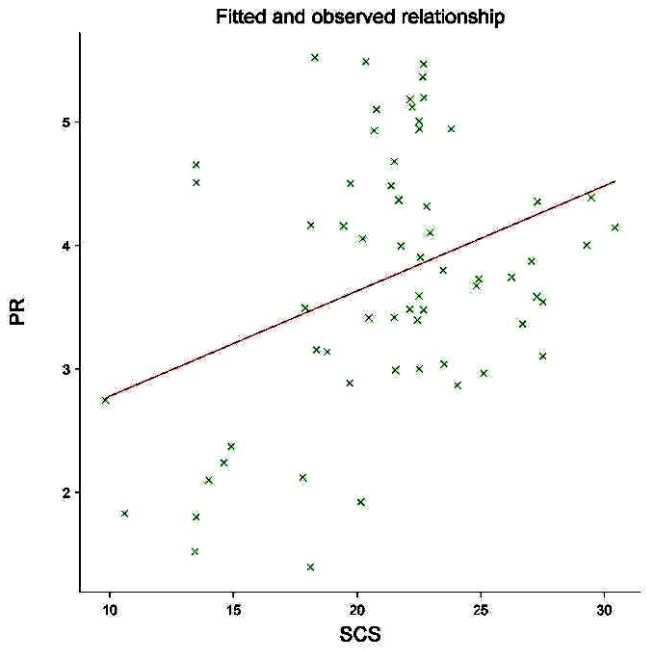

Figure X.14 Scatter plot of the bending moment measured at the depth range of 0.35-0.4 and the soil penetration resistance averaged within the same depth range.

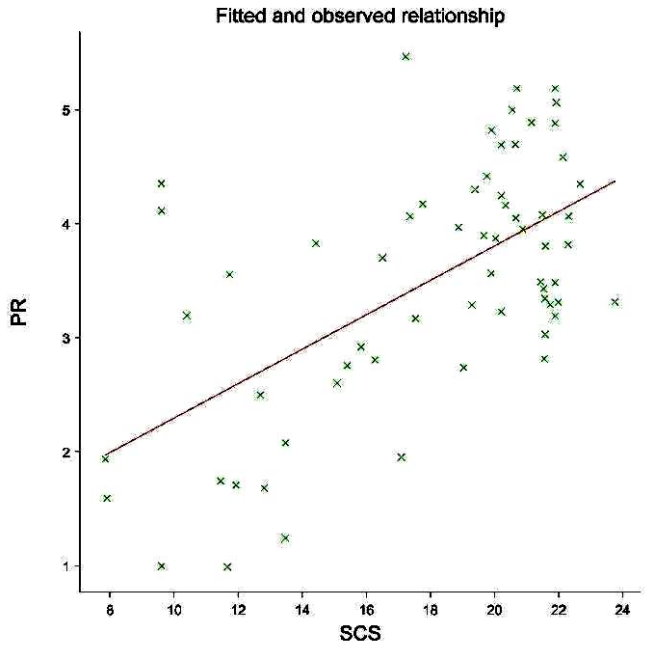

Figure X.15 Scatter plot of the bending moment measured at the depth range of 0.30-0.35 and the soil penetration resistance averaged within the same depth range.

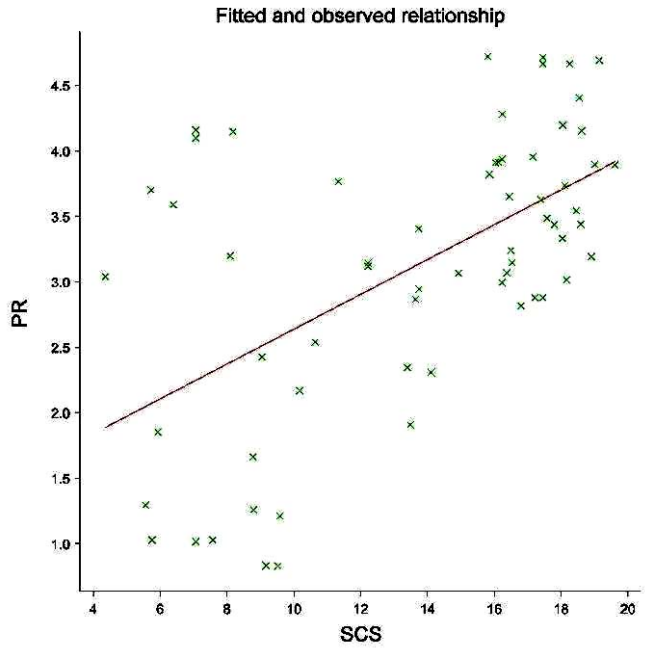

Figure X.16 Scatter plot of the bending moment measured at the depth range of 0.25-0.30 and the soil penetration resistance averaged within the same depth range.

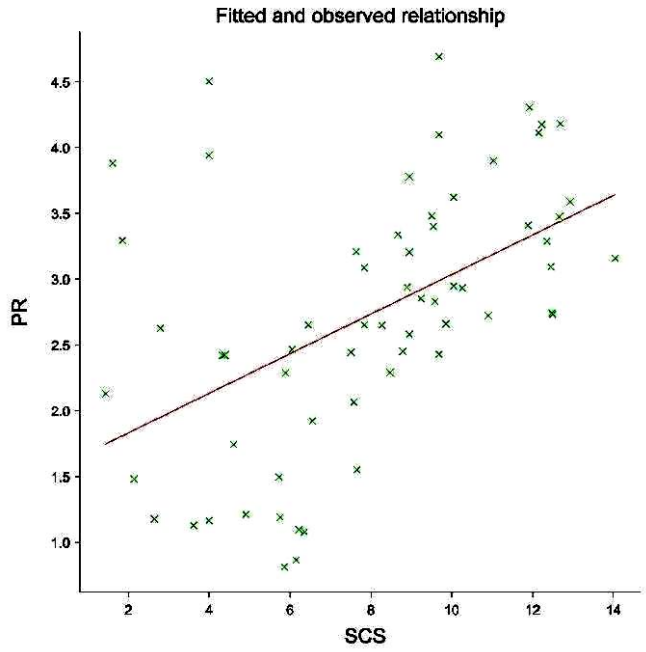

Figure X.17 Scatter plot of the bending moment measured at the depth range of 0.20-0.25 and the soil penetration resistance averaged within the same depth range.

Appendix XI. Maps of EC readings obtained by the Conductometer at speed of 0.05 m.s^{-1}

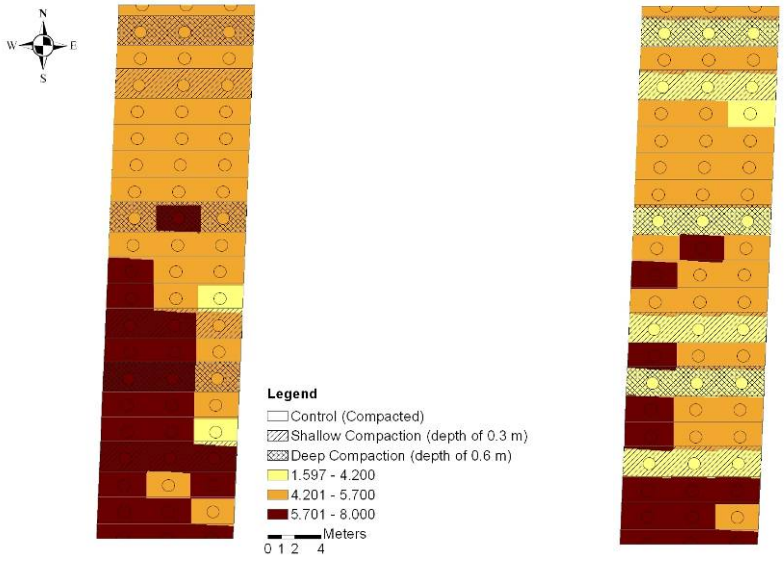

Figure XI.1 Map of EC readings obtained by the Conductometer operated in dynamic mode (speed 0.05 m.s^{-1}) from the trial plot at depth range of 0-0.3 m before (left) and after (right) treatment applying. EC values are displayed in mS.m^{-1}. Yellow areas (right) represent no compaction above 0.3 m.

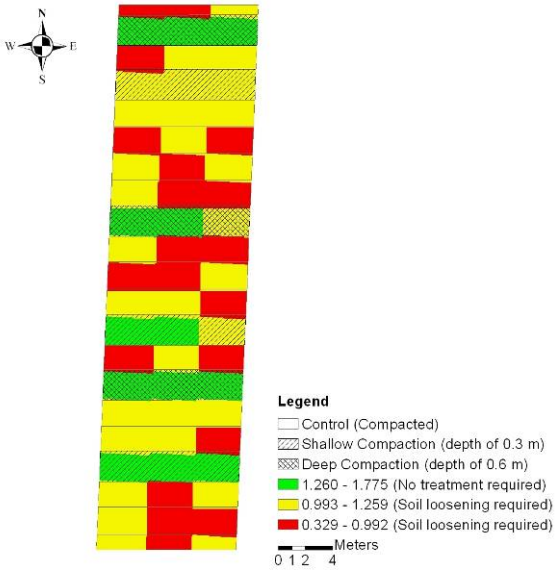

Figure XI.2 Application map created as "EC30 before treatment application / EC30 after treatment application" (simple ratio). The areas displayed by red and yellow are identified as being compacted within whole soil profile.

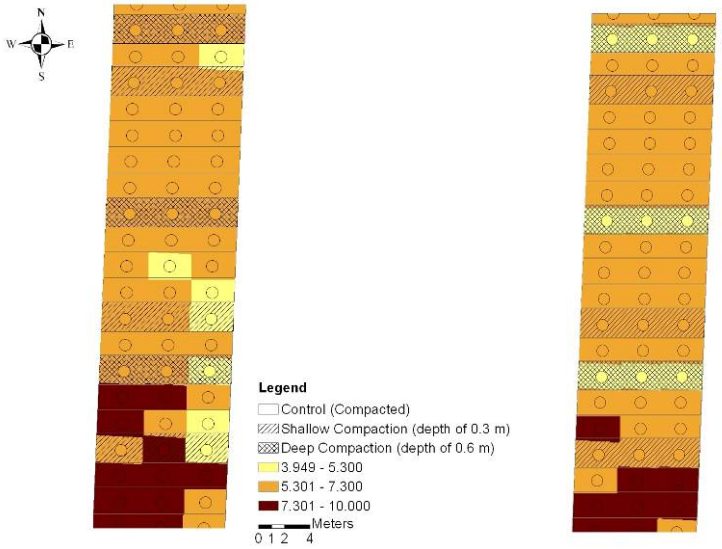

Figure XI.3 Map of EC readings obtained by the Conductometer operated in dynamic mode (speed 0.05 m.s^{-1}) from the trial plot at depth range of 0-0.9 m before (left) and after (right) treatment applying. EC values are displayed in mS.m^{-1}. Yellow areas (right) represent no compaction above 0.6 m.

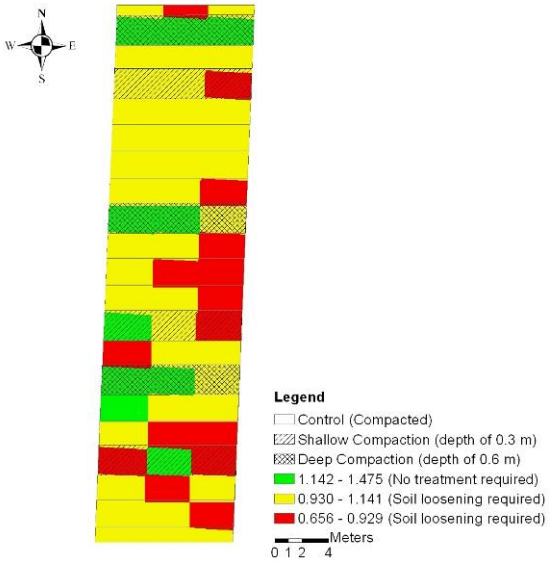

Figure XI.4 Application map created as "EC90 before treatment application / EC90 after treatment application" (simple ratio). The areas displayed by red and yellow are identified as being compacted above 0.6 m.

Appendix XII. Coordinates of EC measurements obtained by the Conductometer in different modes

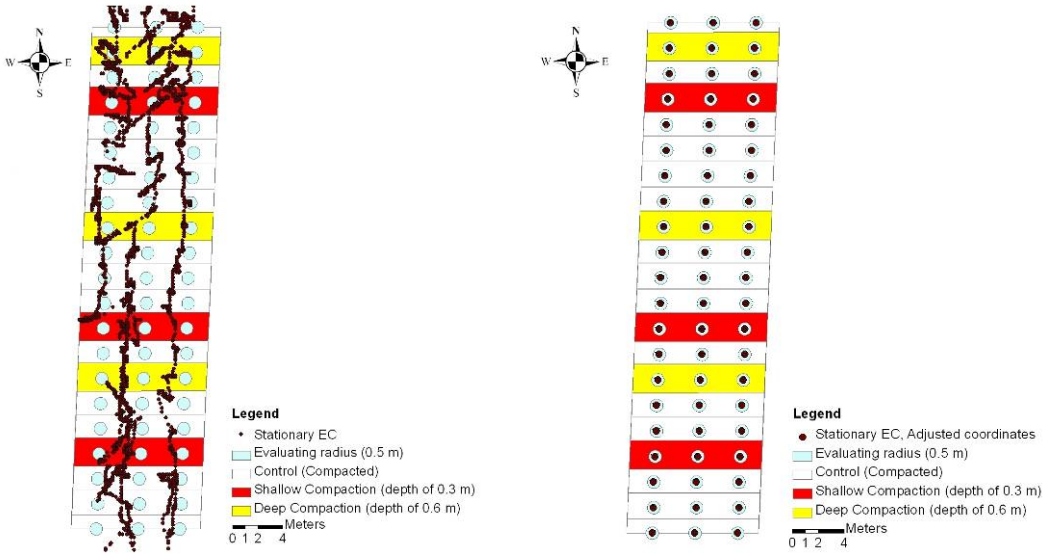

Figure XII.1 Positions of the individual measurements obtained by the Conductometer operated in stationary mode: left – original coordinates, right – adjusted coordinates.

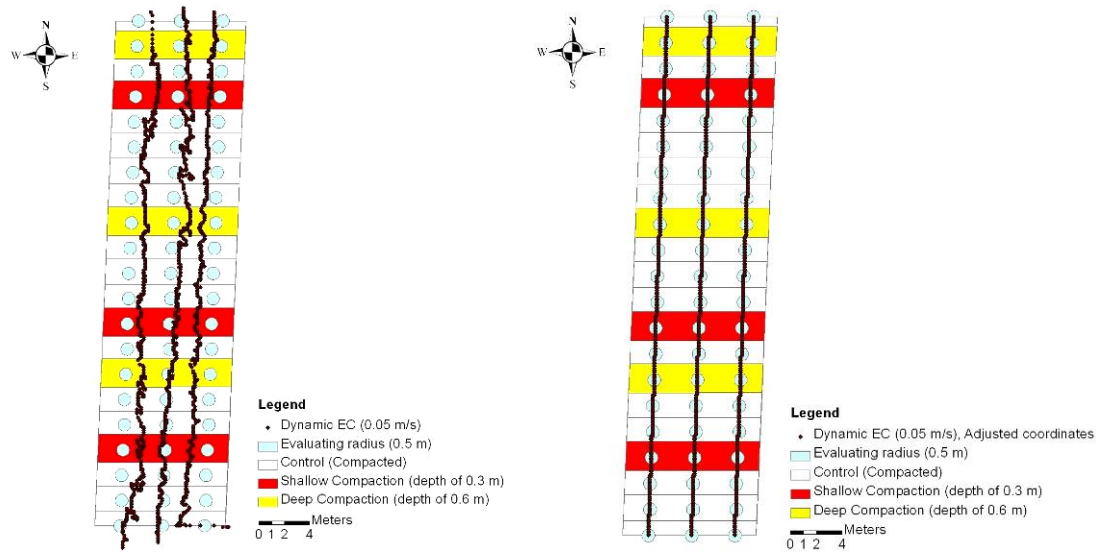

Figure XII.2 Positions of the individual measurements obtained by the Conductometer operated in dynamic mode (speed 0.05 m.s^{-1}): left – original coordinates, right – adjusted coordinates.

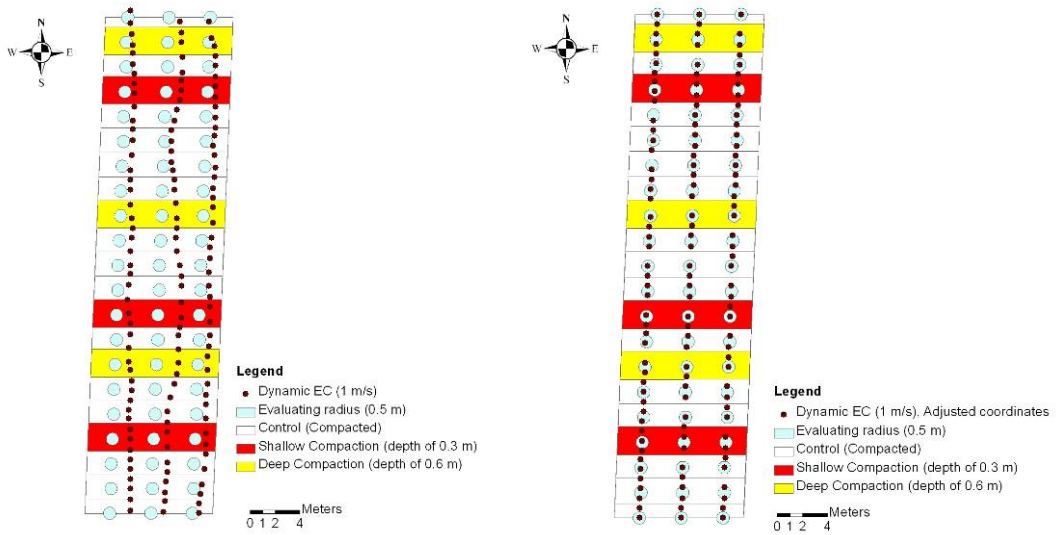

Figure XII.3 Positions of the individual measurements obtained by the Conductometer operated in dynamic mode (speed 1 m.s^{-1}): left – original coordinates, right – adjusted coordinates.